

1 **Rising temperatures drive lower summer minimum flows across hydrologically**
2 **diverse catchments**

3 **S. W. Ruzzante¹ and T. Gleeson¹**

4 ¹University of Victoria, Victoria, BC, Canada

5 Corresponding author: Sacha W. Ruzzante (sruzzante@uvic.ca)

6 **Key Points:**

- 7 • Regression models outperform process-based hydrologic models for minimum summer
8 flow prediction and enable valuable process understanding
9 • Summer low flows are highly sensitive to summer temperature and precipitation, with
10 winter storage historically playing a secondary role
11 • Precipitation variability historically drove low flows but rising temperatures are
12 responsible for recent declines in warmer catchments

13

14 **Abstract**

15 Excessively low stream flows harm ecosystems and societies, so two key goals of low-flow
16 hydrology are to understand their drivers and to predict their severity and frequency. We show
17 that simple linear regressions can accomplish both goals across diverse catchments. We analyse
18 230 unregulated moderate to high relief catchments across rainfall-dominated, hybrid, snowmelt-
19 dominated, and glacial regimes in British Columbia, Canada, with drainage areas spanning 5
20 orders of magnitude from 0.5 to 55,000 km². We find that summer low flows are decreasing in
21 rainfall-dominated and hybrid catchments and are dominantly driven by summer precipitation
22 and temperature, and only weakly influenced by winter storage. We apply this understanding of
23 drivers to create regression models to predict the minimum summer flow using monthly
24 temperature and precipitation data. These models outperform distributed process-based models
25 for every common goodness-of-fit metric; the performance improvement is mostly a result of
26 abandoning the requirement to simulate all parts of the annual hydrograph. We use these
27 regression models to reconstruct streamflow droughts, environmental flow threshold
28 transgressions, and low flow anomalies from 1901-2022. We reproduce recent drying trends in
29 rainfall-dominated and hybrid catchments, but also show that present conditions are comparable
30 to those seen almost one hundred years ago. However, anomalously low flows last century were
31 caused by severe precipitation deficits while current declines are being driven by rising summer
32 temperatures during a period of above-average precipitation.

33 **1 Introduction**

34 **1.1 Environmental flows and streamflow drought**

35 Preserving environmental flows, and especially low flows, is critical to maintaining healthy
36 riverine ecosystems and the societies that depend on them (Arthington et al., 2018; Bradford &
37 Heinonen, 2008). Living things, including humans, can be harmed when rivers carry less water
38 than normal: low flows that are significantly below the natural envelope of variability have been
39 shown to disrupt lifecycles of aquatic species and reduce biodiversity (Poff & Zimmerman,
40 2010), cause economic losses (Folkens et al., 2023), and disrupt cultural practices (Morgan,
41 2012; Tipa & Nelson, 2012). The more evocative term “streamflow drought” has also been
42 coined, presumably to attribute some gravity to a concept that is defined drily as a “sustained
43 period” of “below-normal river discharge” (Van Loon, 2015).

44 Climate change and human activity increasingly threaten environmental flows globally, resulting
45 in severe and probably irreparable harm to riverine ecosystems (Porkka et al., 2022; Richardson
46 et al., 2023; Virkki et al., 2022). Streamflow drought is driven by precipitation (P) and
47 temperature (T) anomalies: in a process called drought propagation, these anomalies cause
48 below-normal storage of groundwater, snow, and soil moisture, resulting in below-normal
49 discharge (Van Loon, 2015). Land use and water abstraction can also affect low flow occurrence
50 and severity (de Graaf et al., 2019; Guzha et al., 2018; Wada et al., 2016). Effective water
51 management requires an understanding of the relative importance of human and climate drivers
52 because land and water use can be managed at local scales, while climate change is a global
53 challenge. Within the category of climate drivers, it is important to distinguish precipitation and

54 temperature effects because climate model projections of temperature are considered highly
55 reliable, while projections of precipitation are less robust (Ukkola et al., 2020).

56 The province of British Columbia (BC), Canada, is a microcosm of the water resource challenges
57 posed by low flows and the hydrologic uncertainties regarding their driving mechanisms. The
58 ecosystems and communities of BC have acutely felt the impacts of streamflow drought. In the
59 late summer and early fall, photographs of drying rivers and dead salmon regularly make
60 national and international news (Cecco, 2022; Hernandez, 2023), and increasingly severe
61 droughts are threatening Indigenous nations' ways of life that have existed for millennia
62 (Cruikshank, 2023; First Nations Fisheries Council of British Columbia, 2020; Wood, 2021).

63 The provincial government enacted, in 2016, legislation declaring their authority to prohibit
64 water use for irrigation when streamflow falls below a critical threshold. This authority has been
65 exercised nine times from 2016 to 2023, alleviating ecosystem stress at the cost of economic
66 hardship for many farmers. Thus, debates about the drivers of low flows are politically charged:
67 is human water use really to blame, or are climate drivers more consequential? If climate is
68 responsible, are increasingly severe low flows primarily driven by rising temperatures (which
69 will almost certainly continue to rise) or decreasing precipitation trends (which may continue, or
70 reverse, or stagnate)?

71 Unfortunately, in BC as in many parts of the world, there is a shortage of scientific evidence to
72 answer these questions. At the most basic level, there is not yet quantitative evidence to confirm
73 the widely-held view that streamflow drought is becoming more common across the province.
74 Assessments of low flow drivers have usually been limited to a small number of catchments and,
75 as we find in Section 3.2, may have placed outsized importance on the role of winter snow
76 storage. Lastly, our ability to project climate change impacts is hindered by hydrologic models
77 that struggle to predict low flows, which is consistent with models developed for other parts of
78 the world.

79 **1.2 Limitations of hydrologic models**

80 Hydrologic models often produce unsatisfactory low flow simulations and forecasts (Newman,
81 2014; Kim et al, 2021; Nicolle et al., 2014; Collins, 2020). One reason for these inaccuracies is
82 that models are usually calibrated to all parts of the annual hydrograph. Low-flow generating
83 mechanisms can differ from those that generate high and medium flows (Smakhtin, 2001), so
84 parameters that are calibrated to reproduce high and medium flows may not accurately reflect
85 hydrologic conditions nor accurately reproduce low flows (Cenobio-Cruz et al, 2023). In
86 addition, since low flows are usually less variable than medium and high flows, low flows exert
87 less influence on model calibration.

88 Various flow transforms can be used to force models to prioritize low flow estimation, but
89 estimation of yearly minimum flows, or zero-flow days, remains challenging. For example, Aryal
90 et al (2020) achieved a median modified Kling-Gupta Efficiency of 0.5 and a median Nash-
91 Sutcliffe Efficiency of about 0.35 for the prediction of zero-flow days in 595 Australian
92 catchments. Using 9 hydrologic models in 10 major river basins worldwide, Huang *et al.*, (2017)
93 found percent bias values from -675% to 98% (median absolute value of 48%) for the flow

94 duration curve low-segment volume and -83% to 1067% (median absolute value of 38%) for the
95 10 and 30-year low flow levels.

96 Studies in the Pacific Northwest region show the same limitations. Whitfield et al., (2003)
97 modelled six watersheds around the Salish Sea (southwestern BC), and found that models
98 produced biased 7-day low flow estimates for pluvial (rain-dominated) catchments. Various
99 authors have used a distributed hydrological model (Variable Infiltration Capacity, or VIC) to
100 model climate impacts in the Fraser River Basin, but found that simulated low flows were
101 systematically lower than measured flows (Islam et al., 2017; Kang et al., 2016; Shrestha et al.,
102 2012). We will return to these VIC simulations in Section 3.3. No comprehensive analysis of
103 summer low flows across BC has been published.

104 **1.3 Low flow drivers**

105 We consider six climatic mechanisms that may influence summer low flows in BC, derived from
106 previous work on low flows and streamflow drought (Smakhtin, 2001; Van Loon, 2015). We
107 group these six mechanisms into three categories of driver: a) below-normal winter storage,
108 which includes groundwater and snowmelt drought b) accelerated summer hydrograph recession,
109 which includes rainfall deficits and storage depletion driven by evapotranspiration (ET), and c)
110 short-term anomalies caused by temperature fluctuation, which include transmission losses and
111 glacier melt drought. These mechanisms are listed in Table 1.

112 Which mechanism is most important? In 2005, Barnett et al. published a widely-cited article
113 showing that warming temperatures would induce snowmelt drought and decrease summer water
114 availability across much of the northern hemisphere. They downplayed potential effects of
115 warming on ET, arguing that actual evapotranspiration (related to temperature) is often much less
116 than potential evapotranspiration in catchments that become water-limited in the summer. This
117 conceptualization has largely dominated the research field for the past two decades, both globally
118 (Adam et al., 2009; Diffenbaugh et al., 2015; Godsey et al., 2014) and in the Pacific Northwest
119 region (Ban et al., 2023; Chang et al., 2012; Clifton et al., 2018; J. R. Dierauer et al., 2018, 2021;
120 Hale et al., 2023; Safeeq et al., 2014).

121 More recently, however, researchers have realized that, in some regions, summer ET may be
122 driving streamflow droughts. Teuling et al. (2013) showed that summer ET was amplifying
123 European droughts; Woodhouse et al. (2016) and Udall and Overpeck (2017), working
124 independently and using different methods, showed that air temperature is increasingly a driver
125 of drought in the Colorado River basin. Floriancic *et al.* (2020) found that summer ET and
126 precipitation controlled drought occurrence, and that winter snow storage had only minor effects
127 on warm-season low flows in Switzerland. Then Brunner et al. (2021) and Floriancic et al.
128 (2021) analysed catchments across the United States and Europe and both found that the
129 importance of temperature as a driver of low flows was increasing or likely to increase in many
130 places. However, Brunner et al. found that the effect of summer temperature was increasing in
131 the Pacific Northwest, while Floriancic et al. argued that summer temperature was not a driver in
132 this region. Boeing et al. (2024) found that increasing evapotranspiration has contributed to
133 water storage deficits in Germany over recent decades.

134 Regional studies focused on the Pacific Northwest do not resolve this inconsistency. Kormos et
135 al. (2016) found that low flows in the Pacific Northwest were more sensitive to precipitation than
136 to temperature. Cooper et al. (2018) found the opposite: that low flows in the western US are
137 more sensitive to ET than to precipitation, but that sensitivity to both climate variables decreases
138 towards the northern end of their study range. Georgiadis and Baker (2023) argued that both
139 temperature and precipitation exert important controls on low flows in the Puget Sound.

140 In addition to climatic drivers, water and land use can alter low flows. In some watersheds,
141 surface and groundwater use substantially reduces low flow discharge. The main land use and
142 land cover disturbance throughout most of British Columbia is forest harvesting, which has been
143 observed to both increase and decrease warm-season low flows (Moore et al., 2020). Coble et al.
144 (2020) reviewed 25 small catchment studies in the Pacific Northwest, and found that there tends
145 to be an increase in low flows following harvesting, sometimes followed by low flows similar to
146 pre-harvest conditions, and then low flows below pre-harvest conditions. However, they also
147 reviewed 19 large-catchment studies from around the world and found that long-term reductions
148 in low flows were observed at large scales.

149 With this study we aim to improve the understanding and prediction of low flows in a well-
150 gauged but understudied region, and in so doing develop novel approaches that can be applied in
151 other locales. Our first objective is to quantify the drivers of low flows in diverse hydroclimatic
152 regimes and whether these drivers are changing over time (Section 3.2). This will contribute to
153 the debate about the importance of winter storage, summer ET, and summer precipitation as
154 drivers of low flows. Second, we aim to extend the statistical analysis of drivers to create
155 predictive regression models, enabling the reconstruction of low flows since 1901 (Sections 3.3
156 and 3.4). This modeling strategy will be of interest to the hydrologic modelling community, as it
157 demonstrates a data-driven approach that improves the simulation of low flows by avoiding
158 many of the challenges posed by traditional process-based hydrologic models, while also
159 providing valuable process understanding by attributing low-flow trends to climate drivers. Our
160 final objective is to apply these methods to produce locally-relevant information about low flow
161 trends and drivers for British Columbia. These results will be of interest to a local audience as
162 well as researchers focused on similar hydrologic environments.

163 **2 Data and methods**

164 **2.1 Study Location**

165 British Columbia occupies an area of almost 1 million km² on the western coast of Canada
166 between 48.3° and 60° latitude. The province is endowed with a rich climatic diversity, ranging
167 from Mediterranean climates in the southwest of the province (southern Vancouver Island) to
168 polar climates at high elevations, with cold arid steppe climates in parts of the Interior (Beck et
169 al., 2018). The geography is dominated by mountains, which rise up to 4653 metres above the
170 Pacific.

171 We focus on the part of the province west of the continental divide (approximately 663,000 km²,
172 roughly the size of Myanmar, or 20% larger than metropolitan France). This excludes the

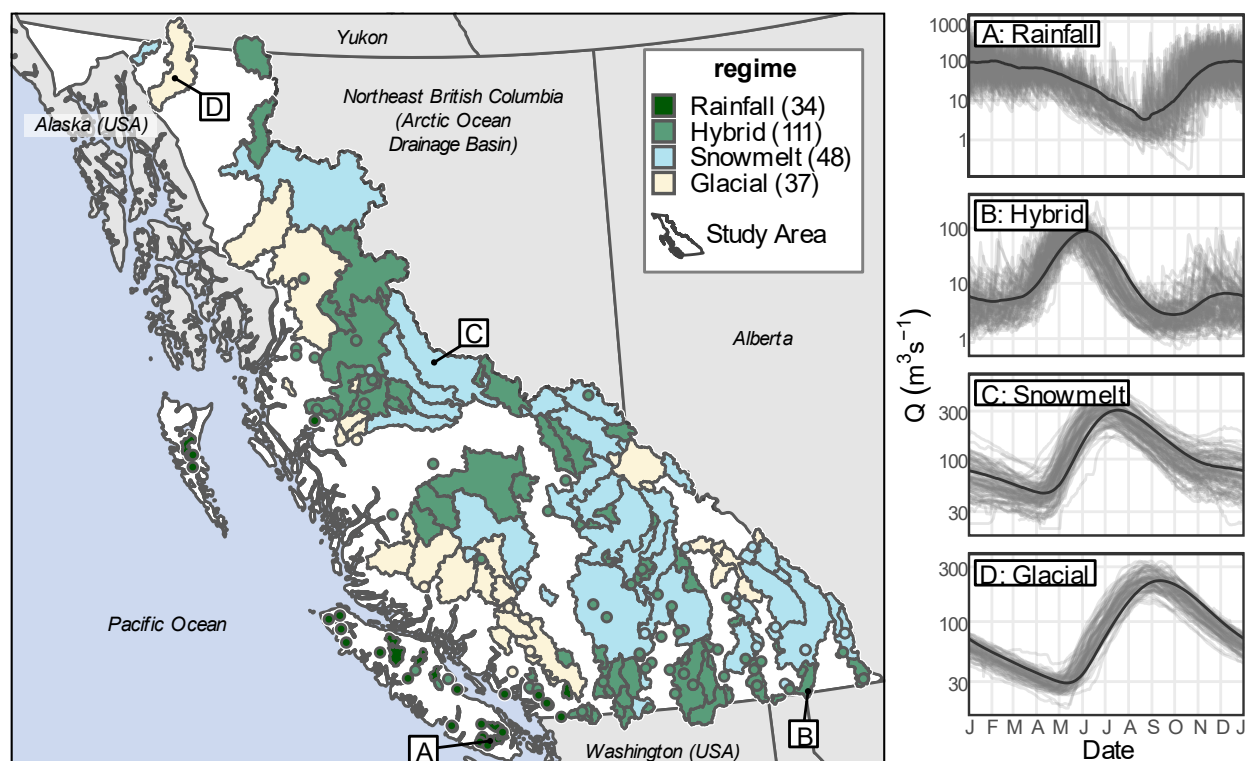
173 northeast of the province, where most precipitation falls in the summer months, leading to high
174 flows in the summer. Also, since one of the chief concerns regarding low flows in British
175 Columbia is the threat to Pacific salmon spawning habitat, it makes sense to focus on the Pacific
176 drainage basin.

177 **2.2 Catchments**

178 We examine records from 230 hydrometric stations in British Columbia, maintained by the Water
179 Survey of Canada. Of the 2235 operational and discontinued stations in British Columbia that
180 measure Pacific-draining streams, 1477 measure unregulated flows. We filter these records for
181 data completeness and recency criteria: at least 20 years of data (from August to October), at
182 least 1 year of continuous year-round operation, and a data record not ending before January 1,
183 2000. 240 stations met the completeness and recency criteria. We then removed 8 intermittent
184 streams, which recorded a zero flow in more than one year, and 2 streams for which urban land
185 use accounted for more than 20% of the catchment area.

186 The average annual hydrographs of these 230 stations were classified as rainfall-dominated,
187 snowmelt-dominated, hybrid, or glacial regimes. Rainfall regimes are those with a single low
188 flow period in late summer, snowmelt regimes are those with a single low flow period in late
189 winter, while hybrid regimes show two distinct low flow periods (Fleming et al., 2007; Wade et
190 al., 2001). The algorithm to identify flow minima is described in Appendix A. Glacial regimes
191 are those where glaciers occupied more than 5% of the catchment area.

192 Figure 1 shows the catchment classification along with example annual hydrographs for each
193 regime. There are 34 rainfall, 111 hybrid, 48 snowmelt, and 37 glacial catchments. We classified
194 the regimes based on all available data for each catchment. However, we note that if we run the
195 classification algorithm separately on 20th and 21st century data, approximately one third of
196 catchments classified as snowmelt-dominated in the 20th century have shifted to the hybrid
197 category in the 21st century (see Appendix A for details).



198
 199 *Figure 1: Regime classification for catchments in our sample. Circles represent catchments of less than 200 km².*
 200 *Example hydrographs are shown for four catchments. A: San Juan River Near Port Renfrew (08HA010), B: Moyie*
 201 *River at Eastport (08NH006), C: Stuart River near Fort St James (08JE001) and D: Atlin River Near Atlin*
 202 *(09AA006). The thick black line in each graph is the 30-day mean flow, averaged across all years. Areas outside of*
 203 *study are shown in grey.*

204 2.3 Definitions

205 We define the warm season as the snow-free season, based on the monthly average snow-water-
 206 equivalent (SWE) for the period 1985-2014, using data from the ERA-5 Reanalysis (Muñoz
 207 Sabater, 2019). We include months with a catchment-average SWE of less than 1 mm. For
 208 catchments with perennial snow or ice cover we defined the warm season as months for which
 209 SWE is within the bottom 10% of the annual range.

210 We define the *low-flow month* based on the timing of the minimum warm-season flow on the
 211 average annual hydrograph of 30-day mean discharge. This minimum is also constrained to
 212 occur after the spring freshet. We define the *low-flow season* as the low-flow month plus the
 213 month before and the month after, if the neighboring months are within the previously defined
 214 warm season.

215 The 7-day flow, Q_7 is the 7-day running mean of discharge. The 7-day low flow, $Q_{7\min}$, is the
 216 minimum value of Q_7 , and can be defined for each month or for the entire low-flow season (the
 217 ‘overall’ low flow).

218 **2.4 Historical Trends**

219 First, we analyze historical trends in low flows. We analyze overall low flows as well as low
 220 flows for July, August, September and October separately. We use Sen’s slope on the log-
 221 transformed values, $\log(Q7_{\min})$, from 1950-2022. Using the logarithm allows the estimated trend
 222 coefficient b to be interpreted as a percentage change per decade:

$$223 \quad \% \Delta_{10} = (\exp(10 \times b) - 1) \times 100\% \quad (1)$$

224 We assess significance at $p < 0.05$ using the modified Mann-Kendall trend test for autocorrelated
 225 data (Hamed & Ramachandra Rao, 1998), implemented in R by Patakamuri and O’Brien (2021).

226 **2.5 Climate and Anthropogenic Drivers**

227 We assess stream sensitivity to the mechanisms discussed in Section 1.2 using several ancillary
 228 datasets. For each catchment, we create a linear regression model with $\log(Q7_{\min})$ as the
 229 dependent variable (Equation 2). All variables are standardized to mean 0 and unit variance.

$$\log(Q7_{\min}) \sim \beta_1 SWE_{max} + \beta_2 BF_{winter} + \beta_3 P_{summer} + \beta_4 T_{summer} + \beta_5 T_7 + \beta_6 Abstraction + \beta_7 ECA_I + \beta_8 ECA_{III} \quad (2)$$

230 β_i are the standardized regression coefficients and the independent variables are defined in
 231 Table 1.

232 Since the objective here is to test a theory, we fit the regression models using forced
 233 simultaneous entry of the predictor variables. We refer to these models as *explanatory*
 234 regressions.

235 The log transformation is used here to increase the influence of the lowest annual low flows and
 236 because $\log(Q7_{\min})$ meets Shapiro-Wilk and Anderson-Darling tests for normality much more
 237 frequently than the untransformed values.

238 Large β coefficients indicate that the mechanism is responsible for a large portion of historical
 239 interannual variability in $\log(Q7_{\min})$. This contrasts with the elasticities reported by Cooper et al.
 240 (2018), which express the % change in y related with % change in x . Low flows are more
 241 variable from year to year in warmer catchments than in colder catchments, so elasticities will
 242 tend to be greater in rainfall-dominated and hybrid catchments. However, we think sensitivities
 243 are better understood in the context of historical variability than in absolute terms, so we prefer
 244 to use the correlation coefficient.

245 There may be nonlinearity in the relationships between low flow discharge and each of the driver
 246 variables. In particular, as temperature increases, there may be thresholds above which no water
 247 is available for evaporation, or when plants close their stomata to regulate transpiration. Since we
 248 are using $\log(Q7_{\min})$, the inherent assumption is that this relationship is loglinear: a unit increase
 249 in temperature will produce a fractional reduction in $Q7_{\min}$, which is consistent with the
 250 expectation that the ratio of actual evapotranspiration to potential evapotranspiration decreases as
 251 water availability decreases.

252 We can statistically test the assumption in two ways. First, we include a squared term in our
 253 regression model, $\beta_9(T_{summer})^2$. If the effect of temperature is less at high temperatures, we
 254 expect that β_9 will be positive.

255 Second, we can substitute space for time and test whether temperature is a weaker driver in
 256 warmer catchments. For each regime, we evaluated the correlation between β_4 (the coefficient of
 257 T_{summer} in equation 2) and the mean summer temperature.

258 *Table 1: Data used to assess sensitivity to climate and anthropogenic drivers*

Driver	Mechanism/ drought type	Variable	Description	Dataset	Dates
Below-normal winter storage	Snowmelt drought	SWE_{max}	Maximum Snow Water Equivalent	ERA5 Land Hourly (Muñoz Sabater, 2019)	1950-present
	Groundwater drought	BF_{winter}	Average baseflow for 30 days prior to SWE_{max}	Eckhardt baseflow separation of discharge time series	Same as discharge
Accelerated summer recession	Rainfall deficit	P_{summer}	Total Precipitation from May to the low-flow month	North American gridded monthly historical climate (~2 km resolution) (MacDonald et al., 2020)	1900-2022
	ET-driven storage depletion	T_{summer}	Average Temperature from May the low-flow month		
Short-term anomalies	ET-driven transmission losses	T_7	7-day mean temperature, concurrent with Q_{7min}	Canadian gridded daily historical climate (~10 km resolution) (Hutchinson et al., 2009)	1949-2020
	Glacier melt drought				
Direct Human Interventions	Water Abstraction	$Abstraction$	Estimated annual water use	Estimated based on water licenses, well construction records, and land use data. See Appendix B.	1863-2023
	Forest Harvesting	ECA_I	Fraction of watershed harvested or burned within 9 years	Calculated from BC Consolidated Cutblocks (Province of BC, 2024b) and Fire Perimeters (Province of BC, 2024a)	1900-2023
		ECA_{III}	Fraction of watershed harvested or burned between 24 and 80 years ago		1900-2023

259

260 We assess below-normal winter snow storage using ERA5-Land reanalysis snow water
261 equivalent (SWE) data (Muñoz Sabater, 2019). Shao et al. (2022) found that these data
262 performed better than other published gridded snow data products, and we also found that this
263 dataset provided a much better match to snow survey data (Vionnet et al., 2021), than a Canadian
264 data product (Environment and Climate Change Canada, 2021). SWE_{max} is the maximum
265 catchment-averaged SWE for each year. We tested an alternative variable definition SWE_{fixed} ,
266 which is the average SWE for the median peak accumulation month.

267 We estimate groundwater drought based on spring baseflow (BF_{winter}). British Columbia's
268 monitoring well network is very sparse (Curran et al., 2023), precluding an analysis based on
269 groundwater levels. We estimate baseflow using an Eckhardt filter, implemented in R in the
270 FlowScreen package (J. Dierauer & Whitfield, 2019). BF_{winter} is the average estimated baseflow
271 for 30 days prior to SWE_{max} . We also test six other baseflow filters, and test using a fixed timing
272 (the same timing as SWE_{fixed}).

273 To estimate the impact of accelerated summer recession, we use the average summer temperature
274 T_{summer} and the total summer precipitation P_{summer} . The summer season is defined as May-August,
275 May-September, or May-October, depending on the low flow month. We use the interpolated,
276 gridded, monthly data produced using the ANUSPLIN algorithm by MacDonald et al. (2020).

277 We investigate ET-driven transmission losses and glacier melt drought using T_7 , 7-day mean
278 temperature for the same 7 days used to calculate $Q7_{min}$. We cannot, unfortunately, separate the
279 drying effects of ET-driven transmission losses from the wetting effects of increased meltflow.
280 However, we may expect that glacial catchments will exhibit more positive (or less negative)
281 streamflow-temperature correlations (Stahl & Moore, 2006). We use the interpolated, gridded,
282 daily data produced using the ANUSPLIN algorithm by Hutchinson et al. (2009).

283 Water abstraction is estimated following the strategy in Barroso and Wainwright (2020). For
284 licensed water use, we converted yearly and daily allocations to m^3/s . Although surface water
285 licensing is thorough in BC, most groundwater use is unlicensed. We spatially joined well
286 construction records to BC Assessment parcels and determined the most likely well use based on
287 the intended well use from the well record (where available) and the property description from
288 the BC Assessment. For most well uses we assigned a representative water use value, but for
289 irrigation wells we estimated water demand based on the size of the property. More details are
290 provided in Appendix B. *Abstraction* is only included for catchments in which the estimated
291 mean annual water use is greater than 10% of the low-flow discharge in any individual year.

292 We include two variables related to forest disturbance: ECA_I and ECA_{III} . These correspond to
293 hydrological periods I and III as described by Coble et al. (2020). Hydrologic period I is
294 expected to be a period of increased low flow discharge, lasting between up to 40 years after the
295 disturbance; the median length in the studies reviewed by Coble *et al.* was 9 years. ECA_I is
296 defined here as the fraction of the catchment with a stand age of 9 years or less. Hydrologic
297 period III is expected to be a period of reduced low flow discharge, beginning some years after
298 the disturbance. The onset of period III has been found to be highly variable, with a median onset
299 timing of 24 years following the disturbance. We defined ECA_{III} as the fraction of the catchment

300 with stand age between 24 and 80 years old. These variables are only included if more than 10%
 301 of the catchment area has ever been logged and if less than 10% of the catchment area is
 302 privately held (where logging records are not public).

303 **2.5.1 Nonlinearity in temperature effects**

304 A common argument is that temperature (or potential evapotranspiration) does not drive droughts
 305 because actual evapotranspiration becomes water limited, not energy-limited as the landscape
 306 dries (Barnett et al., 2005). Thus, we may expect a nonlinear relationship between temperature
 307 and $Q_{7\min}$.

308 Our linear regression models assume that the effect of temperature on $Q_{7\min}$ is loglinear. This
 309 means that a unit increase in temperature will produce a fractional reduction in $Q_{7\min}$, which is
 310 consistent with the expectation that the ratio of actual evapotranspiration to potential
 311 evapotranspiration decreases as water availability decreases. This is a reasonable assumption, but
 312 the real relationship could be either concave up or down on a loglinear plot, and we can
 313 statistically test the assumption in two ways.

314 First, we add a squared term in the linear regressions, $\beta_9(T_{summer})^2$. If the effect of temperatures
 315 is less at high temperatures, we expect that β_9 will be positive. For each regime we use a
 316 binomial test to compare the number of positive coefficients to a binomial distribution with
 317 probability=0.5 as a test for field significance, which is the extent to which the distribution of
 318 results for several catchments differs from a random distribution (Burn and Hag Elnur, 2002). We
 319 also test whether the number of positive or negative significant coefficients exceeds the number
 320 expected by chance, by using binomial test with probability=0.05.

321 Second, we can substitute space for time and test whether temperature is a weaker driver in
 322 warmer catchments. For each regime, we evaluate the correlation between β_4 (the T_{summer}
 323 coefficient) and the mean summer temperature.

324 **2.5.2 Stationarity**

325 The trends that will be shown in Figure 2 are evidence of non-stationary time series, which could
 326 be due to non-stationary drivers and/or non-stationarity in low-flow generating mechanisms. The
 327 latter, which we term ‘mechanistic non-stationarity’ has been variably described as parameter
 328 instability, model non-stationarity, rainfall-runoff non-stationarity, and non-stationarity in
 329 catchment characteristics (Beven, 2016; Niel et al., 2003; Westra et al., 2014). If part of the trend
 330 in low flows is related to mechanistic non-stationarity, then inferences drawn from analysing
 331 historical data will be less useful for making predictions about the future or simulating years
 332 before the calibration period.

333 We can evaluate whether low-flow generating mechanisms have been stationary in the past by
 334 repeating the sensitivity analysis over early and late (recent) time frames. For this analysis we
 335 choose 153 catchments that have at least 20 years of data up to 1997 and at least 20 years from
 336 1998 onwards (this split maximizes the number of catchments meeting the criterion). We fit the
 337 explanatory regression models (Equation 2) to the early (up to 1997) and late (1998 onwards)
 338 datasets.

339 If there is mechanistic non-stationarity, β_{early} and β_{late} will differ. We tested agreement between
340 the two sets of coefficients for each catchment by comparing the test statistic, $\Delta\beta =$
341 $\beta_{late} - \beta_{early}$, to an empirical distribution generated by a Monte Carlo permutation test with
342 10,000 random assignments of the data to the early and late periods. For this analysis we exclude
343 the *Abstraction*, ECA_I , and ECA_{III} variables because a) they are less consistently measured
344 through time, which could lead to erroneous findings of non-stationarity, b) this would also
345 reduce the statistical power to correctly detect non-stationarity in the climate variables, and c)
346 these variables are strongly autocorrelated by construction, which violates the independence
347 assumption necessary for the Monte Carlo permutation test.

348 We assess field significance for this test statistic in with three tests: Test 1 is a binomial test with
349 an expected probability of 0.5 to evaluate if the proportion of catchments with $\Delta\beta > 0$ is more or
350 less than expected. Test 2 is a binomial test with an expected probability of 0.05 to test whether
351 the proportion of catchments with individually significant positive differences is greater than
352 expected. Test 3 is the same as Test 2 but for negative significant differences. Each binomial test
353 is applied 20 times (4 regimes and 5 variables), so we assess significance using the Holm-
354 Bonferroni method to control the family-wise error rate (Holm, 1979).

355 **2.6 Predictive Regression Models**

356 We build on the analysis of low flow drivers to create ordinary least squares regression models
357 that predict the yearly minimum flow, $Q7_{min}$.

358 Despite its simplicity, regression is an appropriate model to simulate summer low flows. In the
359 20th century multiple regression models were often used for streamflow simulation and
360 forecasting (eg. US Soil Conservation Service, 1972; Cayan et al., 1993; Garen, 1992; Vogel et
361 al, 1999). Process-based computer models, though first proposed in the 1960's (Freeze and
362 Harlan, 1969), became more popular in the late 1990s and 2000s with improvements in computer
363 technology (McMahon, 1992; Todini, 2007). More recently, data-driven approaches have made a
364 comeback in the form of machine learning models, with some authors showing that data-driven
365 approaches can outperform process-based models in a wide variety of settings (Kim et al, 2021;
366 Arsenault et al, 2023). Regression is a simple form of machine learning, and its use is thus
367 neither particularly new nor out of step with current practices.

368 We ruled out more complex machine learning models because of limitations in the size of the
369 dataset. We have chosen to predict only the minimum yearly summer/fall low flow, in contrast to
370 many previous low-flow and hydrologic drought studies that analyse flow percentiles or spell
371 durations. The minimum flow has relevance for fish survival, passage, and spawning, has
372 regulatory implications for British Columbia, and is also commonly the portion of the
373 hydrograph that is most poorly predicted by process-based hydrologic models. By abandoning
374 the requirement to simulate all parts of the annual hydrograph, we can more accurately represent
375 the flow-generating mechanisms that are most relevant to low flows. However, we also reduce
376 the size of our calibration data to one observation per year, so a high-order machine learning
377 model would likely be overfit. Regression works well with small datasets and produces models

378 that are straightforward to interpret, whose properties have been studied over more than a
 379 century.

380 **2.6.1 Model Selection**

381 For each catchment we produce one regression model to predict $\log(Q7_{\min})$ for each of the three
 382 months comprising the low-flow season.

383 For each catchment-month combination, we construct the best model using 5-fold cross-
 384 validation, which is repeated 10 times with random partitions of the data into folds. We evaluate
 385 the models using the Kling-Gupta Efficiency (KGE), evaluated jointly on the predicted $Q7_{\min}$ of
 386 the five folds. Due to the known problems with using the KGE on log-transformed flow values
 387 (Santos et al., 2018), we use the square root of $Q7_{\min}$.

388 We start with 15 physically plausible variables and train models for all subsets of variables ($2^{15} =$
 389 32,768 models). The model with the highest average KGE for each catchment-month is selected.
 390 We then evaluate the models using 10 new random partitions of the data into folds.

391 The 15 candidate variables are chosen to represent climate variables and water abstraction
 392 (Equation 3). We only use precipitation (P) and temperature (T) as predictor variables because
 393 they are uniformly available in the historical climate data from 1900-2022. We chose to include
 394 mean T and total P variables over seven averaging times (1, 2, 3, 4, 6, 8, and 12 months prior to
 395 the month being predicted). This allows the cross-validation routine to select the most
 396 appropriate lag times, or combinations thereof, for each catchment. Using overlapping averaging
 397 times ensures that the model will include more recent months, which prevents the construction of
 398 physically implausible models.

399 For month k the full model with all 15 variables is:

$$\begin{aligned} \log(Q7_{\min})_k \sim & b_1 T_{[k-11,k]} + b_2 T_{[k-7,k]} + b_3 T_{[k-5,k]} + b_4 T_{[k-3,k]} + b_5 T_{[k-2,k]} + b_6 T_{[k-1,k]} \quad (3) \\ & + b_7 T_{[k]} + b_8 P_{[k-11,k]} + b_9 P_{[k-7,k]} + b_{10} P_{[k-5,k]} + b_{11} P_{[k-3,k]} \\ & + b_{12} P_{[k-2,k]} + b_{13} P_{[k-1,k]} + b_{14} P_{[k]} + Abstraction \end{aligned}$$

400 b_i are the regression coefficients and the subscripts $[k - m, k]$ indicates the period ending on
 401 month k and beginning m months before. For each year, the predicted minimum summer low
 402 flow is the lowest prediction of the three months comprising the low-flow season.

403 We can compare the model fits to published models for some of the catchments. The Pacific
 404 Climate Impacts Consortium (2020) has created distributed, physically-based hydrologic models
 405 for 56 of the 230 catchments studied here, using a Variable Infiltration Capacity model with a
 406 glacier model (VIC-GL). These 56 models include 21 hybrid, 26 snowmelt, and 9 glacial
 407 regimes. No rainfall-dominated catchments are included. To enable comparison of low-flow
 408 predictions between the VIC-GL models and the regression models developed in this study, we
 409 fit the regression models to the same time period (1945-2012) using the same gridded
 410 meteorological data (Werner et al., 2019). Only the final calibrated model data are available for
 411 the VIC-GL models, so we compare the performance to our final regression models, trained and
 412 evaluated on the all years of data. These performance statistics are referred to as ‘in-sample’
 413 statistics, in contrast to the ‘out of sample’ statistics derived from cross-validation.

414 We evaluate our models for residual autocorrelation and stationarity. We used the Breusch-
 415 Godfrey test for lag-1 autocorrelation (Breusch, 1978; Godfrey, 1978), and evaluated the critical
 416 value of the test statistic using Monte Carlo randomization of the lagged residuals with 10,000
 417 draws. We evaluated residual stationarity by subjecting the residuals to the same trend analysis as
 418 described in Section 2.4. We applied the same binomial tests for field significance as described in
 419 Section 2.5.1.

420 **2.7 Environmental Flow Thresholds**

421 We compare the predicted low flows with two flow thresholds. The BC government has the
 422 authority to set a Critical Environmental Flow Threshold (CEFT) for any stream, which is
 423 defined as the discharge “below which significant or irreversible harm to the stream's aquatic
 424 ecosystem is likely to occur” (Water Sustainability Act, 2016). The presumptive CEFT is often
 425 set using a modified Tennant method, at 5% of the long-term mean annual discharge (McCleary
 426 & Ptolemy, 2017). However, for rainfall-dominated catchments, flows are frequently less than
 427 5% long-term mean annual discharge. As such, the interim CEFT for the Xwulqw’selu
 428 (Koksilah) Watershed (a typical rainfall-dominated catchment) was set close to 2% long-term
 429 mean annual discharge. We follow this strategy and set the presumptive CEFT at 2% long-term
 430 mean annual discharge for rainfall regimes and 5% for other catchments.

431 British Columbia has a separate drought classification framework, which is based on flow
 432 percentiles calculated for each day of the year. The most severe drought level (5) corresponds to
 433 flows below the 2nd percentile (a 1-in-50-year event), while level 4 corresponds to flows below
 434 the 5th percentile, and Level 3 to the 10th percentile. At level 5 “adverse impacts to socio-
 435 economic or ecosystem values are almost certain”, regulatory action to limit water use is “highly
 436 likely”, and the province prepares for “emergency response where risk of failure or loss of
 437 [water] supply exists” (BC Ministry of Water, Land and Resource Stewardship, 2023). The North
 438 American Drought Monitor classifies events below the 10th, 5th and 2nd percentiles as “Severe”,
 439 “Extreme”, and “Exceptional” droughts.

440 We calculate the 10th, 5th, and 2nd percentiles of $Q_{7\min}$, based on available data from 1950 to
 441 present. Compared to British Columbia’s drought monitoring this is somewhat conservative (less
 442 likely to classify events as drought), since the province calculates percentiles for each day of the
 443 year.

444 **2.8 Historical Reconstruction**

445 We reconstruct low flows from 1901 to 2022 using the optimized regression models (Section 2.6)
 446 and the historical monthly temperature and precipitation data. We compare the simulated low
 447 flows to the thresholds described in Section 2.7.

448 We also assess what has driven decadal changes in low flows over the last century. To answer
 449 this question, we estimate the yearly anomaly in $Q_{7\min}$ for each catchment, relative to the average
 450 simulated $Q_{7\min}$ for the 20th century (1901-1999, in the absence of any effect of water
 451 abstraction. This ‘total anomaly’ is composed of anomalies driven by winter and summer
 452 temperature and precipitation, as well as water abstraction.

453 We estimate the $Q_{7\min}$ anomalies and their components using the regression model for the low-
454 flow month for each catchment. First, we find the temperature and precipitation anomaly for
455 each month, year, and catchment. We construct the predictor matrix for each regression model
456 using these anomalies, considering temperature and precipitation separately and winter
457 (November-April) and Summer (May – October) separately and setting all other values to 0. We
458 run these predictor matrices through each regression model; the predicted values, minus the
459 model intercept, are the anomalies in $\log(Q_{7\min})$ associated with each driver.

460 **3 Results**

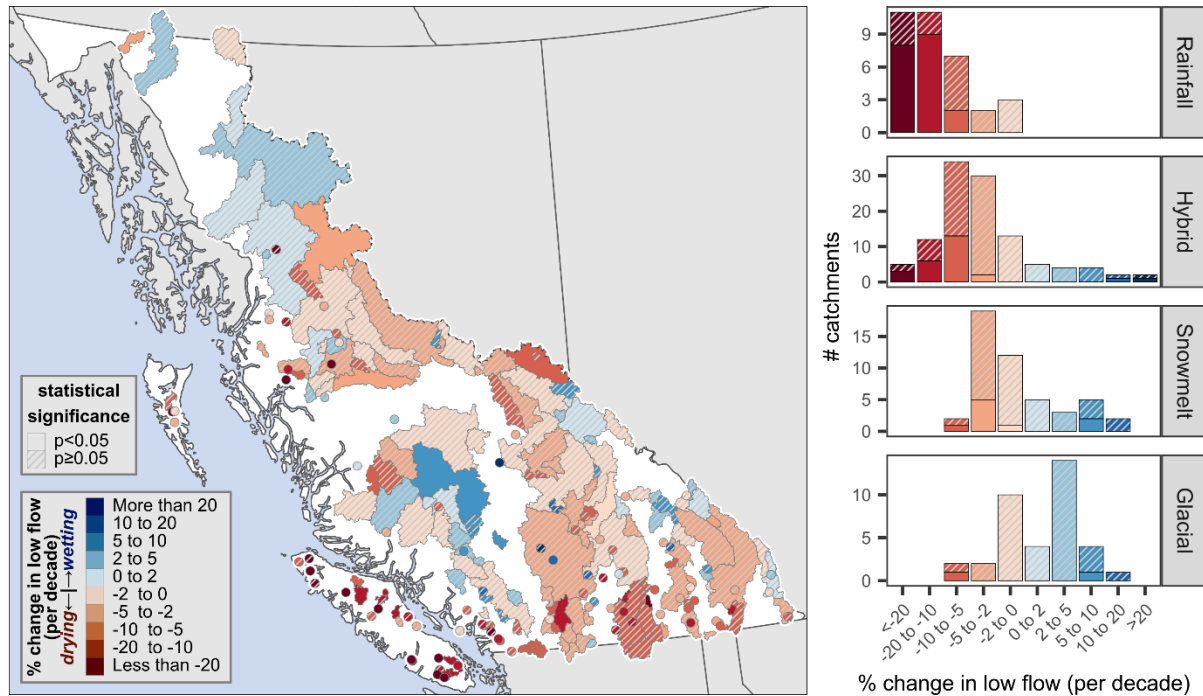
461 **3.1 Dissecting past trends in low flows**

462 Figure 2 shows the trends in summer to fall low flows, from 1950 to 2022. Overall low flows
463 have decreased in 174 of 230 (76%) watersheds. There has been a significant ($p < .05$) decrease in
464 51 watersheds, and only five watersheds have seen a significant increase.

465 Rainfall and hybrid regimes have seen strong drying trends. Low flows in 33 of 34 rainfall-
466 dominated catchments have decreased, with 19 statistically significant trends. 94 of 111 hybrid
467 catchments have seen declines, with 24 significant drying trends. Two hybrid catchments have
468 seen statistically significant increases in low flows; these are small ($< 100 \text{ km}^2$) catchments
469 located beside the largest and second-largest open-pit copper mines in Canada. Although a
470 detailed investigation of these sites is beyond the scope of this study, we hypothesize that
471 historical mining operations (water use and/or mine dewatering) have induced a non-natural
472 streamflow response.

473 Snowfall and glacial regimes show weaker evidence of regional trends. 33 of 48 snowfall-
474 dominated catchments show drying trends, with seven significant drying trends and two
475 significant wetting trends. Over half of glacial catchments (23 of 37) have seen increases in
476 summer low flows, with only one significant increase and one significant decrease.

477 July, August, September, and October trends are shown individually in the Appendix C. Drying
478 trends are strongest in August (210/230 drying, 104 significantly), and weakest in October
479 (121/228 drying, 21 significantly). Glacial regimes have seen more increases than decreases in
480 September and October but across the three other regimes drying trends are more common in all
481 months.



482

483 *Figure 2: Trends for the overall (August – October) low flow in the 230 study catchments, using available data from*
 484 *1950 to present. Hatched polygons denote non-significant trends. Red denotes drying trends and blue denotes*
 485 *wetting trends. 174 of 230 catchments are drying, and 51 of these decreases are statistically significant. Rainfall-*
 486 *dominated and hybrid catchments are drying much more than snowmelt-dominated and glacial catchments. Only*
 487 *five catchments show statistically significant increases (wetting trends).*

488 3.2 Examining sensitivity to key climate variables

489 Figure 3 shows the standardized regression coefficients for regression models with each the
 490 variables listed in Table 1. Figure D1 shows bivariate (Pearson) correlation coefficients for each
 491 of the variables for comparison.

492 Below-normal winter storage has historically had a minor influence on summer low flows. For
 493 winter snow storage, the median coefficient is less than 0.2 across all regimes, with one third
 494 being significant. We found no meaningful differences in the strength of the correlations when
 495 using a fixed timing for the SWE variable (Figure D2) The bivariate correlation coefficients
 496 (Figure D1) were only slightly larger than the standardized coefficients in Figure 3 (median of
 497 0.245 with 42% being significant).

498 Winter snow accumulation also does not necessarily prevent severe low flows. Across the 230
 499 catchments, 35% of the catchment-years in the bottom decile (10th percentile) of $Q7_{min}$ had
 500 above-median winter snow accumulation; 212 of 230 catchments had at least one year with
 501 above-median snow accumulation and $Q7_{min}$ in the bottom decile, and 52 catchments had at least
 502 one year with exceptionally high snow accumulation (top decile) that nevertheless had $Q7_{min}$ in
 503 the bottom decile, including 5 rainfall-dominated, 25 hybrid, 14 snowfall-dominated, and 8
 504 glacial catchments.

505 Correlations with end-of winter baseflow (BF_{winter}) are small in all hydroclimatic regimes. The
 506 median coefficient is 0.07. Only 11% are significant and positive, which is slightly more than the

507 5% that would be expected by chance. The bivariate correlation coefficients (Figure C1) were
 508 similar to the standardized coefficients in Figure 3 (median of 0.11 with 14% being significant).
 509 We tested six other baseflow filtering algorithms (Figure D3). Although the baseflow time series
 510 were considerably different, we did not find meaningful differences in the correlations with
 511 $\log(Q7_{\min})$. We also tried holding the timing constant and calculating the average baseflow over
 512 the same month for each year (the median peak SWE accumulation month) and found even
 513 weaker correlations.

514 As another robustness check on our conclusions about the importance of winter storage, we tried
 515 including winter (November to April) T and P in place of SWE_{\max} and BF_{winter} (Figure D4).
 516 The coefficients of T_{winter} and P_{winter} were similar in magnitude to the correlations with
 517 SWE_{\max} , indicating that these variables serve as reasonable proxies for snow accumulation.

518 Summer precipitation, P_{summer} , shows large positive correlations for most catchments across all
 519 regimes (median of 0.48), and 80% of these correlations are statistically significant. Summer
 520 temperature, T_{summer} , shows negative coefficients for most rainfall-dominated and hybrid
 521 catchments, with median coefficients of -0.28 and -0.21, and 41% and 35% significant,
 522 respectively. In snowmelt-dominated catchments the median coefficient for T_{summer} is close to
 523 zero and in glacial catchments it is positive.

524 We note that bivariate correlation coefficients (Figure D1) for T_{summer} are considerably more
 525 negative than the coefficient from the multiple linear regression. For rainfall-dominated and
 526 hybrid catchments, the median bivariate correlations for T_{summer} are about -0.55 and -0.49,
 527 respectively, which are approximately equal and opposite to the correlations for P_{summer} . The
 528 discrepancy between the bivariate correlations and the coefficients of the multiple linear
 529 regression occurs because T_{summer} tends to be correlated with many of the other predictor
 530 variables, especially P_{summer} , T_7 , Abstraction, ECA_I and ECA_{III} .

531 There are both positive and negative coefficients with T_7 , but most of these relationships are
 532 weak. The coefficients are more likely to be negative in rainfall and hybrid catchments, which is
 533 similar to the pattern for T_{summer} .

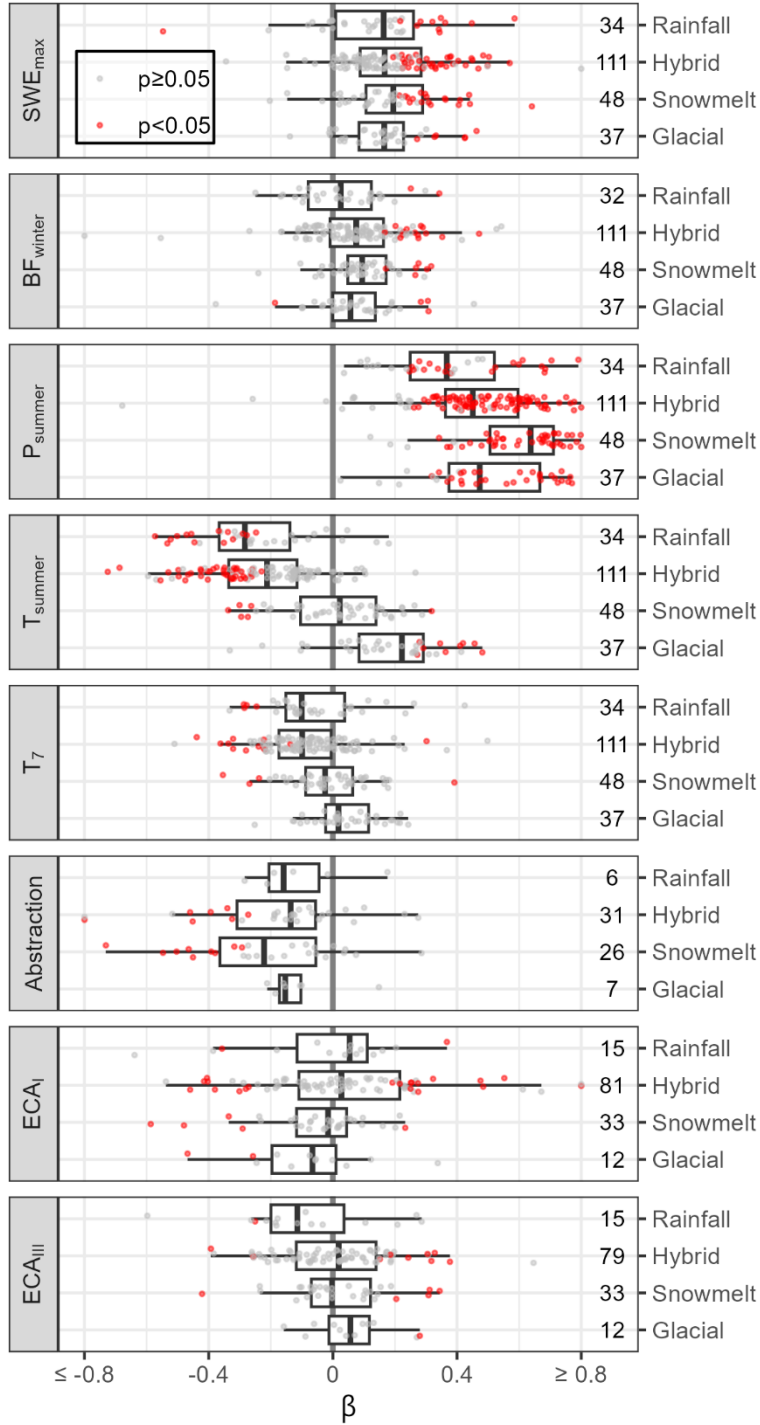
534 Abstraction tends to reduce low flows, as expected. However, the magnitude of the effect varies
 535 widely, probably because the magnitude of water use varies. Most catchments in our sample had
 536 very little water use.

537 The two forest harvesting variables, ECA_I and ECA_{III} , do not show the expected behaviour of
 538 low flow increases in period I and decreases in period III. Both positive and negative coefficients
 539 are common for ECA_I and ECA_{III} and the median is near zero in all regimes.

540 We also performed a more detailed analysis of the effect of forest disturbances on low flows
 541 (Appendix E), using four different Equivalent Clearcut Area functions and the pre-whitening
 542 strategy applied by Zhang and Wei (2012) and various other authors. This analysis also showed
 543 mixed and mostly non-significant results for most regimes. We found that pre-whitening resulted
 544 in extremely low statistical power to detect even relatively large effects, so we also conducted an
 545 analysis without pre-whitening. There was moderately strong evidence that forest disturbance

546 lowers low flows in snowmelt-dominated catchments, but we were unable to detect effects in the
547 three other regimes.

548 We note that the standardized regression coefficients, β , measure the effect of each explanatory
549 variable as a fraction of the standard deviation of $\log(Q7_{\min})$. However, this variance tends to be
550 smaller in cold catchments: the average coefficient of variation of $Q7_{\min}$ is 0.54 in rainfall
551 regimes, 0.46 in hybrid regimes, and 0.30 in snowmelt and glacial regimes. This means that, all
552 else being equal, the same β indicates a greater effect on the magnitude of the low flow in
553 rainfall-dominated catchments than in colder catchments.



554
 555 *Figure 3: Standardized regression coefficients for log-transformed summer low flows with 8 explanatory variables.*
 556 *Analogous graphs with bivariate Pearson correlation coefficients are shown in Figure D1. The numbers indicate the*
 557 *number of catchments.*

558 3.2.1 Nonlinearity of temperature effects

559 The first test for non-linearity in the effect of temperature was to include $(T_{summer})^2$ in our
 560 explanatory regression models. The coefficient for $(T_{summer})^2$ is positive 59%, 78%, 67%, and

561 68% of rainfall, hybrid, snowmelt, and glacial catchments; these rates are field-significant
562 (greater than would be expected by chance) for hybrid, snowmelt, and glacial catchments and not
563 significant for rainfall-dominated catchments. The rate of positive *significant* coefficients is was
564 not significant for any regime. These results suggest that the effect of temperature on $\log(Q7_{\min})$
565 may be slightly nonlinear, and that the effect of temperature diminishes off at high temperatures
566 for all but rainfall-dominated catchments.

567 The second test for nonlinearity was to examine whether the effect of temperature was weaker in
568 warmer catchments. We found the opposite: for all regimes, the coefficient for T_{summer} was
569 larger (more negative) in warmer catchments, and this relationship was statistically significant
570 for all but the rainfall regime.

571 **3.2.2 Testing stationarity**

572 We did not find evidence of significant non-stationarity in most of the correlations. Tests 2 and 3
573 (the number of positive and negative significant correlations) were non-significant for all
574 variables and regimes, even before applying the Holm-Bonferroni method.

575 Test 1 was significant for T_{summer} in hybrid and snowmelt-dominated regimes (for most
576 catchments the coefficients were less negative in the late period), indicating that the influence of
577 summer temperature may be decreasing. However, the influence of T_7 appears to be increasing in
578 snowmelt-dominated regimes (most catchments had more negative coefficients in the later
579 period). Test 1 was also significant for SWE_{max} in hybrid and snowmelt-dominated regimes,
580 indicating that the influence of winter snow accumulation may be decreasing. P_{summer} and BF_{winter}
581 did not show evidence of non-stationarity in this analysis.

582 We tested the robustness of our analysis by using univariate regressions for each predictor
583 variable, and by splitting the data at years 1995, 1996, and 1998. All results are included in
584 Appendix D.

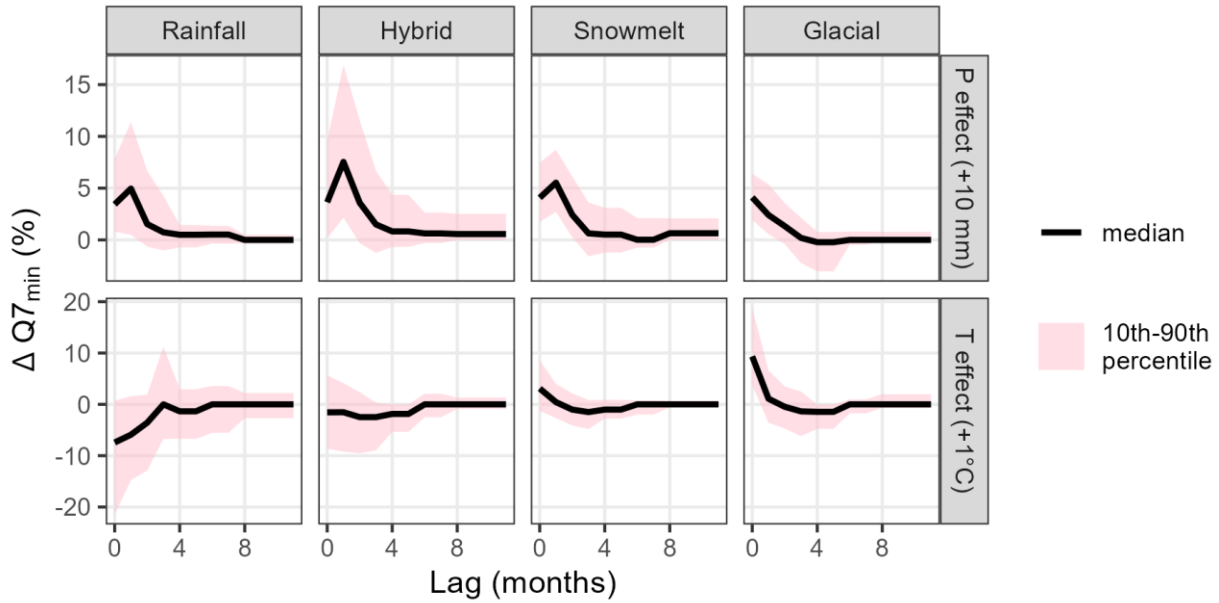
585 **3.3: Parsimonious predictive regression models**

586 Figure 4 shows the modelled response (change in low flow as a percentage) to temperature and
587 precipitation anomalies, based on the predictive regression models (Section 2.6). The x-axis
588 indicates the lag time between the anomaly and the low-flow month. The top row shows the
589 response to 10 mm of additional precipitation, and the bottom row shows the response to a 1°C
590 increase in temperature over a single month.

591 All regimes show increases in $Q7_{\min}$ related to precipitation events over a period of about 4
592 months. The lag-0 effect is smaller for some catchments because low-flow events can occur early
593 in the month, before large precipitation events. Some hybrid and snowmelt-dominated
594 catchments have longer lag times (up to 11 months) which is probably related to winter snow
595 accumulation that persists into the summer.

596 The response to temperature for the low-flow month (lag 0) is strongly negative in rainfall
597 regimes and variable in hybrid regimes. For snowmelt and glacial regimes, increased temperature
598 leads to higher flows over the short term (up to a lag of 1 month) probably because of increased
599 meltflow, but lower flows over the longer term (3-6 months) because of storage depletion. The

600 short term increase could also be partly related to catchments where low-flow month
 601 precipitation falls as snow in particularly cold years.



602
 603 *Figure 4: The modelled response to precipitation and temperature anomalies occurring 0 to 11 months before the*
 604 *month for which the low flow is predicted. The top row shows responses to 10 mm of additional precipitation and the*
 605 *bottom row shows responses to a 1°C increase in temperature over a single month.*

606 Table 2 shows the KGE, NSE, and R^2 statistics for the predictive regression models, derived
 607 from 10 repeated 5-fold cross-validations. The median KGE for the overall low-flow prediction
 608 is 0.64, with a range from 0.18 to 0.92. All the models perform significantly better than the
 609 benchmark KGE of -0.41 (Knoben et al., 2019). Three models have negative NSEs.

610 Based on the R^2 values, the models explain between 6% and 86% of the historical variance, with
 611 a median of 51%. The residual error may be due to unobserved variables (eg. land use change)
 612 and measurement errors in streamflow, climate, and water use variables. Some of the error can
 613 also be attributed to variability in the timing of precipitation events during the month of interest.

614 *Table 2: Median goodness of fit statistics for best regression models selected for the 230 catchments. Minimum and*
 615 *maximum values are provided in brackets.*

	Rainfall	Hybrid	Snowfall	Glacial
N	34	111	48	37
KGE(Q7_{min}^{1/2})	0.67 (0.28, 0.87)	0.71 (0.19, 0.91)	0.64 (0.14, 0.85)	0.57 (0.26, 0.77)
NSE(log(Q7_{min}))	0.47 (-0.09, 0.68)	0.52 (-0.29, 0.82)	0.45 (-0.1, 0.76)	0.35 (-0.07, 0.63)
R²(Q7_{min})	0.52 (0.16, 0.78)	0.57 (0.06, 0.86)	0.48 (0.07, 0.78)	0.41 (0.13, 0.71)
PBIAS(Q7_{min})	-3.21 (-24.58, 3.78)	-0.59 (-18.16, 6.38)	-0.66 (-4.83, 2.32)	-0.52 (-5.17, 6.51)

616
 617 In terms of predicting the overall summer low flow, the regression models presented here
 618 generally outperform the VIC-GL models (Pacific Climate Impacts Consortium, 2020).
 619 KGE(Q7_{min}) and NSE(Q7_{min}) for the regression models are better in 95% and 98% of the

620 catchments, respectively. Evaluated on transformed flow values, $KGE(Q7_{min}^{1/2})$ and
 621 $NSE(\log(Q7_{min}))$ are better in 89% and 98% of the catchments. Table 3 shows the median and
 622 range of NSE and KGE for the regression and VIC-GL models. Strikingly, $NSE(\log(Q7_{min}))$ is
 623 negative for 40 of 56 of the VIC-GL models but none of the regression models.

624 *Table 3: Median Nash-Sutcliffe and Kling-Gupta Efficiencies for regression and VIC-GL models. Minimum and*
 625 *maximum statistics are provided in brackets.*

	Regression	VIC-GL	Regression outperforms VIC-GL
KGE(Q7_{min})	0.78 (0.37, 0.93)	0.43 (-1.71, 0.86)	53/56 catchments
KGE(Q7_{min}^{1/2})	0.78 (0.41, 0.92)	0.46 (-0.48, 0.88)	50/56 catchments
NSE(Q7_{min})	0.69 (0.25, 0.88)	-0.22 (-70.6, 0.75)	55/56 catchments
NSE(log(Q7_{min}))	0.68 (0.33, 0.85)	-0.56 (-44.74, 0.7)	55/56 catchments
PBIAS(Q7_{min})	-0.4 (-9.8, 4.4)	-11.5 (-88, 129.1)	52/56 catchments

626

627 We also evaluated 27 common goodness-of-fit statistics included in the hydroGOF R package
 628 (Zambrano-Bigiarini, 2024) under square-root, log, and identity transformations (81 statistics
 629 total). The regression models outperformed the VIC-GL models for every one of these statistics;
 630 on average for the 81 statistics, the regression models outperformed VIC-GL in 53 of 56
 631 catchments.

632 The efficiency statistics in Table 3 are evaluated using in-sample statistics to ensure a like-with-
 633 like comparison. However, the regression models outperform the VIC-GL models even if we
 634 give the regressions an artificial disadvantage by using their cross-validated efficiency statistics
 635 (Table 2). The cross-validated regression $KGE(Q^{1/2})$ scores are better than the in-sample scores
 636 for the VIC-GL in 43 of 56 (77%) catchments, and the cross-validated Regression $NSE(\log(Q))$
 637 are better than the in-sample VIC-GL scores of 54 of 56 (96%) catchments.

638 The VIC-GL models are not poorly calibrated overall. When calculated on daily flows for the
 639 entire time series, the median $NSE(\log(Q))$ and $KGE(Q^{1/2})$ for these models are 0.76 and 0.84.
 640 Only one VIC-GL model has a negative $KGE(Q^{1/2})$, and only five have a negative $NSE(\log(Q))$.
 641 However, the models clearly perform poorly for low-flow prediction. The VIC-GL models were
 642 not calibrated with the sole purpose of predicting low flows, so general conclusions about the
 643 relative suitability of regression vs process-based models for predicting low flows may not be
 644 appropriate. It is possible that process-based models calibrated to optimize low-flow prediction
 645 could outperform the regression models presented here, but a rigorous benchmarking of different
 646 models and calibration techniques is out of the scope of the current work.

647 We found little evidence of residual autocorrelation. Overall, the Breusch-Godfrey test was
 648 significant for 8% of the catchments. Snowmelt-dominated regimes were most likely to be
 649 autocorrelated (10%), followed by hybrid catchments (9%), rainfall-dominated catchments (6%)
 650 and glacial catchments (3%). Based on binomial tests, these rates of significant results are not
 651 field-significant (not greater than expected by chance), which indicates that ignoring interannual
 652 catchment storage in the models is a reasonable choice.

653 We also found little evidence of non-stationarity in the model residuals. We found individually
654 significant trends in 13% of the catchments (9% of rainfall catchments, 14% of hybrid
655 catchments, 10% of snowmelt catchments and 16% of glacial catchments). Approximately half
656 (49%) of all catchments had positive trends in the residuals. Based on binomial tests, none of the
657 regimes had an abnormal number of positive/negative trends nor an abnormal number of
658 significant positive/negative trends.

659 **3.4: Hindcasted low-flow conditions**

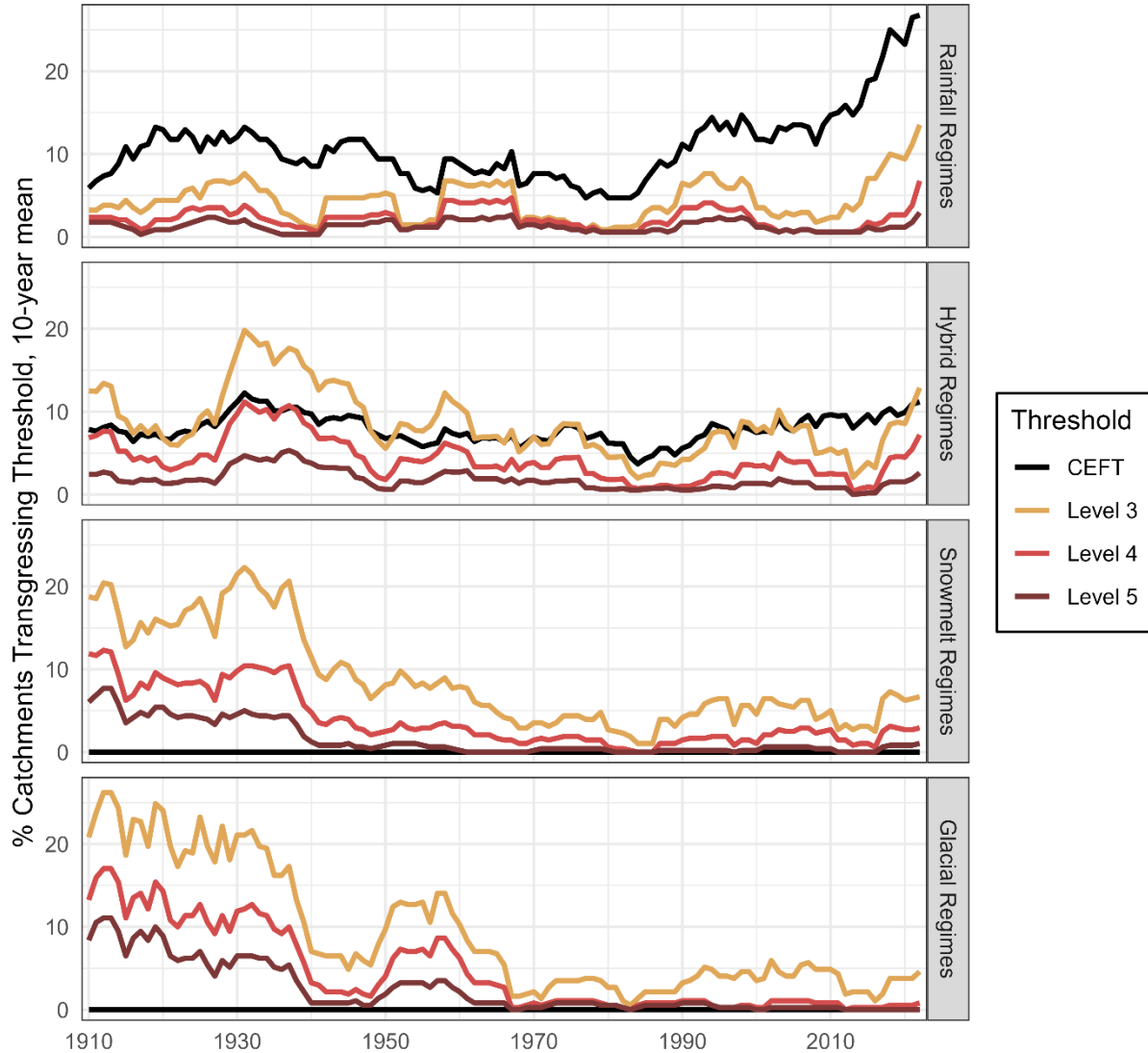
660 We use the regression models to simulate past low flows from 1901-2022 and compare low flows
661 to the Critical Environmental Flow Threshold (CEFT) and drought thresholds. Figure 5 shows
662 the percentage of catchments within each regime that transgress these thresholds smoothed using
663 a running mean of 10 years.

664 Rainfall-dominated catchments are, in general, more likely to transgress the CEFT than hybrid
665 catchments, even though the CEFT for these catchments is set at 2% of long-term mean annual
666 discharge for rainfall-dominated catchments and 5% for hybrid catchments. This is because low
667 flows in these catchments are more variable from year to year than low flows in colder
668 catchments, as was noted in Section 3.2. This larger envelope of variability means that low flows
669 transgress the CEFT more frequently.

670 Warm-season low flows in snowmelt-dominated and glacial catchments almost never fall below
671 the CEFT because these catchments tend to see their lowest flows in the winter months.
672 However, drought thresholds were defined on a seasonal basis, and these catchments do
673 experience warm-season droughts.

674 Drought and CEFT transgressions in rainfall-dominated catchments have risen erratically but
675 persistently since the 1980s. There has also been a recent increase in transgressions for hybrid
676 regimes over the same period, although it has been less dramatic than the trend in rainfall
677 regimes. These simulated trends are consistent with the declining trends in measured $Q_{7\min}$
678 observed in Figure 2.

679 Another remarkable detail in Figure 5 is that, for hybrid, snowmelt, and glacial regimes, drought
680 was more common 100 years ago than it is currently. Although Critical Environmental Flow
681 Threshold transgressions are rising in hybrid regimes, they are currently no more common than
682 they were throughout the warm and dry 1920's and 1930's.



683

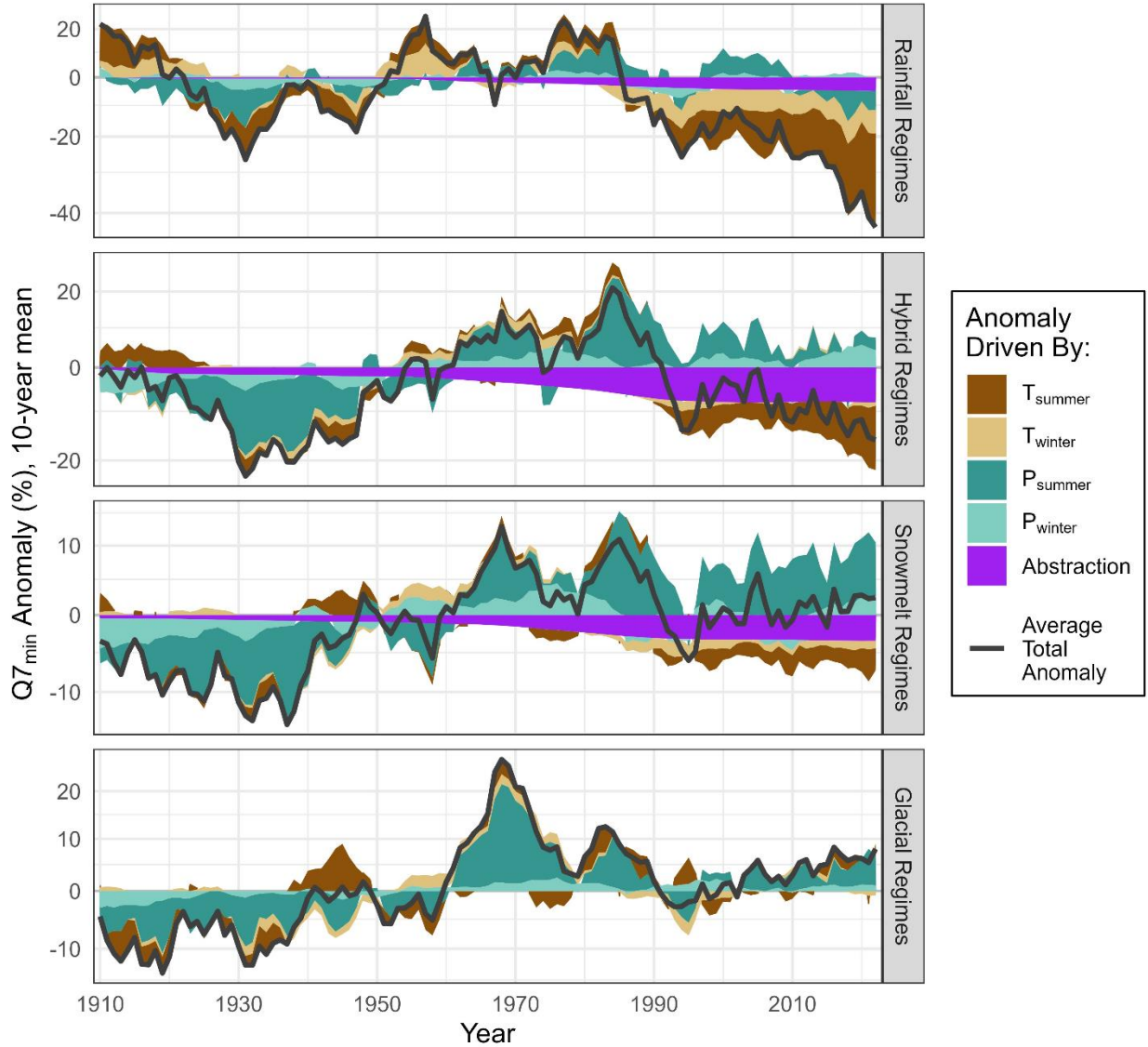
684 *Figure 5: The simulated percentage of catchments transgressing the Critical Environmental Flow Threshold (CEFT)*
 685 *as well as Drought Levels 3, 4, and 5. A 10-year rolling mean (beginning in 1900) is used to smooth the data.*

686 Figure 6 shows the total anomaly in $Q7_{min}$ (black line) and the components of this anomaly that
 687 can be attributed to winter and summer temperature and precipitation. Low flows in the early
 688 20th century were considerably below-average in hybrid, snowmelt, and glacial regimes, and this
 689 was mostly related to a long-term precipitation deficit. Variability in precipitation drove most of
 690 the overall low-flow variability throughout the 20th century.

691 In recent years temperature has begun to play a much larger role. Since 1990, warm summer
 692 temperatures have been substantial enough to counteract above-average precipitation in rainfall-
 693 dominated and hybrid regimes, leading to negative total anomalies. The anomaly associated with
 694 temperature has grown since 1990.

695 Increasing water abstraction began in earnest around 1950 and the effect on low flows has grown
 696 ever since. On average, in 2022 abstraction is estimated to have reduced flows by 5%, 8%, and

697 3% in rainfall, hybrid, and snowmelt-dominated catchments. Note that this is an average across
 698 all studied catchments, many of which have little or no water use; the effect on some catchments
 699 is much larger.



700

701 *Figure 6: The average total anomaly in $Q7_{min}$ (relative to the period 1950-2022, with no water abstraction) is shown*
 702 *as a black for each catchment. The total anomaly is composed of anomalies driven by winter and summer*
 703 *temperature and precipitation, as well as abstraction. The y-axis is log-scaled so the width of the coloured ribbons*
 704 *can be directly compared.*

705 **4 Discussion**

706 With regard to our first objective, we found that low flows in rainfall-dominated catchments are
 707 currently lower than at any point during the 20th century, and there are strong drying trends over
 708 the last few decades. There are similar drying trends in hybrid catchments, but drought was about

709 as common during the 1920's and 1930's as it is now. We did not find strong trends in snowmelt
710 or glacial catchments since 1950, but our hindcasts indicate that low flows in the early 20th
711 century were probably substantially lower than they are now.

712 Our second objective was to analyse the drivers of low flows, with particular attention to the
713 debate surrounding the impact of changing winter snow accumulation (Barnett et al., 2005) and
714 recent work indicating that the impact of evapotranspiration and summer temperature may be
715 increasing (Boeing et al., 2024; Brunner et al., 2021).

716 We found low flows have not been very sensitive to winter storage of snow and groundwater. In
717 section 3.2 we found small correlations between winter maximum snow water equivalent and
718 near-zero correlations with end-of-winter baseflow. We also found some evidence that the effect
719 of snowpack has been non-stationary (the correlations have shrunk in recent years) in hybrid and
720 snowmelt-dominated catchments. Low flows below the 10th percentile occur regularly in years
721 with above-average snowpack and have even been observed in years with snowpack above the
722 90th percentile. In Section 3.4 we found that winter precipitation and temperature anomalies have
723 not contributed substantially to decadal variability in $Q_{7\min}$. These findings are consistent with
724 some past sensitivity analyses, including Cooper et al. (2018) who found low sensitivities to
725 snow in the northwestern United States, and Floriancic et al. (2020) who found similar results in
726 Switzerland.

727 However, sensitivity analyses rely on historical data, and the magnitude of future declines in
728 snow accumulation may be much larger than the variability in the historical record. A very large
729 decline multiplied by a small sensitivity could still result in a large impact to low flows, as
730 predicted by Barnett et al. (2005) and Dierauer et al.(2021). We also found that sensitivities to
731 groundwater storage were usually smaller than sensitivities to snow storage, suggesting that
732 groundwater will not adequately buffer against the effects of declining snowpack. We propose
733 that studies that investigate low flow drivers should consider both historical sensitivities and the
734 magnitude of projected changes in each driver.

735 Across all regimes, accelerated summer recession has been the most important driver of summer
736 low flows. In section 3.2 we found that on average, a 1 standard deviation-increase summer
737 precipitation leads to half a standard deviation increase in $\log(Q_{7\min})$. The opposite is probably
738 true for T_{summer} in hybrid and rainfall regimes, although this relationship is obscured by
739 collinearity with several other predictors. The correlations with T_{summer} are weaker in snowmelt-
740 dominated catchments, probably because these regimes are more water-limited than energy-
741 limited: the average mean annual precipitation in snowmelt-dominated catchments is only 760
742 mm, compared to 2130 mm in rainfall-dominated, 930 mm in hybrid, and 1120 mm in glacial
743 catchments. In glacial catchments correlations with T_{summer} are often positive, probably because
744 increasing meltflow contributions at higher temperatures offset losses due to increased ET.

745 Our predictive regression models tell a similar story. These models predict that low flows are
746 most influenced by temperature and precipitation over a period of about 4 months (Figure 4).
747 Temperature generally exerts a negative influence on low flows, except for short-term

748 temperature (up to 1 month) in snowmelt-dominated and glacial catchments, where it tends to
749 increase flows.

750 We hindcasted anomalies in $Q_{7\min}$ from 1901-2022 and found that these anomalies were
751 primarily driven by precipitation variability except in rainfall-dominated catchments where
752 temperature has also played a dominant role. Warmer temperatures over the last 30 years have
753 also exerted negative pressures on $Q_{7\min}$ in hybrid and snowmelt-dominated catchments (Figure
754 6).

755 These results align with those of Brunner et al. (2021) and Kormos et al. (2016), who studied the
756 US portion of the Pacific Northwest. However, our finding that summer temperature is an
757 important driver of low flows stands in contrast to the conclusion of Floriancic *et al.* (2021) who
758 argued that summer ET was not a driver of low flows in this region. Their argument relied on the
759 fact that low flow timing in this region (late August – October) is not coincident with the timing
760 of maximum ET (July or August). However, their analysis did not consider that precipitation
761 often remains low across the region until mid-Autumn, so the water balance typically remains in
762 deficit even though ET is not at a maximum in September and October. We have shown here that
763 temperature over a period of about 4 months (not just the 30-day windows used by Floriancic
764 and colleagues) strongly influences the severity of low flows in the late summer and early
765 autumn.

766 The effect of temperature on low flows may be changing, but the evidence is mixed. By
767 including $(T_{\text{summer}})^2$ in our explanatory regressions, we found some evidence of nonlinearity (that
768 the effect of summer temperature dissipates at high temperatures) in colder catchments. This is
769 corroborated by the finding that the effect of summer temperature in hybrid and snowmelt-
770 dominated catchments has been nonstationary, and has decreased in more recent (warmer) years.
771 These findings are physically plausible if evapotranspiration in these catchments is becoming
772 more water-limited, rather than energy-limited (Barnett et al., 2005). On the other hand, when
773 substituting space for time, we found that the effect of temperature tends to be stronger in
774 warmer catchments within each regime: this is opposite to the expected behaviour if the warmest
775 catchments are the most water limited. We also did not find evidence of non-stationarity in the
776 residuals of the predictive regression models, so we conclude that any mechanistic non-
777 stationarity has probably had minor effects on overall low-flow behaviour.

778 Importantly, in rainfall-dominated catchments, which have seen the most severe declines in low
779 flows, and where rising summer temperatures have had the largest effect, the effect of
780 temperature does not appear to dissipate at high temperatures and has remained robust in recent
781 years.

782 Transmission losses appear to play a secondary role in controlling low flows. We found mostly
783 negative but small correlations of T_7 with $\log(Q_{7\min})$, particularly occur in rainfall and hybrid
784 catchments. These represent transmission losses: when temperatures are high, ET from open
785 water and from riparian zones increases. This leads to a temporary reduction in streamflow that
786 may rebound once temperatures decrease. On the other hand, in snowmelt-dominated and glacial

787 regimes temporary increases in temperature can lead to increased meltflow (Stahl & Moore,
788 2006).

789 We note that our catchment classification was static in time, but when we separately classified
790 20th and 21st century hydrographs, there was a large net shift (30%) from snowmelt-dominated to
791 hybrid regimes (Appendix A). With further warming this shift is likely to continue, and many
792 currently snowmelt-dominated catchments may behave more like hybrid catchments. They may
793 begin to see negative trends in low flows, and may become more sensitive to summer
794 temperature.

795 Beginning in earnest around 1950, surface and groundwater abstraction has reduced summer low
796 flows in many parts of the province. We estimated that total water use has exceeded 10% of low
797 flow discharge in 30% of the catchments studied. Although the regime-average anomalies in
798 $Q_{7\min}$ associated with abstraction are estimated to be small (0% in glacial catchments, up to 8%
799 in hybrid catchments), many individual catchments have seen much larger reductions.

800 We were unable to find strong evidence of the impact of harvesting on low flows, although
801 several of our analyses did point towards reduced low flows for 5-20 years post-harvest in
802 snowmelt-dominated catchments. This is the opposite of the typical response reported in the
803 literature, but several reviews have shown that responses are highly heterogeneous and difficult
804 to predict (Coble et al., 2020; Goeking & Tarboton, 2020; Moore et al., 2020). Moore et al.
805 (2020) point out that longitudinal analyses of streamflow in disturbed catchments (as presented
806 here) are less robust and statistically powerful than paired catchment studies. The issues they
807 raised are compounded here by the gradual nature and low levels of disturbance in most of the
808 studied catchments as well as the uncertain quality and completeness of historical forestry data.

809 Our third objective was to build regression models to predict and hindcast low flows from 1901-
810 2022. Our predictive regression models predict low flows much more accurately than models
811 currently being used for climate change impact assessment (Pacific Climate Impacts Consortium,
812 2020). We found that the regression models had low levels of residual autocorrelation and non-
813 stationarity. Some caveats do apply to our historical reconstructions. Land use changes over the
814 past century may have led to other forms of mechanistic non-stationarity. Our analysis of
815 stationarity was based on a before/after analysis split at 1997; we do not have enough data to
816 evaluate stationarity at the time scale of a century. The climate data on which the models are
817 based are slightly less accurate for the early 20th century because meteorological stations were
818 more sparsely distributed (MacDonald et al., 2020). Nevertheless, streamflow records from the
819 few hydrometric stations with continuous records throughout the 1920's and 1930's largely
820 confirm very low flows in these decades. Long-term records for some select stations are shown
821 in Appendix F. See, for example Figure F14 (South Thompson River, a tributary of the Fraser),
822 or Figure F20 (the Columbia River).

823 We can also look to anecdotal evidence to confirm historical droughts. In our reconstruction,
824 1929 was the year with the highest number of hybrid catchments experiencing Level 5 drought.
825 Newspaper records show that the region was so dry in 1929 that Vancouver and Seattle's

826 hydroelectric reservoirs almost ran out of water¹, water was rationed², wells ran dry, and Catholic
827 clergy appealed for divine intervention³. In those years newspapers also regularly ran headlines
828 with dire warnings that salmon stocks were disappearing⁴. Most Canadian articles from the time
829 blamed dwindling salmon stocks on overfishing, American traps, seals, and dam construction,
830 but in 1929 the Washington State Supervisor of Fisheries, Charles Pollock, identified that
831 “Drought is imperiling the fish industry of the Pacific northwest”⁵.

832 For rainfall-dominated catchments, the most drought-stricken year in our reconstruction was
833 1958 which, according to tree-ring data from Vancouver Island, may have been the driest year for
834 350 years (Coulthard et al., 2016). In snowmelt-dominated and glacial catchments 1905 claimed
835 the top spot in our reconstruction of drought events; 1905 took 5th place in the reconstruction
836 presented by [Coulthard et al. \(2016\)](#) and 2nd place in a separate 300-year tree-ring reconstruction
837 of snow droughts (Mood et al., 2020).

838 **5 Conclusions**

839 We have shown that linear regression provides a simple, highly interpretable, and surprisingly
840 accurate way of analysing and predicting low flows across a diverse range of hydrologic
841 regimes. First, we assessed low-flow sensitivities to various climate and anthropogenic drivers
842 and examined whether these sensitivities were changing. We then developed predictive
843 regression models that outperformed process-based models on every standard goodness-of-fit
844 metric. These regression models require just monthly temperature, precipitation, and water
845 abstraction data, so we were able to hindcast droughts, environmental flow transgressions, and
846 low flow anomalies to 1901. Due to the additive nature of the models, we were able to
847 disaggregate these anomalies by driving mechanism, and so corroborate our sensitivity analysis.
848 We propose that these regression techniques could be useful for explaining and predicting low
849 flows and droughts in other regions.

850 Rainfall-dominated and hybrid catchments have seen large and statistically significant decreasing
851 trends in the annual summer minimum flow. Rainfall-dominated catchments are now
852 experiencing streamflow drought and environmental flow transgressions more often than at any
853 point over the past 122 years. Hybrid catchments, on the other hand, are experiencing conditions
854 about as dry as the 1930’s. However, negative low flow anomalies through the Great Depression
855 were caused by lack of precipitation while present-day low flows are being driven by warming
856 temperatures, despite above-average precipitation.

¹ [Capilano Flow Hits New Low](#) (1929, December 3). *The Vancouver Daily Province*, p. 5.

² [Plan to Curtail Street Lighting As Power Economy](#) (1929, November 27). *The Vancouver Sun*, p. 1.

³ [Prayers for Rain Ordered by Archbishop](#) (1929, November 29). *The Vancouver Daily Province*, p. 1.

⁴ See, for example: [B.C. Salmon Run Tends to Decline](#) (1933, August 11). *The Vancouver Daily Province*, p. 1.; Malloy, M. (1921, October 9). [What is a Poor Fish to do? Government Conservation Tactics Fail to Protect the Fraser River’s Former Wealth; Sockeye Salmon, under Conservation, are Disappearing](#). *The Vancouver Sun*, p. 30; Y, E. M. (1920, February 15). [Preservation of Salmon Problem for Authorities](#). *The Vancouver Sun*, p. 7; [Says Salmon Runs Facing Destruction](#) (1922, September 22). *The Vancouver Sun*, p. 1;

⁵ Associated Press: [Fish Affected](#) (1929, December 6). *The Vancouver Sun*, p.14.

857 Summer low flows in snowmelt-dominated and glacial catchments have not shown strong trends
858 since the 1950s but are substantially higher than flows seen during the early 20th century. We
859 found that these catchments are primarily sensitive to summer rainfall. Sensitivity to temperature
860 is low, probably because high temperatures induce melting which offsets increased evaporative
861 losses in glacial catchments and because snowmelt-dominated catchments tend to more water-
862 limited than energy-limited. However, we note that our catchment classification indicated that
863 about one third of previously snowmelt-dominated catchments have become hybrid. If this shift
864 continues then many catchments currently classified as snowmelt-dominated may become more
865 sensitive to temperature and summer low flows may begin to decline.

866 We found that winter conditions and annual snow accumulation have historically only weakly
867 driven variability in low flows. However, climate-change-induced reductions in snowpack and
868 glacial extent will probably be large compared to historical variability, and this large change
869 combined with a weak sensitivity could still result in large reductions in low flow (J. R. Dierauer
870 et al., 2021; Schnorbus et al., 2014).

871 **Acknowledgments**

872 We have no conflicts of interest to disclose.

873 We wish to thank Drs. Dan Moore, Thorsten Wagener, Sandra Walde and Daniel Ruzzante for their
874 feedback, which improved the manuscript.

875 **Open Research**

876 All code developed for this project is available at <https://github.com/sruzzante/low-flows-BC>

877 **References**

- 878 Adam, J. C., Hamlet, A. F., & Lettenmaier, D. P. (2009). Implications of global climate change for
879 snowmelt hydrology in the twenty-first century. *Hydrological Processes*, 23(7), 962–972.
880 <https://doi.org/10.1002/hyp.7201>
- 881 Arthington, A. H., Bhaduri, A., Bunn, S. E., Jackson, S. E., Tharme, R. E., Tickner, D., Young, B.,
882 Acreman, M., Baker, N., Capon, S., Horne, A. C., Kendy, E., McClain, M. E., Poff, N. L.,
883 Richter, B. D., & Ward, S. (2018). The Brisbane Declaration and Global Action Agenda on
884 Environmental Flows (2018). *Frontiers in Environmental Science*, 6.
885 <https://www.frontiersin.org/articles/10.3389/fenvs.2018.00045>
- 886 Ban, Z., Li, D., & Lettenmaier, D. P. (2023). The Increasing Role of Seasonal Rainfall in Western U.S.
887 Summer Streamflow. *Geophysical Research Letters*, 50(9), e2023GL102892.
888 <https://doi.org/10.1029/2023GL102892>
- 889 Barnett, T. P., Adam, J. C., & Lettenmaier, D. P. (2005). Potential impacts of a warming climate on water
890 availability in snow-dominated regions. *Nature*, 438(7066), Article 7066.
891 <https://doi.org/10.1038/nature04141>
- 892 Barroso, S., & Wainwright, M. (2020). *Water Use and Management Options in the Koksilah River*
893 *Watershed: Preliminary analysis and recommendations for future work* (WSS2020-02; Water
894 Science Series).
895 https://a100.gov.bc.ca/pub/acat/documents/r59126/Koksilah_wateruse_1620692372737_E9980F7
896 DAE.pdf
- 897 BC Ministry of Water, Land and Resource Stewardship. (2023). *British Columbia Drought and Water*
898 *Scarcity Response Plan* (pp. 1–54). Government of British Columbia.
899 [https://www2.gov.bc.ca/assets/gov/environment/air-land-water/water/drought-](https://www2.gov.bc.ca/assets/gov/environment/air-land-water/water/drought-info/drought_response_plan_final.pdf)
900 [info/drought_response_plan_final.pdf](https://www2.gov.bc.ca/assets/gov/environment/air-land-water/water/drought-info/drought_response_plan_final.pdf)
- 901 Beck, H. E., Zimmermann, N. E., McVicar, T. R., Vergopolan, N., Berg, A., & Wood, E. F. (2018). Present
902 and future Köppen-Geiger climate classification maps at 1-km resolution. *Scientific Data*, 5(1),
903 Article 1. <https://doi.org/10.1038/sdata.2018.214>
- 904 Beven, K. (2016). Facets of uncertainty: Epistemic uncertainty, non-stationarity, likelihood, hypothesis
905 testing, and communication. *Hydrological Sciences Journal*, 61(9), 1652–1665.
906 <https://doi.org/10.1080/02626667.2015.1031761>
- 907 Boeing, F., Wagener, T., Marx, A., Rakovec, O., Kumar, R., Samaniego, L., & Attinger, S. (2024).
908 Increasing influence of evapotranspiration on prolonged water storage recovery in Germany.
909 *Environmental Research Letters*, 19(2), 024047. <https://doi.org/10.1088/1748-9326/ad24ce>
- 910 Bradford, M. J., & Heinonen, J. S. (2008). Low Flows, Instream Flow Needs and Fish Ecology in Small
911 Streams. *Canadian Water Resources Journal / Revue Canadienne Des Ressources Hydriques*,
912 33(2), 165–180. <https://doi.org/10.4296/cwrj3302165>
- 913 Breusch, T. S. (1978). Testing for Autocorrelation in Dynamic Linear Models*. *Australian Economic*
914 *Papers*, 17(31), 334–355. <https://doi.org/10.1111/j.1467-8454.1978.tb00635.x>
- 915 Brunner, M. I., Swain, D. L., Gilleland, E., & Wood, A. W. (2021). Increasing importance of temperature
916 as a contributor to the spatial extent of streamflow drought. *Environmental Research Letters*,
917 16(2), 024038. <https://doi.org/10.1088/1748-9326/abd2f0>
- 918 Burn, D. H., & Hag Elnur, M. A. (2002). Detection of hydrologic trends and variability. *Journal of*
919 *Hydrology*, 255(1), 107–122. [https://doi.org/10.1016/S0022-1694\(01\)00514-5](https://doi.org/10.1016/S0022-1694(01)00514-5)
- 920 Cecco, L. (2022, October 5). Thousands of salmon found dead as Canada drought dries out river. *The*
921 *Guardian*. [https://www.theguardian.com/environment/2022/oct/05/canada-dead-salmon-drought-](https://www.theguardian.com/environment/2022/oct/05/canada-dead-salmon-drought-british-columbia)
922 [british-columbia](https://www.theguardian.com/environment/2022/oct/05/canada-dead-salmon-drought-british-columbia)
- 923 Chang, H., Jung, I.-W., Steele, M., & Gannett, M. (2012). Spatial Patterns of March and September
924 Streamflow Trends in Pacific Northwest Streams, 1958–2008. *Geographical Analysis*, 44(3),
925 177–201. <https://doi.org/10.1111/j.1538-4632.2012.00847.x>

- 926 Clifton, C. F., Day, K. T., Luce, C. H., Grant, G. E., Safeeq, M., Halofsky, J. E., & Staab, B. P. (2018).
927 Effects of climate change on hydrology and water resources in the Blue Mountains, Oregon,
928 USA. *Climate Services*, 10, 9–19. <https://doi.org/10.1016/j.cliser.2018.03.001>
- 929 Coble, A. A., Barnard, H., Du, E., Johnson, S., Jones, J., Keppeler, E., Kwon, H., Link, T. E., Penaluna, B.
930 E., Reiter, M., River, M., Puettmann, K., & Wagenbrenner, J. (2020). Long-term hydrological
931 response to forest harvest during seasonal low flow: Potential implications for current forest
932 practices. *Science of The Total Environment*, 730, 138926.
933 <https://doi.org/10.1016/j.scitotenv.2020.138926>
- 934 Cooper, M. G., Schaperow, J. R., Cooley, S. W., Alam, S., Smith, L. C., & Lettenmaier, D. P. (2018).
935 Climate Elasticity of Low Flows in the Maritime Western U.S. Mountains. *Water Resources*
936 *Research*, 54(8), 5602–5619. <https://doi.org/10.1029/2018WR022816>
- 937 Coulthard, B., Smith, D. J., & Meko, D. M. (2016). Is worst-case scenario streamflow drought
938 underestimated in British Columbia? A multi-century perspective for the south coast, derived
939 from tree-rings. *Journal of Hydrology*, 534, 205–218.
940 <https://doi.org/10.1016/j.jhydrol.2015.12.030>
- 941 Cruickshank, A. (2023, September 21). Restoring the flow: Tsleil-Waututh’s race to save salmon habitat in
942 drought stricken southwest B.C. *The Narwhal*. [https://thenarwhal.ca/tsleil-waututh-nation-](https://thenarwhal.ca/tsleil-waututh-nation-salmon-restoration/)
943 [salmon-restoration/](https://thenarwhal.ca/tsleil-waututh-nation-salmon-restoration/)
- 944 Curran, D., Gleeson, T., & Huggins, X. (2023). Applying a science-forward approach to groundwater
945 regulatory design. *Hydrogeology Journal*, 31(4), 853–871. [https://doi.org/10.1007/s10040-023-](https://doi.org/10.1007/s10040-023-02625-6)
946 [02625-6](https://doi.org/10.1007/s10040-023-02625-6)
- 947 de Graaf, I. E. M., Gleeson, T., van Beek, L. P. H. (Rens), Sutanudjaja, E. H., & Bierkens, M. F. P.
948 (2019). Environmental flow limits to global groundwater pumping. *Nature*, 574, 90–94.
949 <https://doi.org/10.1038/s41586-019-1594-4>
- 950 Dierauer, J. R., Allen, D. M., & Whitfield, P. H. (2021). Climate change impacts on snow and streamflow
951 drought regimes in four ecoregions of British Columbia. *Canadian Water Resources Journal /*
952 *Revue Canadienne Des Ressources Hydriques*, 46(4), 168–193.
953 <https://doi.org/10.1080/07011784.2021.1960894>
- 954 Dierauer, J. R., Whitfield, P. H., & Allen, D. M. (2018). Climate Controls on Runoff and Low Flows in
955 Mountain Catchments of Western North America. *Water Resources Research*, 54(10), 7495–7510.
956 <https://doi.org/10.1029/2018WR023087>
- 957 Dierauer, J., & Whitfield, P. (2019). *FlowScreen: Daily Streamflow Trend and Change Point Screening*
958 (1.2.6) [Computer software]. <https://cran.r-project.org/web/packages/FlowScreen/index.html>
- 959 Diffenbaugh, N. S., Swain, D. L., & Touma, D. (2015). Anthropogenic warming has increased drought
960 risk in California. *Proceedings of the National Academy of Sciences*, 112(13), 3931–3936.
961 <https://doi.org/10.1073/pnas.1422385112>
- 962 Environment and Climate Change Canada. (2021). *Historical gridded snow water equivalent and snow*
963 *cover fraction over Canada from remote sensing and land surface models* [dataset].
964 <https://climate-scenarios.canada.ca/?page=blended-snow-data>
- 965 First Nations Fisheries Council of British Columbia. (2020). *Environmental Flow Needs—A Primer for*
966 *First Nations* (pp. 1–11). [https://www.fnfisheriescouncil.ca/wp-content/uploads/2022/01/WFF-](https://www.fnfisheriescouncil.ca/wp-content/uploads/2022/01/WFF-ENVIRONMENTAL-FLOW-NEEDS-2020.pdf)
967 [ENVIRONMENTAL-FLOW-NEEDS-2020.pdf](https://www.fnfisheriescouncil.ca/wp-content/uploads/2022/01/WFF-ENVIRONMENTAL-FLOW-NEEDS-2020.pdf)
- 968 Fleming, S. W., Whitfield, P. H., Moore, R. D., & Quilty, E. J. (2007). Regime-dependent streamflow
969 sensitivities to Pacific climate modes cross the Georgia–Puget transboundary ecoregion.
970 *Hydrological Processes*, 21(24), 3264–3287. <https://doi.org/10.1002/hyp.6544>
- 971 Floriancic, M. G., Berghuijs, W. R., Jonas, T., Kirchner, J. W., & Molnar, P. (2020). Effects of climate
972 anomalies on warm-season low flows in Switzerland. *Hydrology and Earth System Sciences*,
973 24(11), 5423–5438. <https://doi.org/10.5194/hess-24-5423-2020>
- 974 Floriancic, M. G., Berghuijs, W. R., Molnar, P., & Kirchner, J. W. (2021). Seasonality and Drivers of Low
975 Flows Across Europe and the United States. *Water Resources Research*, 57(9), e2019WR026928.
976 <https://doi.org/10.1029/2019WR026928>

- 977 Folkens, L., Bachmann, D., & Schneider, P. (2023). Driving Forces and Socio-Economic Impacts of Low-
 978 Flow Events in Central Europe: A Literature Review Using DPSIR Criteria. *Sustainability*,
 979 *15*(13), Article 13. <https://doi.org/10.3390/su151310692>
- 980 Georgiadis, N. J., & Baker, J. E. (2023). A multidecadal oscillation in precipitation and temperature series
 981 is pronounced in low flow series from Puget Sound streams. *JAWRA Journal of the American*
 982 *Water Resources Association*, *59*(5), 970–983. <https://doi.org/10.1111/1752-1688.13129>
- 983 Godfrey, L. G. (1978). Testing Against General Autoregressive and Moving Average Error Models when
 984 the Regressors Include Lagged Dependent Variables. *Econometrica*, *46*(6), 1293–1301.
 985 <https://doi.org/10.2307/1913829>
- 986 Godsey, S. E., Kirchner, J. W., & Tague, C. L. (2014). Effects of changes in winter snowpacks on summer
 987 low flows: Case studies in the Sierra Nevada, California, USA. *Hydrological Processes*, *28*(19),
 988 5048–5064. <https://doi.org/10.1002/hyp.9943>
- 989 Goeking, S. A., & Tarboton, D. G. (2020). Forests and Water Yield: A Synthesis of Disturbance Effects on
 990 Streamflow and Snowpack in Western Coniferous Forests. *Journal of Forestry*, *118*(2), 172–192.
 991 <https://doi.org/10.1093/jofore/fvz069>
- 992 Guzha, A. C., Rufino, M. C., Okoth, S., Jacobs, S., & Nóbrega, R. L. B. (2018). Impacts of land use and
 993 land cover change on surface runoff, discharge and low flows: Evidence from East Africa.
 994 *Journal of Hydrology: Regional Studies*, *15*, 49–67. <https://doi.org/10.1016/j.ejrh.2017.11.005>
- 995 Hale, K. E., Jennings, K. S., Musselman, K. N., Livneh, B., & Molotch, N. P. (2023). Recent decreases in
 996 snow water storage in western North America. *Communications Earth & Environment*, *4*(1),
 997 Article 1. <https://doi.org/10.1038/s43247-023-00751-3>
- 998 Hamed, K. H., & Ramachandra Rao, A. (1998). A modified Mann-Kendall trend test for autocorrelated
 999 data. *Journal of Hydrology*, *204*(1), 182–196. [https://doi.org/10.1016/S0022-1694\(97\)00125-X](https://doi.org/10.1016/S0022-1694(97)00125-X)
- 1000 Hernandez, J. (2023, July 21). Drought conditions threatening B.C. salmon as river levels drop | CBC
 1001 News. *CBC*. [https://www.cbc.ca/news/canada/british-columbia/drought-hurting-b-c-salmon-](https://www.cbc.ca/news/canada/british-columbia/drought-hurting-b-c-salmon-1.6912670)
 1002 [1.6912670](https://www.cbc.ca/news/canada/british-columbia/drought-hurting-b-c-salmon-1.6912670)
- 1003 Holm, S. (1979). A Simple Sequentially Rejective Multiple Test Procedure. *Scandinavian Journal of*
 1004 *Statistics*, *6*(2), 65–70.
- 1005 Huang, S., Kumar, R., Flörke, M., Yang, T., Hundecha, Y., Kraft, P., Gao, C., Gelfan, A., Liersch, S.,
 1006 Lobanova, A., Strauch, M., van Ogtrop, F., Reinhardt, J., Haberlandt, U., & Krysanova, V. (2017).
 1007 Evaluation of an ensemble of regional hydrological models in 12 large-scale river basins
 1008 worldwide. *Climatic Change*, *141*(3), 381–397. <https://doi.org/10.1007/s10584-016-1841-8>
- 1009 Hutchinson, M. F., McKenney, D. W., Lawrence, K., Pedlar, J. H., Hopkinson, R. F., Milewska, E., &
 1010 Papadopol, P. (2009). Development and Testing of Canada-Wide Interpolated Spatial Models of
 1011 Daily Minimum–Maximum Temperature and Precipitation for 1961–2003. *Journal of Applied*
 1012 *Meteorology and Climatology*, *48*(4), 725–741. <https://doi.org/10.1175/2008JAMC1979.1>
- 1013 Islam, S. ul, Déry, S. J., & Werner, A. T. (2017). Future Climate Change Impacts on Snow and Water
 1014 Resources of the Fraser River Basin, British Columbia. *Journal of Hydrometeorology*, *18*(2),
 1015 473–496. <https://doi.org/10.1175/JHM-D-16-0012.1>
- 1016 Kang, D. H., Gao, H., Shi, X., Islam, S. ul, & Déry, S. J. (2016). Impacts of a Rapidly Declining
 1017 Mountain Snowpack on Streamflow Timing in Canada’s Fraser River Basin. *Scientific Reports*,
 1018 *6*(1), Article 1. <https://doi.org/10.1038/srep19299>
- 1019 Knoben, W. J. M., Freer, J. E., & Woods, R. A. (2019). *Technical note: Inherent benchmark or not?*
 1020 *Comparing Nash-Sutcliffe and Kling-Gupta efficiency scores* [Preprint]. Catchment
 1021 hydrology/Modelling approaches. <https://doi.org/10.5194/hess-2019-327>
- 1022 Kormos, P. R., Luce, C. H., Wenger, S. J., & Berghuijs, W. R. (2016). Trends and sensitivities of low
 1023 streamflow extremes to discharge timing and magnitude in Pacific Northwest mountain streams.
 1024 *Water Resources Research*, *52*(7), 4990–5007. <https://doi.org/10.1002/2015WR018125>
- 1025 MacDonald, H., McKenney, D. W., Papadopol, P., Lawrence, K., Pedlar, J., & Hutchinson, M. F. (2020).
 1026 North American historical monthly spatial climate dataset, 1901–2016. *Scientific Data*, *7*(1),
 1027 Article 1. <https://doi.org/10.1038/s41597-020-00737-2>

- 1028 McCleary, R., & Ptolemy, R. (2017). *Setting Critical Environmental Flow Thresholds for Drought*
 1029 *Response: Coldwater River Case Study* (FNR-2017-72956; p. 23).
 1030 http://docs.openinfo.gov.bc.ca/Response_Package_FNR-2017-72956.pdf
 1031 Mood, B. J., Coulthard, B., & Smith, D. J. (2020). Three hundred years of snowpack variability in
 1032 southwestern British Columbia reconstructed from tree-rings. *Hydrological Processes*, *34*(25),
 1033 5123–5133. <https://doi.org/10.1002/hyp.13933>
 1034 Moore, R. D. (Dan), Gronsdahl, S., & McCleary, R. (2020). Effects of Forest Harvesting on Warm-Season
 1035 Low Flows in the Pacific Northwest: A Review. *Confluence: Journal of Watershed Science and*
 1036 *Management*, *4*(1), Article 1. <https://doi.org/10.22230/jwsm.2020v4n1a35>
 1037 Morgan, M. (2012). Cultural Flows: Asserting Indigenous Rights and Interests in the Waters of the
 1038 Murray-Darling River System, Australia. In B. R. Johnston, L. Hiwasaki, I. J. Klaver, A. Ramos
 1039 Castillo, & V. Strang (Eds.), *Water, Cultural Diversity, and Global Environmental Change:*
 1040 *Emerging Trends, Sustainable Futures?* (pp. 453–466). Springer Netherlands.
 1041 https://doi.org/10.1007/978-94-007-1774-9_31
 1042 Muñoz Sabater, J. (2019). *ERA5-Land hourly data from 2001 to present* [dataset]. Copernicus Climate
 1043 Change Service (C3S) Climate Data Store (CDS). <https://doi.org/10.24381/CDS.E2161BAC>
 1044 Niel, H., Paturel, J.-E., & Servat, E. (2003). Study of parameter stability of a lumped hydrologic model in
 1045 a context of climatic variability. *Journal of Hydrology*, *278*(1), 213–230.
 1046 [https://doi.org/10.1016/S0022-1694\(03\)00158-6](https://doi.org/10.1016/S0022-1694(03)00158-6)
 1047 Pacific Climate Impacts Consortium. (2020). *VIC-GL BCCAQ CMIP5 RVIC: Station Hydrologic Model*
 1048 *Output*. [dataset]. University of Victoria. [https://www.pacificclimate.org/data/station-hydrologic-](https://www.pacificclimate.org/data/station-hydrologic-model-output)
 1049 [model-output](https://www.pacificclimate.org/data/station-hydrologic-model-output)
 1050 Patakamuri, S. K., & O'Brien, N. (2021). *modifiedmk: Modified Versions of Mann Kendall and*
 1051 *Spearman's Rho Trend Tests* (1.6) [Computer software]. [https://cran.r-](https://cran.r-project.org/web/packages/modifiedmk/)
 1052 [project.org/web/packages/modifiedmk/](https://cran.r-project.org/web/packages/modifiedmk/)
 1053 Poff, N. L., & Zimmerman, J. K. H. (2010). Ecological responses to altered flow regimes: A literature
 1054 review to inform the science and management of environmental flows. *Freshwater Biology*,
 1055 *55*(1), 194–205. <https://doi.org/10.1111/j.1365-2427.2009.02272.x>
 1056 Porkka, M., Virkki, V., Wang-Erlandsson, L., Gerten, D., Gleeson, T., Mohan, C., Fetzer, I., Jaramillo, F.,
 1057 Staal, A., Wierik, S. te, Tobian, A., Ent, R. van der, Döll, P., Flörke, M., Gosling, S., Hanasaki, N.,
 1058 Satoh, Y., Schmied, H. M., Wanders, N., ... Kummu, M. (2022). *Global water cycle shifts far*
 1059 *beyond pre-industrial conditions – planetary boundary for freshwater change transgressed*.
 1060 <https://eartharxiv.org/repository/view/3438/>
 1061 Province of BC. (2024a). *Fire Perimeters—Historical* [dataset].
 1062 <https://catalogue.data.gov.bc.ca/dataset/22c7cb44-1463-48f7-8e47-88857f207702>
 1063 Province of BC. (2024b). *Harvested Areas of BC (Consolidated Cutblocks)* [dataset].
 1064 <https://catalogue.data.gov.bc.ca/dataset/harvested-areas-of-bc-consolidated-cutblocks->
 1065 Richardson, K., Steffen, W., Lucht, W., Bendtsen, J., Cornell, S. E., Donges, J. F., Drüke, M., Fetzer, I.,
 1066 Bala, G., von Bloh, W., Feulner, G., Fiedler, S., Gerten, D., Gleeson, T., Hofmann, M., Huiskamp,
 1067 W., Kummu, M., Mohan, C., Nogués-Bravo, D., ... Rockström, J. (2023). Earth beyond six of
 1068 nine planetary boundaries. *Science Advances*, *9*(37), eadh2458.
 1069 <https://doi.org/10.1126/sciadv.adh2458>
 1070 Safeeq, M., Grant, G. E., Lewis, S. L., Kramer, M. G., & Staab, B. (2014). A hydrogeologic framework
 1071 for characterizing summer streamflow sensitivity to climate warming in the Pacific Northwest,
 1072 USA. *Hydrology and Earth System Sciences*, *18*(9), 3693–3710. [https://doi.org/10.5194/hess-18-](https://doi.org/10.5194/hess-18-3693-2014)
 1073 [3693-2014](https://doi.org/10.5194/hess-18-3693-2014)
 1074 Santos, L., Thirel, G., & Perrin, C. (2018). Technical note: Pitfalls in using log-transformed flows within
 1075 the KGE criterion. *Hydrology and Earth System Sciences*, *22*(8), 4583–4591.
 1076 <https://doi.org/10.5194/hess-22-4583-2018>

- 1077 Schnorbus, M., Werner, A., & Bennett, K. (2014). Impacts of climate change in three hydrologic regimes
 1078 in British Columbia, Canada. *Hydrological Processes*, 28(3), 1170–1189.
 1079 <https://doi.org/10.1002/hyp.9661>
- 1080 Shao, D., Li, H., Wang, J., Hao, X., Che, T., & Ji, W. (2022). Reconstruction of a daily gridded snow
 1081 water equivalent product for the land region above 45°N based on a ridge regression
 1082 machine learning approach. *Earth System Science Data*, 14(2), 795–809.
 1083 <https://doi.org/10.5194/essd-14-795-2022>
- 1084 Shrestha, R. R., Schnorbus, M. A., Werner, A. T., & Berland, A. J. (2012). Modelling spatial and temporal
 1085 variability of hydrologic impacts of climate change in the Fraser River basin, British Columbia,
 1086 Canada. *Hydrological Processes*, 26(12), 1840–1860. <https://doi.org/10.1002/hyp.9283>
- 1087 Smakhtin, V. U. (2001). Low flow hydrology: A review. *Journal of Hydrology*, 240(3), 147–186.
 1088 [https://doi.org/10.1016/S0022-1694\(00\)00340-1](https://doi.org/10.1016/S0022-1694(00)00340-1)
- 1089 Stahl, K., & Moore, R. D. (2006). Influence of watershed glacier coverage on summer streamflow in
 1090 British Columbia, Canada. *Water Resources Research*, 42(6).
 1091 <https://doi.org/10.1029/2006WR005022>
- 1092 Teuling, A. J., Van Loon, A. F., Seneviratne, S. I., Lehner, I., Aubinet, M., Heinesch, B., Bernhofer, C.,
 1093 Grünwald, T., Prasse, H., & Spank, U. (2013). Evapotranspiration amplifies European summer
 1094 drought. *Geophysical Research Letters*, 40(10), 2071–2075. <https://doi.org/10.1002/grl.50495>
- 1095 Tipa, G., & Nelson, K. (2012). Identifying Cultural Flow Preferences: Kakaunui River Case Study.
 1096 *Journal of Water Resources Planning and Management*, 138(6), 660–670.
 1097 [https://doi.org/10.1061/\(ASCE\)WR.1943-5452.0000211](https://doi.org/10.1061/(ASCE)WR.1943-5452.0000211)
- 1098 Udall, B., & Overpeck, J. (2017). The twenty-first century Colorado River hot drought and implications
 1099 for the future. *Water Resources Research*, 53(3), 2404–2418.
 1100 <https://doi.org/10.1002/2016WR019638>
- 1101 Ukkola, A. M., De Kauwe, M. G., Roderick, M. L., Abramowitz, G., & Pitman, A. J. (2020). Robust
 1102 Future Changes in Meteorological Drought in CMIP6 Projections Despite Uncertainty in
 1103 Precipitation. *Geophysical Research Letters*, 47(11), e2020GL087820.
 1104 <https://doi.org/10.1029/2020GL087820>
- 1105 Van Loon, A. F. (2015). Hydrological drought explained. *WIREs Water*, 2(4), 359–392.
 1106 <https://doi.org/10.1002/wat2.1085>
- 1107 Vionnet, V., Mortimer, C., Brady, M., Arnal, L., & Brown, R. (2021). Canadian historical Snow Water
 1108 Equivalent dataset (CanSWE, 1928–2020). *Earth System Science Data*, 13(9), 4603–4619.
 1109 <https://doi.org/10.5194/essd-13-4603-2021>
- 1110 Virkki, V., Alanärrä, E., Porkka, M., Ahopelto, L., Gleeson, T., Mohan, C., Wang-Erlandsson, L., Flörke,
 1111 M., Gerten, D., Gosling, S. N., Hanasaki, N., Müller Schmied, H., Wanders, N., & Kummu, M.
 1112 (2022). Globally widespread and increasing violations of environmental flow envelopes.
 1113 *Hydrology and Earth System Sciences*, 26(12), 3315–3336. [https://doi.org/10.5194/hess-26-3315-](https://doi.org/10.5194/hess-26-3315-2022)
 1114 [2022](https://doi.org/10.5194/hess-26-3315-2022)
- 1115 Wada, Y., Flörke, M., Hanasaki, N., Eisner, S., Fischer, G., Tramberend, S., Satoh, Y., van Vliet, M. T. H.,
 1116 Yillia, P., Ringler, C., Burek, P., & Wiberg, D. (2016). Modeling global water use for the 21st
 1117 century: The Water Futures and Solutions (WFaS) initiative and its approaches. *Geoscientific*
 1118 *Model Development*, 9(1), 175–222. <https://doi.org/10.5194/gmd-9-175-2016>
- 1119 Wade, N. L., Martin, J., & Whitfield, P. H. (2001). Hydrologic and Climatic Zonation of Georgia Basin,
 1120 British Columbia. *Canadian Water Resources Journal / Revue Canadienne Des Ressources*
 1121 *Hydriques*, 26(1), 43–70. <https://doi.org/10.4296/cwrj2601043>
- 1122 Water Sustainability Act, [SBC 2014] CHAPTER 15 § 87 (2016).
 1123 <https://www.bclaws.gov.bc.ca/civix/document/id/complete/statreg/14015>
- 1124 Werner, A. T., Schnorbus, M. A., Shrestha, R. R., Cannon, A. J., Zwiers, F. W., Dayon, G., & Anslow, F.
 1125 (2019). A long-term, temporally consistent, gridded daily meteorological dataset for northwestern
 1126 North America. *Scientific Data*, 6(1), Article 1. <https://doi.org/10.1038/sdata.2018.299>

- 1127 Westra, S., Thyer, M., Leonard, M., Kavetski, D., & Lambert, M. (2014). A strategy for diagnosing and
1128 interpreting hydrological model nonstationarity. *Water Resources Research*, *50*(6), 5090–5113.
1129 <https://doi.org/10.1002/2013WR014719>
- 1130 Whitfield, P. H., Wang, J. Y., & Cannon, A. J. (2003). Modelling Future Streamflow Extremes—Floods
1131 and Low Flows in Georgia Basin, British Columbia. *Canadian Water Resources Journal / Revue*
1132 *Canadienne Des Ressources Hydriques*, *28*(4), 633–656. <https://doi.org/10.4296/cwrj2804633>
- 1133 Wood, S. K. (2021, December 21). ‘The salmon will come back again’: First Nations document
1134 devastating low returns on B.C.’s central coast. *The Narwhal*. [https://thenarwhal.ca/bc-salmon-](https://thenarwhal.ca/bc-salmon-central-coast-2021-run/)
1135 [central-coast-2021-run/](https://thenarwhal.ca/bc-salmon-central-coast-2021-run/)
- 1136 Woodhouse, C. A., Pederson, G. T., Morino, K., McAfee, S. A., & McCabe, G. J. (2016). Increasing
1137 influence of air temperature on upper Colorado River streamflow. *Geophysical Research Letters*,
1138 *43*(5), 2174–2181. <https://doi.org/10.1002/2015GL067613>
- 1139 Zambrano-Bigiarini, M. (2024). *hydroGOF: Goodness-of-Fit Functions for Comparison of Simulated and*
1140 *Observed Hydrological Time Series (0.5-4)* [Computer software]. [https://cran.r-](https://cran.r-project.org/web/packages/hydroGOF/index.html)
1141 [project.org/web/packages/hydroGOF/index.html](https://cran.r-project.org/web/packages/hydroGOF/index.html)
- 1142 Zhang, M., & Wei, X. (2012). The effects of cumulative forest disturbance on streamflow in a large
1143 watershed in the central interior of British Columbia, Canada. *Hydrology and Earth System*
1144 *Sciences*, *16*(7), 2021–2034. <https://doi.org/10.5194/hess-16-2021-2012>
- 1145

1 Appendix A: Catchment Classification

2 CONTENTS

3	Algorithm	1
4	Comparison to Previous Classification Schemes.....	3
5	Regime changes	5
6	References	6

8 Tables

9	<i>Table A1: Contingency table for regime classification, comparison to Wenger et al. (2010)</i>	3
10	<i>Table A2: Contingency table for regime classification, comparison to Chang et al. (2010)</i> ..	3
11	<i>Table A3: Contingency table for regime classification, comparison to Cooper et al (2018)</i>	4
12	<i>Table A4: Contingency table for regime classification, comparison to Wade et al. (2001)</i>	4
13	<i>Table A5: Contingency table for regime classification, comparison to Fleming et al. (2007)</i>	4
14	<i>Table A6: Contingency table for regime classification, comparison to Déry et al. (2009)</i>	5
15	<i>Table A7: Contingency table comparing catchments classifications using data from 1903-1997 and 1998-2022</i>	5

17 Algorithm

18 A variety of catchment classification schemes have been proposed in the literature for Pacific Northwest
19 streams. Wade et al. (2001) classified streams by qualitatively analysing annual hydrographs and runoff
20 calculations. Similarly, Fleming et al. (2007) used a qualitative evaluation of the average annual
21 hydrograph of each river; hybrid regimes were those that “consistently display two seasonal peaks.”
22 Wenger et al. (2010) and later Kormos et al. (2016) classified streams by the centre of timing of
23 streamflow (CT, days since start of water year) with $CT < 150$, $150 \leq CT \leq 200$, and $CT > 200$ corresponding to
24 pluvial, transitional, and nival regimes. (Chang et al., 2012) classified catchments by mean basin
25 elevation. (Cooper et al., 2018) used the ratio of snow-water equivalent to total annual precipitation to
26 distinguish rain-dominated and snow-dominated catchments. (Islam et al., 2019) use a snowmelt pulse
27 detection technique based on the work of Cayan et al. (2001) and Fritze et al. (2011). Mohan et al.
28 (2023) classified regions of BC as rainfall-dominant when low flows occur in late summer and snowfall-
29 dominant when low flows occur in winter. Déry et al. (2009) qualitatively classified 9 BC streams as
30 Pluvial, Nival, and Glacial.

31 For the purposes of low flow analysis, the definition proposed by Fleming et al. (2007) is the most
32 relevant. The consistent appearance of two seasonal peaks also guarantees the appearance of two
33 seasonal low flow periods. Thus, we define pluvial regimes as those with a single low flow period in the
34 warm season. Nival regimes are those with a single low flow period in cold seasons, and hybrid regimes
35 are those that have two distinct low flow period.

36 We define the warm season as the snow-free season, based on the monthly average snow-water-
37 equivalent (SWE) for the period 1985-2014, using data from the ERA-5 Reanalysis (Muñoz Sabater,
38 2019). We define the snow disappearance date (SDD) and snow appearance date (SAD) as the first (last)
39 month of the year for which the catchment-average SWE is less than 1 mm. For catchments with
40 perennial snow or ice cover in parts, we define the SDD (SAD) as the first (last) month for which SWE is

41 within the bottom 10% of the annual range. The snow maximum date (SMD) is the month with the
42 highest average snow accumulation.

43 We designed an algorithm to classify the catchments by their annual hydrographs. We construct the
44 annual hydrograph by averaging the 30-day flows (Q30) from all available years.

45 We define the *low-flow month* based on the timing of the minimum warm-season flow on the average
46 annual hydrograph. We also define the *low-flow season* as the low-flow month ± 1 , as long as the
47 neighboring months are within the previously defined warm season.

48 The following equations refer to the average Q30.

49 We define four variables:

50 $Q_{min.Winter}$ is the minimum cold-season flow.

51 $Q_{max.Freshet}$ is the maximum spring flow, which occurs after $Q_{min.Winter}$, during or after the month of
52 maximum snow accumulation (SMD), and during or before the month of the snow disappearance date
53 (SDD). This flow is attributed to the freshet peak.

54 $Q_{min.Summer}$ is the *low-flow season* minimum flow.

55 $Q_{max.Autumn}$ is the maximum Autumn-Winter flow (October to December). This flow is attributed to
56 increase autumn-winter rainfall. $Q_{max.Autumn}$ is also constrained to occur after $Q_{min.Summer}$.

57 We define **snow-affected catchments** as those with a substantial freshet (at least 2X larger than the
58 winter minimum flow):

$$snow.affected = Q_{max.Freshet} > 2 \times Q_{min.Winter}$$

59 We define **rain-affected catchments** as those where the autumn rainfall peak exceeds the summer
60 minimum. In these catchments, increased autumn rainfall more than compensates for catchment
61 drainage from summer to autumn. Autumn precipitation also typically falls as rain, rather than snow. To
62 account for small amounts of noise in some of the annual hydrographs, we require that $Q_{max.Autumn}$

$$rain.affected = Q_{max.Autumn} > 1.025 \times Q_{min.Summer}$$

63 If both *rain.affected* and *snow.affected* are true, then the catchment is classified as **hybrid**. If only
64 *snow.affected* is true, then the catchment is **snowmelt-dominated**, and if only *rain.affected* is true
65 then the catchment is **rainfall-dominated**.

66 Lastly, if over 5% of the catchment area is glaciated, we classify the catchment to be **glacial**, overriding
67 any prior classification. extents were found by spatially overlaying catchment polygons with historical
68 glacial extents (GeoBC, 2023).

69 Two catchments on the island of Haida Gwaii (Honna River Near the Mouth, 08OA004 and Tarundl Creek
70 Near Queen Charlotte, 08HA005) have few years of winter data, so their annual hydrographs are noisier
71 than the hydrographs for other catchments. These catchments are pluvial, but the algorithm incorrectly
72 identified winter rainfall-induced runoff peaks as freshets, so the catchments were incorrectly classified
73 as hybrid.

74 Comparison to Previous Classification Schemes

75 The classification presented here differs somewhat from previous classifications. We implemented
 76 algorithms proposed by Wenger et al. (2010), Chang et al. (2012), and Cooper et al. (2018). The
 77 following contingency tables compare our classification algorithm with the algorithms used by these
 78 authors. We also compare our classification against the qualitative classifications published by Wade et
 79 al. (2001), Fleming et al. (2007), and Déry et al. (2009).

80 Table A1 presents a confusion matrix comparing the regimes as classified here against those predicted
 81 by the algorithm of Wenger et al. (2010), based on the centre of timing. Overall, there is only 53%
 82 agreement. However, this disagreement occurs because our “hybrid” category is much more expansive
 83 than Wenger’s “transitional” category (111 catchments in our hybrid category and only 8 in Wenger’s
 84 classification). The two schemes agree on the rainfall-dominated regime: only 2 watersheds classified as
 85 rainfall-dominated in this scheme are classified as “transitional” in Wenger’s scheme.

86 **Table A1: Contingency table for regime classification, comparison to Wenger et al. (2010). Cells denoting agreement are**
 87 **bolded.**

		Wenger et al. (2010)		
		Rainfall	Transitional	Snowmelt
This study	Rainfall	32	2	0
	Hybrid	0	6	105
	Snowmelt	0	0	48
	Glacial	0	0	37

88

89 Table A2 compares our classification to the elevation-based classification used by Chang et al. (2012).
 90 There is 60% agreement between the two schemes but troublingly, Change et al. classify as rainfall-
 91 dominated 4 catchments that we classify as snowmelt-dominated or glacial. Also, their scheme classifies
 92 only six catchments as snowmelt-dominated (mean elevation above 2000 m above sea level).

93 **Table A2: Contingency table for regime classification, comparison to Chang et al. (2010). Cells denoting agreement are**
 94 **bolded.**

		Chang et al. (2012)		
		Rainfall	Hybrid	Snowmelt
This study	Rainfall	34	0	0
	Hybrid	14	97	0
	Snowmelt	3	42	3
	Glacial	1	33	3

95

96 Table A3 compares our classification to the scheme used by Cooper et al. (2018). They classified
 97 catchments according to the ratio of maximum snow water equivalent to annual precipitation.
 98 Catchments with a ratio greater than 0.2 were classified as snow-dominated. Although their scheme did
 99 not classify as rainfall-dominated any catchments that we classified as hybrid, snowmelt, or glacial, their
 100 scheme is highly skewed towards the snowmelt category. They also did not include a hybrid category.
 101 Overall there was only 47% agreement.

102 **Table A3: Contingency table for regime classification, comparison to Cooper et al (2018). Cells denoting agreement are**
 103 **bolded.**

		(Cooper et al., 2018)	
		Rainfall	Snowmelt
This study	Rainfall	24	10
	Hybrid	0	111
	Snowmelt	0	48
	Glacial	0	37

104

105 Twenty-three (23) catchments in our study were also classified by Wade et al. (2001) based on
 106 consideration of climate, hydrologic, and elevation data. Table A4 shows a comparison of their
 107 classification with ours. Overall, our classification agrees with (Wade et al., 2001) in 18/23 (70%) of the
 108 catchments.

109 **Table A4: Contingency table for regime classification, comparison to Wade et al. (2001). Cells denoting agreement are**
 110 **bolded.**

		(Wade et al., 2001)		
		Rainfall	Hybrid	Snowmelt/Glacial
This study	Rainfall	8	4	0
	Hybrid	0	4	2
	Snowmelt	0	0	0
	Glacial	0	1	4

111

112 Six catchments in our study were also classified by Fleming et al. (2007), based on a qualitative
 113 assessment of the hydrographs. Table A5 shows a comparison of their classification with ours. Their
 114 classification combined snowmelt-dominated and glacial catchments into one 'nival' category but
 115 otherwise there is perfect (100%) agreement between our classification and theirs.

116 **Table A5: Contingency table for regime classification, comparison to Fleming et al. (2007). Cells denoting agreement are**
 117 **bolded.**

		Fleming et al. (2007)		
		Pluvial	Hybrid	Nival
This study	Rainfall	3	0	0
	Hybrid	0	2	0
	Snowmelt	0	0	0
	Glacial	0	0	1

118

119 Eight catchments in our study were also qualitatively classified by Déry et al. (2009). Table A6 shows a
 120 comparison of their classification with ours. They assigned pluvial, nival, and glacial categories (no hybrid
 121 category). The catchments in our study classified as hybrid were classified by Déry et al. as nival, but
 122 otherwise there is perfect agreement between our classification and theirs.

123 **Table A6: Contingency table for regime classification, comparison to Déry et al. (2009). Cells denoting agreement are bolded.**

		Déry et al. (2009)		
		Pluvial	Nival	Glacial
This study	Rainfall	2	0	0
	Hybrid	0	3	0
	Snowmelt	0	0	0
	Glacial	0	0	3

124

125 Our scheme relies on direct observations of the dominant processes, rather than somewhat arbitrary
 126 cutoffs based on the center of timing, elevation, or the ratio of maximum snow water equivalent to
 127 precipitation. Our classification agrees reasonably well with past qualitative assessments, but has the
 128 benefit of reproducibility over qualitative assessments.

129 Regime changes

130 We also evaluated whether regimes have changed. We ran the classification algorithm separately on
 131 data up to 1997 and from 1998 onwards. This split was selected to coincide with the split used to assess
 132 stationarity (Section 3.2) The definition of the ‘warm season’ was the same for both periods. We didn’t
 133 analyse regime change in glacial catchments because the glacial extent data are static in time. We only
 134 evaluated catchments with at least 10 years of data in both periods (154 catchments in total).

135 Table A7 shows a contingency table comparing the classifications based on the early and late periods.
 136 There was an overall shift towards the hybrid catchment classification. Two (2) previously rainfall-
 137 dominated catchments were reclassified as hybrid, two (2) hybrid catchments were reclassified as
 138 snowfall-dominated, and nineteen (19) moved from snowfall-dominated to hybrid. As a result, the
 139 hybrid category grew by 23% and the snowmelt-dominated category shrunk by 31%.

140 **Table A7: Contingency table comparing catchment classifications using data from 1903-1997 and 1998-2022.**

		2000-2022		
		Rainfall	Hybrid	Snowmelt
1903-1999	Rainfall	17	2	0
	Hybrid	0	79	2
	Snowmelt	0	19	36

141

142

143 References

- 144 Cayan, D. R., Kammerdiener, S. A., Dettinger, M. D., Caprio, J. M., & Peterson, D. H. (2001). Changes in
145 the Onset of Spring in the Western United States. *Bulletin of the American Meteorological Society*, *82*(3),
146 399–416. [https://doi.org/10.1175/1520-0477\(2001\)082<0399:CITOOS>2.3.CO;2](https://doi.org/10.1175/1520-0477(2001)082<0399:CITOOS>2.3.CO;2)
- 147 Chang, H., Jung, I.-W., Steele, M., & Gannett, M. (2012). Spatial Patterns of March and September
148 Streamflow Trends in Pacific Northwest Streams, 1958–2008. *Geographical Analysis*, *44*(3), 177–201.
149 <https://doi.org/10.1111/j.1538-4632.2012.00847.x>
- 150 Cooper, M. G., Schaperow, J. R., Cooley, S. W., Alam, S., Smith, L. C., & Lettenmaier, D. P. (2018). Climate
151 Elasticity of Low Flows in the Maritime Western U.S. Mountains. *Water Resources Research*, *54*(8),
152 5602–5619. <https://doi.org/10.1029/2018WR022816>
- 153 Déry, S. J., Stahl, K., Moore, R. D., Whitfield, P. H., Menounos, B., & Burford, J. E. (2009). Detection of
154 runoff timing changes in pluvial, nival, and glacial rivers of western Canada. *Water Resources Research*,
155 *45*(4). <https://doi.org/10.1029/2008WR006975>
- 156 Fleming, S. W., Whitfield, P. H., Moore, R. D., & Quilty, E. J. (2007). Regime-dependent streamflow
157 sensitivities to Pacific climate modes cross the Georgia–Puget transboundary ecoregion. *Hydrological*
158 *Processes*, *21*(24), 3264–3287. <https://doi.org/10.1002/hyp.6544>
- 159 Fritze, H., Stewart, I. T., & Pebesma, E. (2011). Shifts in Western North American Snowmelt Runoff
160 Regimes for the Recent Warm Decades. *Journal of Hydrometeorology*, *12*(5), 989–1006.
161 <https://doi.org/10.1175/2011JHM1360.1>
- 162 GeoBC. (2023). *Freshwater Atlas Glaciers* [dataset].
163 <https://catalogue.data.gov.bc.ca/dataset/freshwater-atlas-glaciers>
- 164 Islam, S. U., Curry, C. L., Déry, S. J., & Zwiers, F. W. (2019). Quantifying projected changes in runoff
165 variability and flow regimes of the Fraser River Basin, British Columbia. *Hydrology and Earth System*
166 *Sciences*, *23*(2), 811–828. <https://doi.org/10.5194/hess-23-811-2019>
- 167 Kormos, P. R., Luce, C. H., Wenger, S. J., & Berghuijs, W. R. (2016). Trends and sensitivities of low
168 streamflow extremes to discharge timing and magnitude in Pacific Northwest mountain streams. *Water*
169 *Resources Research*, *52*(7), 4990–5007. <https://doi.org/10.1002/2015WR018125>
- 170 Mohan, C., Gleeson, T., Forstner, T., Famiglietti, J. S., & de Graaf, I. (2023). Quantifying Groundwater's
171 Contribution to Regional Environmental-Flows in Diverse Hydrologic Landscapes. *Water Resources*
172 *Research*, *59*(6), e2022WR033153. <https://doi.org/10.1029/2022WR033153>
- 173 Muñoz Sabater, J. (2019). *ERA5-Land hourly data from 2001 to present* [dataset]. Copernicus Climate
174 Change Service (C3S) Climate Data Store (CDS). <https://doi.org/10.24381/CDS.E2161BAC>
- 175 Wade, N. L., Martin, J., & Whitfield, P. H. (2001). Hydrologic and Climatic Zonation of Georgia Basin,
176 British Columbia. *Canadian Water Resources Journal / Revue Canadienne Des Ressources Hydriques*,
177 *26*(1), 43–70. <https://doi.org/10.4296/cwrj2601043>
- 178 Wenger, S. J., Luce, C. H., Hamlet, A. F., Isaak, D. J., & Neville, H. M. (2010). Macroscale hydrologic
179 modeling of ecologically relevant flow metrics. *Water Resources Research*, *46*(9).
180 <https://doi.org/10.1029/2009WR008839>

1 **APPENDIX B: WATER USE ESTIMATION**

2 We estimated both surface water and groundwater use. The total water use for each year is the sum of
3 the two estimates. We followed the estimation framework used by Barroso and Wainwright (2020).

4 **Licensed Surface and Ground Water**

5 Geo-located data on surface and ground water licenses were downloaded from British Columbia’s data
6 warehouse (BC Ministry of Forests, 2023) on August 29, 2023. We excluded licences for uses in the
7 winter or early spring as well as licenses that represent non-consumptive use. Table B1 lists the license
8 purpose codes for licenses located within the 230 studied catchments.

9 We assumed that all users draw the maximum licensed amount each year from the license priority date
10 to the date when the licenses is cancelled or abandoned. We did not account for license expiry dates,
11 but only 20 (less than 0.1%) of the licenses have expired.

12 **Unlicensed Groundwater Use**

13 Groundwater licensing began in British Columbia in 2016 but most groundwater users are not licensed.
14 We estimated groundwater use for unlicensed wells based on provincial well records (BC Ministry of
15 Environment and Climate Change Strategy, 2023) and property assessment data collected by the (BC
16 Assessment Authority, 2022).

17 First, we spatially filtered wells to the 230 studied catchments and removed wells whose tag numbers
18 were also found in the water license data. We then filtered to wells with “Well Class” of *Water Supply* or
19 *Unknown*, and removed wells with an “Intended Use” of *Observation Well*, *Test*, or *Open Loop*
20 *Geoexchange*. We spatially joined the remaining wells to the BC Assessment parcels (individual
21 properties).

22 For wells with an “Intended Use” of *Private Domestic* we assumed water consumption of 1.75 m³/day.
23 For wells with an “Intended Use” of *Irrigation* we assumed a standard irrigation duty of 1 acre-foot per
24 year, over a reference area of half the property size.

25 For wells with other “Intended Use” codes, located within properties used as for a variety of commercial
26 and community purposes, we assumed water consumption of 1-10 times the domestic rate. This
27 included campgrounds, seasonal resorts, motels, restaurants, service stations, churches, and community
28 halls.

29 For wells located within golf courses we assumed a standard irrigation duty of 1 acre-foot per year over
30 the full property area.

31 At this point, we assumed any wells for which use had not already been estimated, and for which the
32 property use was “Grain & Forage”, “Vegetable & Truck” or other agricultural purposes, had a standard
33 irrigation duty of 1 acre-foot per year, over half the property. For orchards and vineyards 0.5 acre-feet
34 per year was assumed.

35 For other property uses, including sawmills, various types of mining operations, airports, sand and gravel
36 quarries, concrete plants, we analysed water licenses located within the same property use type and
37 assigned a reasonable value to unlicensed wells.

38 Lastly, for wells that were still not assigned an estimated water use rate we assumed private domestic
39 use (1.75 m³/day).

40 For properties with more than one well with the same intended use (eg. two irrigation wells) we divided
41 the use for each well by the total number of wells.

42 We assumed water use started when the well was constructed.

43

44 **References**

45 Barroso, S., & Wainwright, M. (2020). *Water Use and Management Options in the Koksilah River*
46 *Watershed: Preliminary analysis and recommendations for future work* (WSS2020-02; Water
47 Science Series).
48 [https://a100.gov.bc.ca/pub/acat/documents/r59126/Koksilah_wateruse_1620692372737_E998](https://a100.gov.bc.ca/pub/acat/documents/r59126/Koksilah_wateruse_1620692372737_E9980F7DAE.pdf)
49 [0F7DAE.pdf](https://a100.gov.bc.ca/pub/acat/documents/r59126/Koksilah_wateruse_1620692372737_E9980F7DAE.pdf)

50 BC Assessment Authority. (2022). *BC Assessment Data Advice, 2022-* (Version V8) [dataset]. Abacus Data
51 Network. <https://hdl.handle.net/11272.1/AB2/NXRVP9>

52 BC Ministry of Environment and Climate Change Strategy. (2023). *Groundwater Wells* [dataset]. BC Data
53 Catalogue. <https://catalogue.data.gov.bc.ca/dataset/e4731a85-ffca-4112-8caf-cb0a96905778>

54 BC Ministry of Forests. (2023). *Water Rights Licences—Public* [dataset]. BC Data Catalogue.
55 <https://catalogue.data.gov.bc.ca/dataset/water-rights-licences-public>

56

57

58

59 **Table B1: Summary of included and excluded licences**

Code	Purpose	# Licenses	Included?
01A	Domestic	10527	YES
03B	Irrigation: Private	6056	YES
	Livestock & Animal:		
02I31	Stockwatering	960	YES
WSA08	Livestock & Animal	406	YES
WSA01	Domestic (WSA01)	391	YES
00A	Waterworks: Local Provider	383	YES
02D	Comm. Enterprise: Enterprise	342	YES
00B	Waterworks (other than LP)	154	YES
05D	Mining: Placer	149	YES
WSA03	Commercial Enterprise	133	YES
WSA02	Camps & Public Facilities	115	YES
02F	Lwn, Fairway & Grdn: Watering	114	YES
03A	Irrigation: Local Provider	106	YES
02E	Pond & Aquaculture	104	YES
02I42	Lwn, Fairway & Grdn: Res L/G	104	YES
02I08	Transport Mgmt: Dust Control	84	YES
02B	Processing & Mfg: Processing	47	YES
02I37	Camps & Pub Facil: Work Camps	40	YES
02I12	Misc Ind'l: Fire Protection	37	YES
05C	Mining: Processing Ore	33	YES
WSA11	Lawn, Fairway & Garden	33	YES
02I27	Misc Ind'l: Sediment Control	28	YES
02G	Fresh Water Bottling	27	YES
	Camps & Pub Facil: Non-Work		
02I02	Camps	24	YES
02C	Cooling	21	YES
05A	Mining: Hydraulic	17	YES
	Camps & Pub Facil: Public		
02I25	Facility	16	YES
WSA09	Processing & Manufacturing	16	YES
02I17	Grnhouse & Nursery: Grnhouse	15	YES
02I21	Camps & Pub Facil: Institutions	14	YES
WSA10	Well Drill/Transprt Mgmt	12	YES
02I35	Waterworks: Water Delivery	11	YES
WSA05	Greenhouse & Nursery	10	YES
WSA12	Vehicle & Equipment	9	YES
02I38	Fish Hatchery	8	YES
05B	Mining: Washing Coal	8	YES
09B	Mineralized Water: Comm. Pool	8	YES

60

02I24	Misc Ind'l: Overburden Disposal	7	YES
02I22	Grnhouse & Nursery: Nursery	6	YES
09A	Mineralized Water: Bottling & Dist	6	YES
Table B1 (continued)			
Code	Purpose	# Licenses	Included?
02I03	Camps & Pub Facil: Church/Com Hall	5	YES
02I11	Processing & Mfg: Fire Prevention	4	YES
02I39	Vehicle & Eqpt: Mine & Quarry	4	YES
02I46	Transport Mgmt: Road Maint.	4	YES
02A	Pulp Mill	3	YES
02I07	Ind'l Waste Mgmt: Effluent	3	YES
02I33	Vehicle & Eqpt: Truck & Eq Wash	3	YES
02I09	Camps & Pub Facil: Exhibition Grnds	2	YES
02I18	Heat Exchanger	2	YES
02I32	Swimming Pool	2	YES
02I47	Heat Exchanger, Residential	2	YES
WSA04	Crop: Harvest/Protect/Compost	2	YES
02H	Bulk Shipment for Marine Trans	1	YES
02I01	Vehicle & Eqpt: Brake Cooling	1	YES
02I04	Conveying (Inactiv	1	YES
02I09	Camp & Pub Facil: Exhibition Grnds	1	YES
02I16	Ind'l Waste Mgmt: Garbage Dump	1	YES
02I26	River Improvement	1	YES
02I28	Ind'l Waste Mgmt: Sewage Disposal	1	YES
02I43	Transport Mgmt: Tunnelling/Well Drilling	1	YES
04B	Land Improve: Rehab/Remed	1	YES
08A	Stream Storage: Non-Power	1026	NO
11A	Conservation: Storage	251	NO
04A	Land Improve: General	237	NO
07A	Power: Residential	166	NO
11B	Conservation: Use of Water	109	NO
07C	Power: General	74	NO
11C	Conservation: Construct Works	73	NO
WSA07	Misc Indust	47	NO
01A01	Incidental - Domestic	39	NO
07B	Power: Commercial	39	NO

02I30	Ice & Snow Making: Snow	21	NO
12A	Stream Storage: Power	17	NO
02I06	Misc Ind'l: Dewatering	5	NO
08B	Aquifer Storage: NP	4	NO
02I14	Crops: Frost Protection	1	NO
WSA06	Ice & Snow Making	1	NO

61

62

1 **Appendix C: Trend Tests**

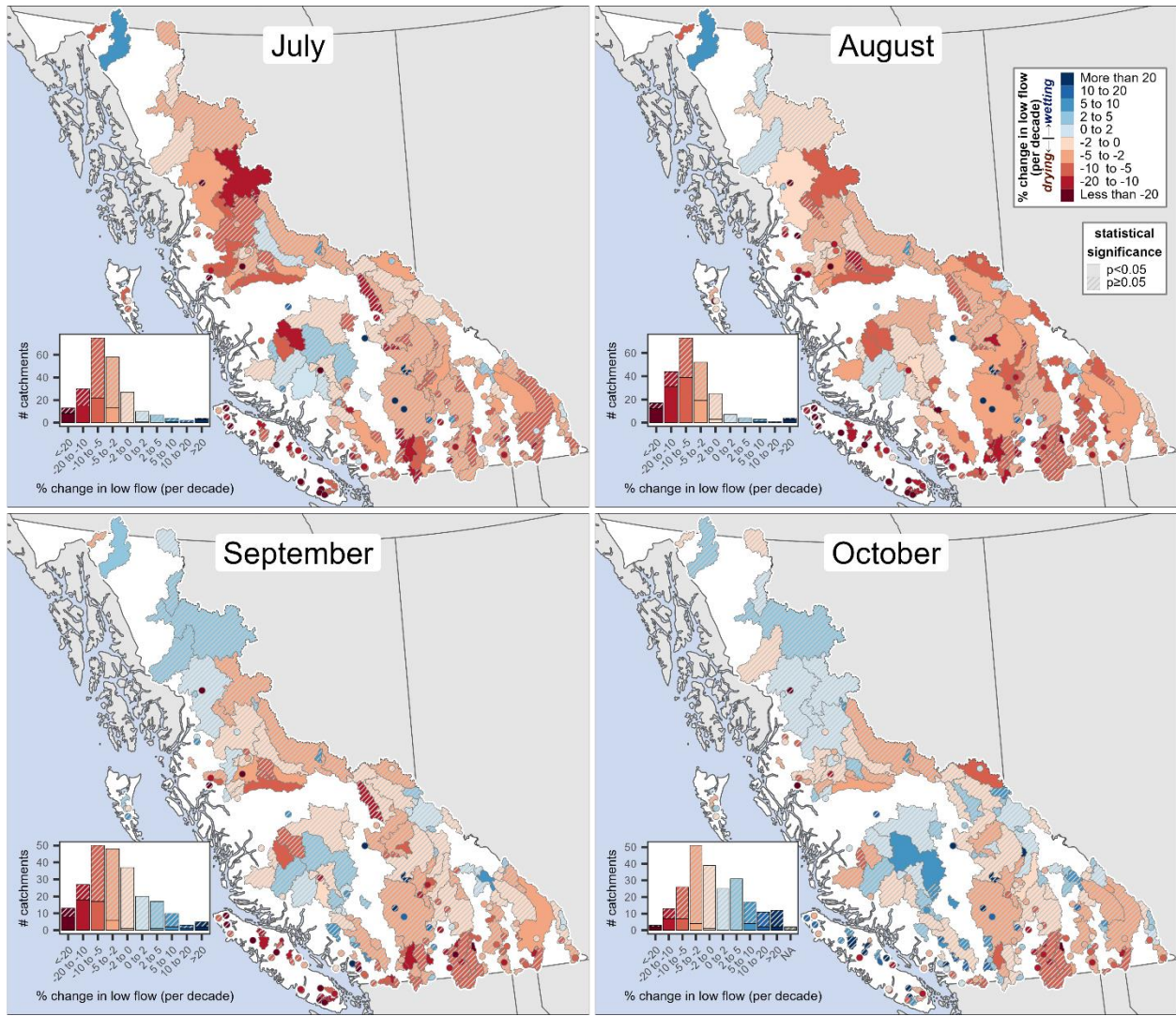
2 Table C1 shows the number positive and negative, and significant trends for all regimes and months, as
 3 well as for the low-flow season (*overall*). Figure B1 shows maps of the trends for the low flow in each
 4 month.

5 **Table C1: Overall and month-specific trends in $\log(Q7_{min})$. The trend direction is based on Sen's slope. The numbers in**
 6 **parentheses indicate the number of significant trends, based on a Mann-Kendall trend test for autocorrelated data (Hamed**
 7 **& Ramachandra Rao, 1998).**

Regime	Month	# Negative Trends (# significant)	# Positive Trends (# significant)	Total
All	Overall	174 (51)	56 (5)	230
	July	201 (58)	29 (5)	230
	August	210 (104)	20 (4)	230
	September	174 (50)	56 (6)	230
	October	131 (21)	97 (8)	228
Rainfall	Overall	33 (19)	1 (0)	34
	July	32 (16)	2 (0)	34
	August	33 (19)	1 (0)	34
	September	29 (13)	5 (0)	34
	October	17 (4)	15 (0)	32
Hybrid	Overall	94 (24)	17 (2)	111
	July	101 (26)	10 (3)	111
	August	101 (47)	10 (3)	111
	September	91 (31)	20 (3)	111
	October	69 (12)	42 (4)	111
Snowmelt	Overall	33 (7)	15 (2)	48
	July	42 (10)	6 (0)	48
	August	47 (25)	1 (0)	48
	September	39 (5)	9 (0)	48
	October	32 (5)	16 (2)	48
Glacial	Overall	14 (1)	23 (1)	37
	July	26 (6)	11 (2)	37
	August	29 (13)	8 (1)	37
	September	15 (1)	22 (3)	37
	October	13 (0)	24 (2)	37

8

9



10
 11 **Figure C1: Trends for the overall monthly low flows in the 230 study catchments, using available data from 1950 to present.**
 12 **Hatched polygons denote non-significant trends. Red denotes drying trends and blue denotes wetting trends.**

13

1 **Appendix D: Sensitivity**

2 This appendix provides additional robustness checks for Section 3.2.

3 Figure D1 shows Pearson correlation coefficients for each of the eight tested variables. This differs from
4 the analysis presented in Figure 3 in the main text, where we showed the coefficients from a multiple
5 regression model with all variables standardized to mean of 0 and unit variance. We found correlations
6 with SWE_{max} were generally slightly stronger but still not very large. Correlations with BF_{winter} were
7 similarly small, and correlations with P_{summer} were similarly large or slightly larger. Pearson correlations
8 with T_{summer} and T₇ were substantially larger than the standardized regression coefficients, due to
9 multicollinearity with other variables in the multiple regression. Correlations with abstraction, ECA_I, and
10 ECA_{III} varied somewhat but not predictably.

11 Figure D2 shows results using a fixed annual timing for the SWE variable, rather than the maximum
12 accumulation for each year. There were no major differences.

13 Figure D3 shows results using 14 different definitions of the baseflow variable. All results indicate minor
14 effects of winter baseflow/groundwater storage on summer low flows.

15 Figure D4 shows a figure analogous to Figure 3 in the main text, but using P_{winter} and T_{winter} instead of
16 BF_{winter} and SWE_{max}. The effect of these variables was similar.

17 Figure D5 shows figures analogous to Figure 3 in the main text but computed for each month between
18 July and October (instead of using the overall Q7_{min}). SWE_{max} and T_{summer} have larger impacts on flows
19 earlier in the season (July and August), while P_{summer} has a larger impact later in the season. The effect of
20 all other variables is small in all seasons.

21 Tables D1-D4 show results of our stationarity tests, splitting the data at 1995, 1996, 1997, and 1998.
22 Test 1 evaluates the percentage of catchments that show positive changes in each coefficient, while
23 Tests 2 and 3 evaluate the percentage of catchments showing positive and significant changes. Overall
24 there is little evidence of non-stationarity in most variables. However, in hybrid and snowmelt-
25 dominated regimes, we do see consistent reductions in the effect of SWE_{max} (coefficients mostly
26 decrease) and in T_{summer} (coefficients mostly become less negative).

27

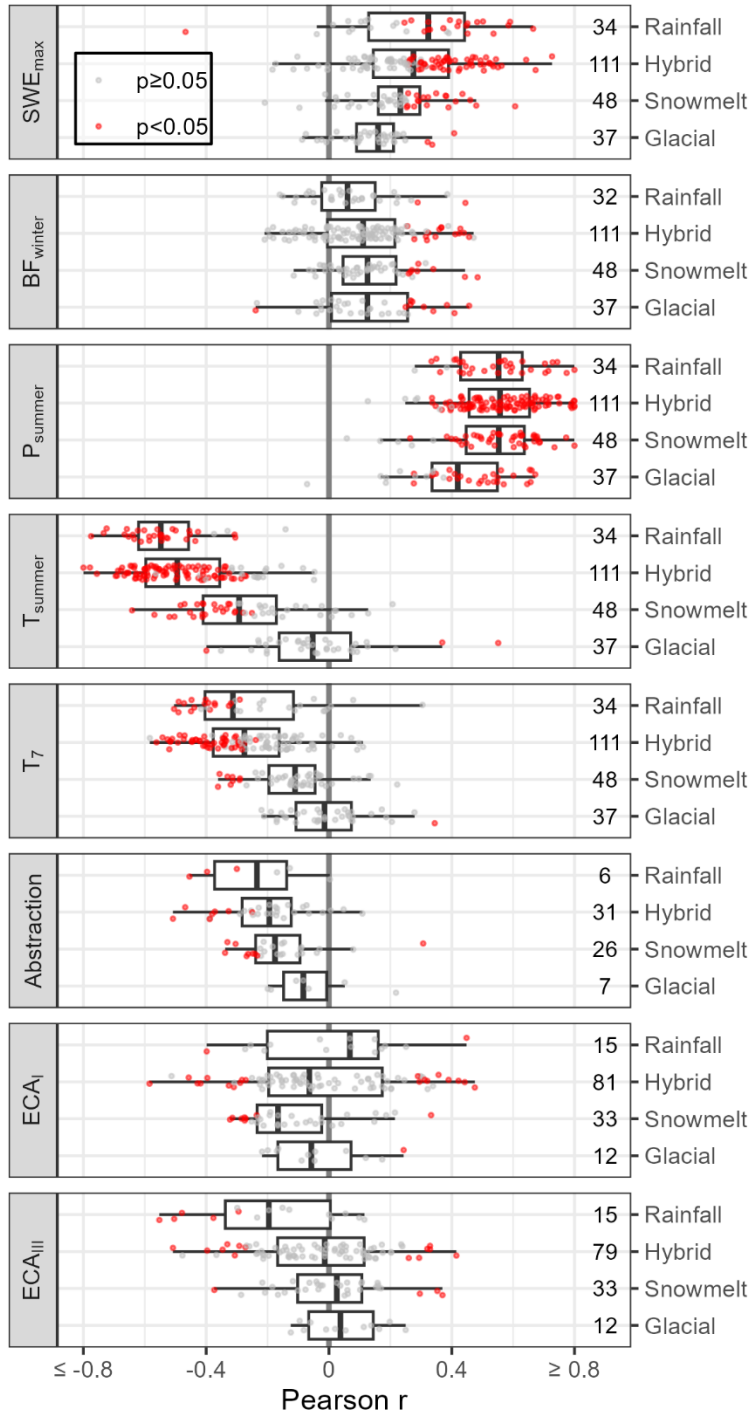
28 **Tables**

29	Table D1: Stationarity tests with split year 1995.....	7
30	Table D2: Stationarity tests with split year 1995.....	8
31	Table D3: Stationarity tests with split year 1997.....	9
32	Table D4: Stationarity tests with split year 1997.....	10

33 **Figures**

34	Figure D1: Bivariate Pearson correlation coefficients for log-transformed summer low flows.....	2
35	Figure D2: Standardized regression coefficients using two definitions of the SWE variable.....	3
36	Figure D3: Fourteen difference baseflow variables.....	4
37	Figure D4: Standardized regression coefficients using winter temperature and precipitation instead of 38 SWE _{max} and BF _{winter}	5
39	Figure D5: Standardized regression coefficients for log-transformed monthly low flows.....	6

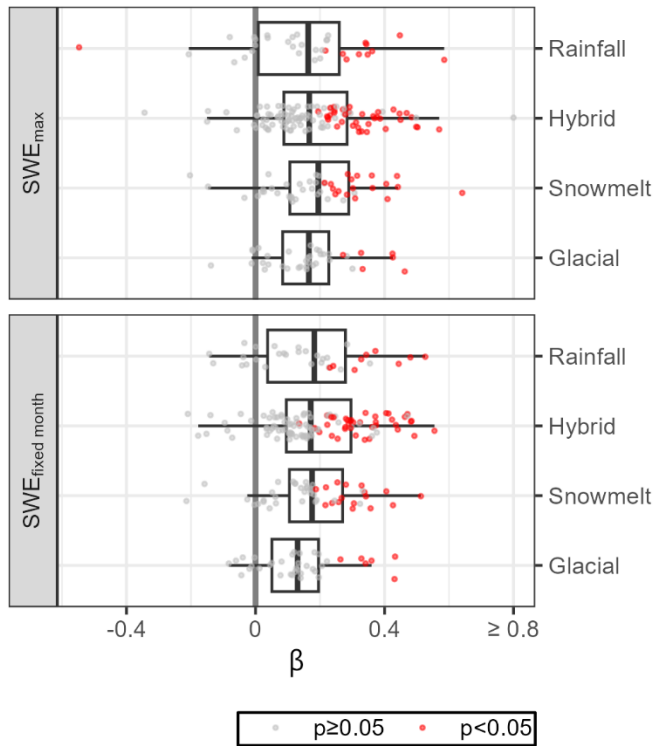
40



41

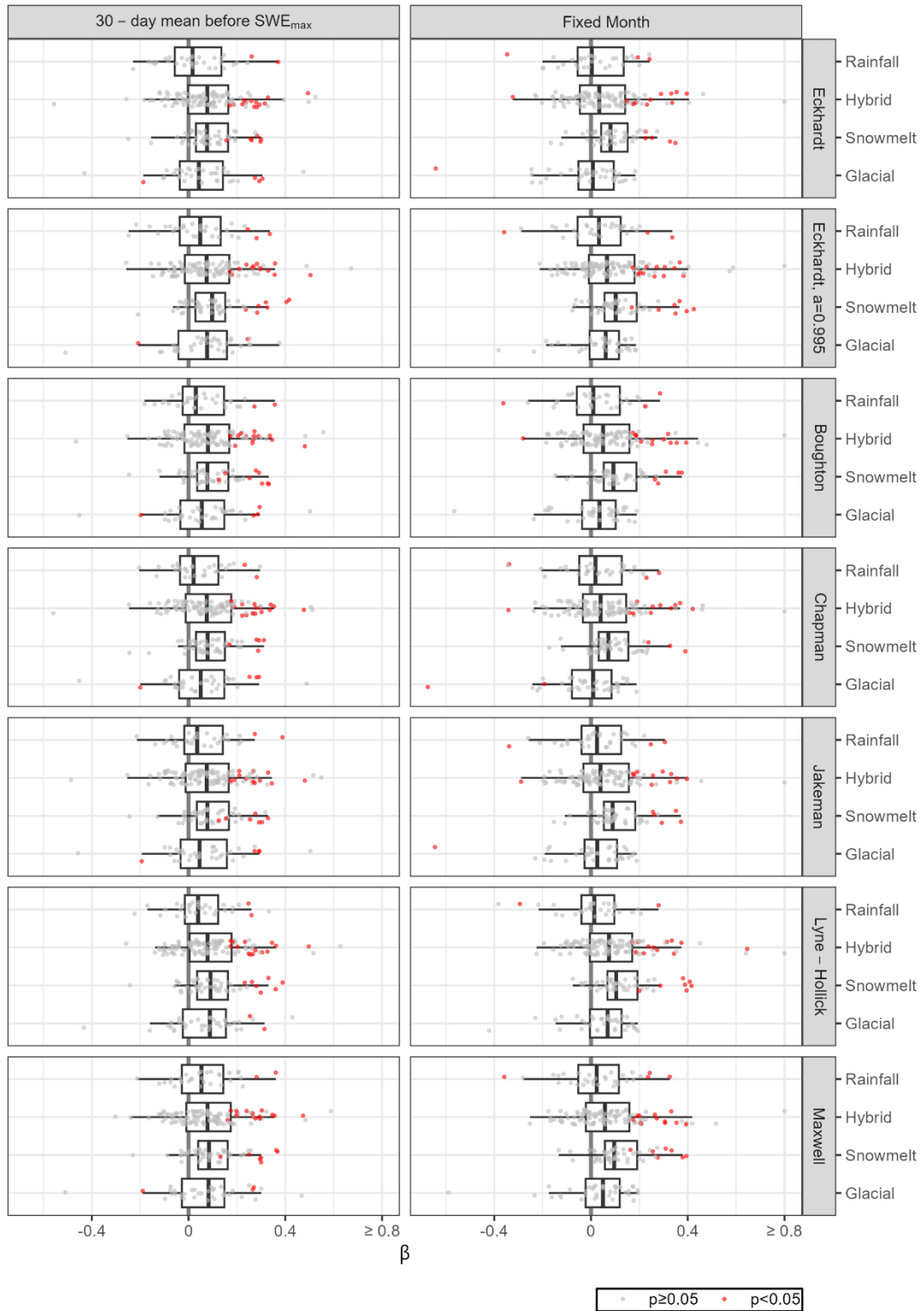
42

Figure D1: Bivariate Pearson correlation coefficients for log-transformed summer low flows with 8 explanatory variables.



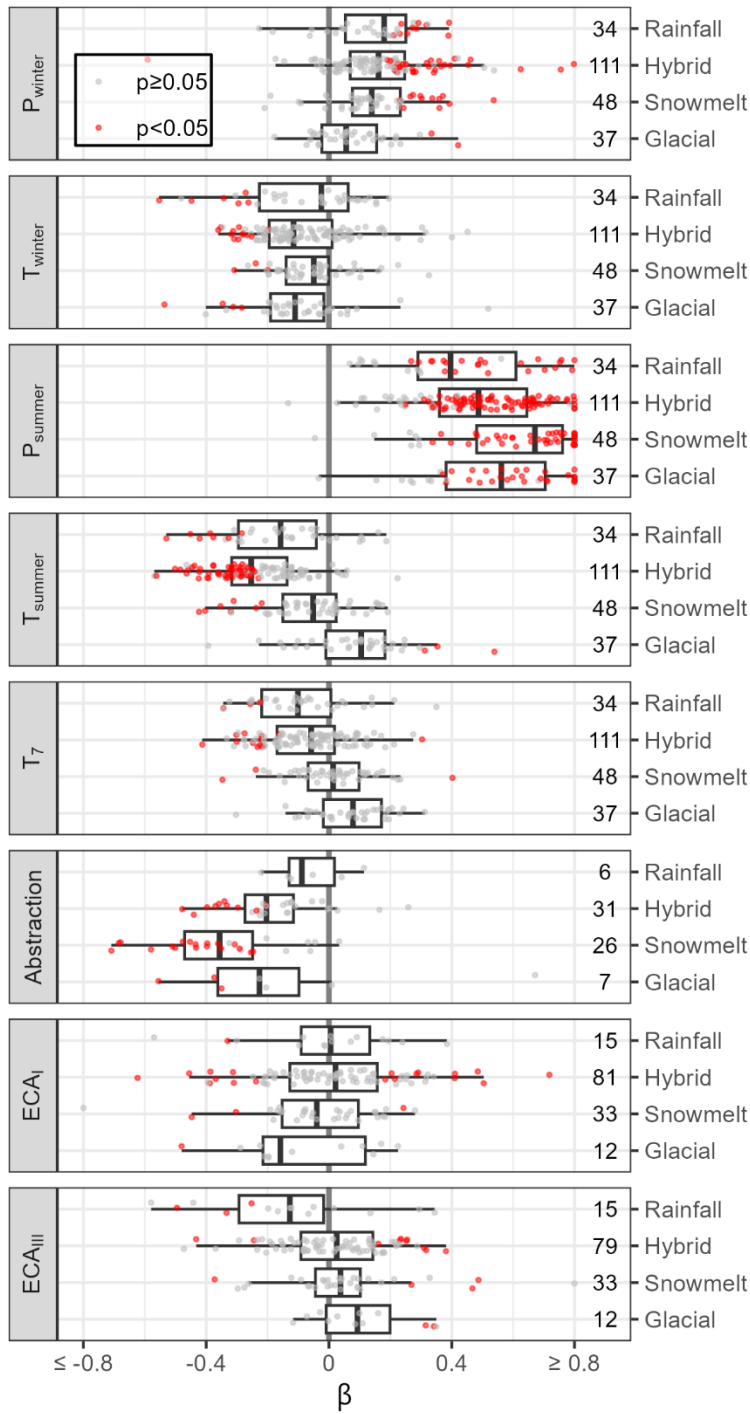
43

44 **Figure D2: Standardized regression coefficients using two definitions of the SWE variable. The top panel shows results using**
 45 **the maximum accumulation for each year (as in the manuscript). The bottom panel shows $SWE_{fixed\ month}$, which is the monthly**
 46 **average SWE for the median peak accumulation month.**



47

48 **Figure D3: Fourteen different baseflow variables all show very small effects. The left column uses the average baseflow for**
 49 **30 days prior to SWE_{max} . The right column uses the average baseflow over the same month as SWE_{fixed} . Each row is a**
 50 **different baseflow filtering algorithm. The top row (Eckhardt) is used in the manuscript, with $\alpha = 0.97$, and the second row**
 51 **uses $\alpha = 0.995$.**



52

53 **Figure D4: Standardized regression coefficients for log-transformed summer low flows with 8 explanatory variables. In**
 54 **contrast to Figure 3 in the manuscript here we use the winter temperature and precipitation instead of SWE_{max} and BF_{winter} .**

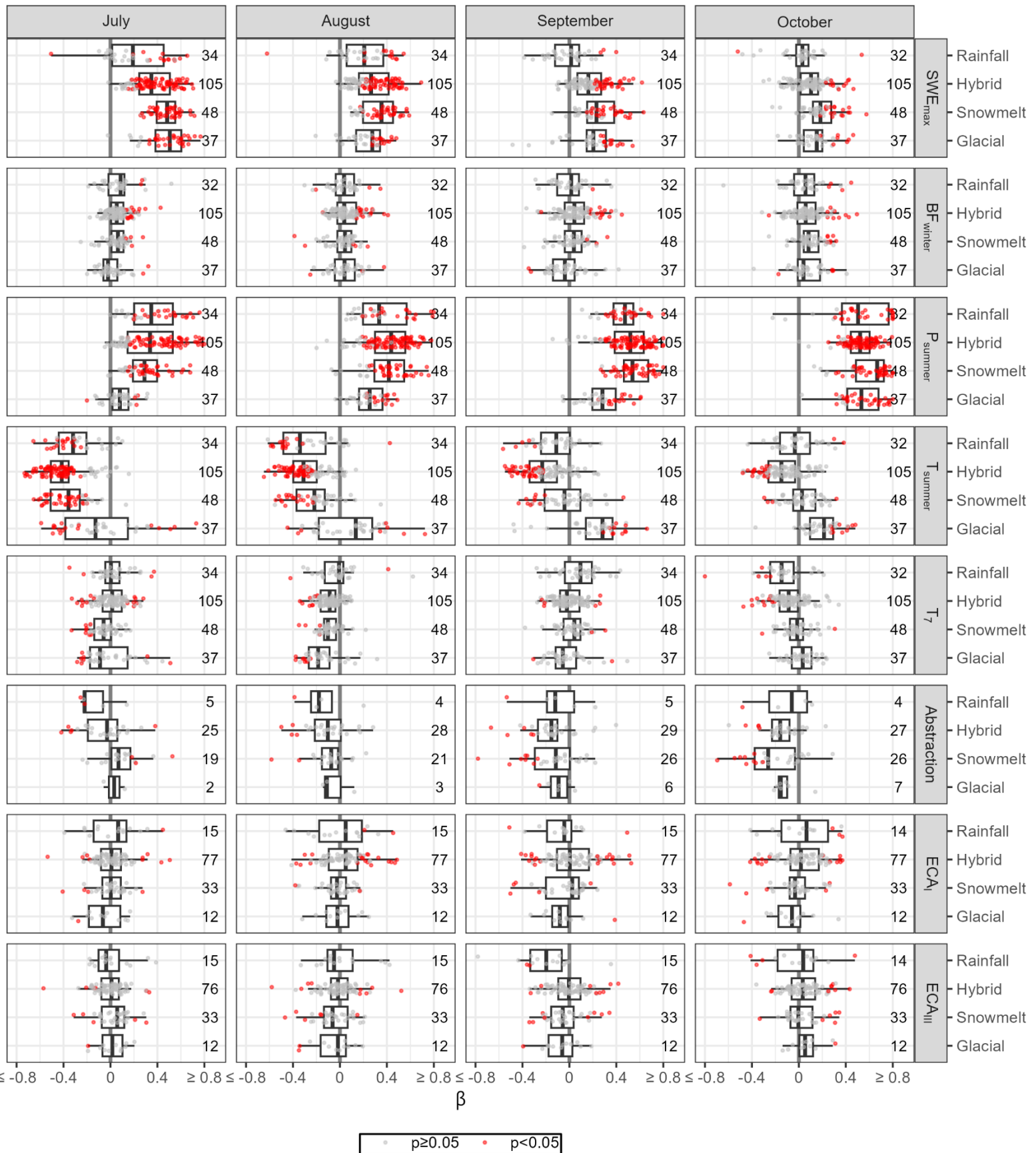


Figure D5: Standardized regression coefficients for log-transformed monthly low flows. The effect of SWE is larger earlier in the summer. The effect of BF_{winter} is minimal in all months. The effect of P_{summer} is largest in the later months, while the effect of temperature is strongest earlier in the season. The effects of the four other variables are small and mostly non-significant.

Table D1: Stationarity tests with split year 1995. The three tests correspond to the significance tests described in Section 2.4. The H-B test columns refer to the Holm-Bonferroni method. Significant results after applying the Holm-Bonferroni method are bolded.

Variable	Regime	N	Test 1 (positive)			Test 2 (positive, significant)		Test 3 (negative, significant)			
			% positive	p	H-B test	% positive & significant	p	H-B test	% negative & significant	p	H-B test
SWE _{max}	Rainfall	15	27%	0.12		0%	1		7%	0.54	
	Hybrid	68	29%	0.001	*	0%	1		4%	0.67	
	Snowmelt	41	34%	0.06		2%	0.88		0%	1	
	Glacial	23	48%	1		0%	1		0%	1	
BF _{winter}	Rainfall	15	13%	0.007		0%	1		0%	1	
	Hybrid	68	63%	0.04		6%	0.44		1%	0.97	
	Snowmelt	41	66%	0.06		5%	0.61		2%	0.88	
	Glacial	23	78%	0.01		4%	0.69		0%	1	
P _{summer}	Rainfall	15	80%	0.04		0%	1		0%	1	
	Hybrid	68	40%	0.11		1%	0.97		3%	0.86	
	Snowmelt	41	63%	0.12		0%	1		0%	1	
	Glacial	23	78%	0.01		9%	0.32		0%	1	
T _{summer}	Rainfall	15	60%	0.61		7%	0.54		0%	1	
	Hybrid	68	63%	0.04		7%	0.25		1%	0.97	
	Snowmelt	41	80%	0.0001	**	0%	1		0%	1	
	Glacial	23	65%	0.21		9%	0.32		0%	1	
T ₇	Rainfall	15	60%	0.61		0%	1		0%	1	
	Hybrid	68	54%	0.54		1%	0.97		0%	1	
	Snowmelt	41	15%	<0.0001	***	0%	1		12%	0.05	
	Glacial	23	39%	0.40		0%	1		9%	0.32	

Holm-Bonferroni significance levels: * p<0.05, **p<0.01, ***p<0.001

Table D2: Stationarity tests with split year 1995. The three tests correspond to the significance tests described in Section 2.4. The H-B test columns refer to the Holm-Bonferroni method. Significant results after applying the Holm-Bonferroni method are bolded.

Variable	Regime	N	Test 1 (positive)			Test 2 (positive, significant)		Test 3 (negative, significant)			
			% positive	p	H-B test	% positive & significant	p	H-B test	% negative & significant	p	H-B test
SWE _{max}	Rainfall	16	38%	0.45		0%	1		6%	0.56	
	Hybrid	72	32%	0.003		0%	1		3%	0.88	
	Snowmelt	41	32%	0.03		2%	0.88		0%	1	
	Glacial	23	52%	1.000		0%	1		0%	1	
BF _{winter}	Rainfall	16	19%	0.02		0%	1		0%	1	
	Hybrid	72	69%	0.001	*	4%	0.70		0%	1	
	Snowmelt	41	68%	0.03		5%	0.61		2%	0.88	
	Glacial	23	74%	0.04		4%	0.69		0%	1	
P _{summer}	Rainfall	16	88%	0.004		0%	1		0%	1	
	Hybrid	72	49%	0.91		3%	0.88		1%	0.98	
	Snowmelt	41	63%	0.12		5%	0.61		0%	1	
	Glacial	23	78%	0.011		17%	0.03		0%	1	
T _{summer}	Rainfall	16	62%	0.45		6%	0.56		0%	1	
	Hybrid	72	69%	0.001	*	7%	0.29		1%	0.98	
	Snowmelt	41	85%	<0.0001	***	5%	0.61		0%	1	
	Glacial	23	78%	0.01		9%	0.32		0%	1	
T ₇	Rainfall	16	62%	0.45		0%	1		0%	1	
	Hybrid	72	50%	1		1%	0.98		0%	1	
	Snowmelt	41	24%	0.001	*	0%			15%	0.02	
	Glacial	23	43%	0.67		0%	1		9%	0.32	

Holm-Bonferroni significance levels: * p<0.05, **p<0.01, ***p<0.001

Table D3: Stationarity tests with split year 1997. The three tests correspond to the significance tests described in Section 2.4. The H-B test columns refer to the Holm-Bonferroni method. Significant results after applying the Holm-Bonferroni method are bolded.

Variable	Regime	N	Test 1 (positive)			Test 2 (positive, significant)		Test 3 (negative, significant)			
			% positive	p	H-B test	% positive & significant	p	H-B test	% negative & significant	p	H-B test
SWE _{max}	Rainfall	16	31%	0.21		0%	1		12%	0.19	
	Hybrid	71	28%	0.0003	**	0%	1		1%	0.97	
	Snowmelt	40	22%	0.0007	*	2%	0.87		0%	1	
	Glacial	23	48%	1		0%	1		0%	1	
BF _{winter}	Rainfall	16	19%	0.02		0%	1		0%	1	
	Hybrid	71	69%	0.002		4%	0.70		0%	1	
	Snowmelt	40	65%	0.08		5%	0.60		2%	0.87	
	Glacial	23	74%	0.03		4%	0.69		0%	1	
P _{summer}	Rainfall	16	69%	0.21		6%	0.56		0%	1	
	Hybrid	71	46%	0.64		1%	0.97		3%	0.88	
	Snowmelt	40	57%	0.43		0%	1		0%	1	
	Glacial	23	78%	0.01		9%	0.32		0%	1	
T _{summer}	Rainfall	16	69%	0.21		6%	0.56		0%	1	
	Hybrid	71	73%	0.0001	**	7%	0.28		1%	0.97	
	Snowmelt	40	82%	<0.0001	**	0%	1		0%	1	
	Glacial	23	70%	0.09		0%	1		0%	1	
T ₇	Rainfall	16	62%	0.45		0%	1		0%	1	
	Hybrid	71	49%	1		0%	1		0%	1	
	Snowmelt	40	25%	0.002		2%	0.87		12%	0.05	
	Glacial	23	43%	0.68		0%	1		9%	0.32	

Holm-Bonferroni significance levels: * p<0.05, **p<0.01, ***p<0.001

Table D4: Stationarity tests with split year 1998. The three tests correspond to the significance tests described in Section 2.4. The H-B test columns refer to the Holm-Bonferroni method. Significant results after applying the Holm-Bonferroni method are bolded.

Variable	Regime	N	Test 1 (positive)			Test 2 (positive, significant)		Test 3 (negative, significant)		
			% positive	p	H-B test	% positive & significant	p	H-B test	% negative & significant	p
SWE _{max}	Rainfall	15	33%	0.30		0%	1		0%	1
	Hybrid	68	29%	0.001	*	0%	1		0%	1
	Snowmelt	39	26%	0.003		0%	1		3%	0.86
	Glacial	24	42%	0.54		0%	1		0%	1
BF _{winter}	Rainfall	15	20%	0.04		0%	1		0%	1
	Hybrid	68	66%	0.01		1%	0.97		0%	1
	Snowmelt	39	59%	0.34		8%	0.31		0%	1
	Glacial	24	71%	0.06		4%	0.71		0%	1
P _{summer}	Rainfall	15	67%	0.30		7%	0.54		0%	1
	Hybrid	68	49%	0.90		1%	0.97		1%	0.97
	Snowmelt	39	62%	0.20		0%	1		0%	1
	Glacial	24	79%	0.007		8%	0.34		0%	1
T _{summer}	Rainfall	15	67%	0.30		7%	0.54		0%	1
	Hybrid	68	60%	0.11		4%	0.67		0%	1
	Snowmelt	39	79%	0.0003	**	3%	0.86		3%	0.86
	Glacial	24	62%	0.31		0%	1		0%	1
T ₇	Rainfall	15	67%	0.30		0%	1		0%	1
	Hybrid	68	47%	0.72		0%	1		1%	0.97
	Snowmelt	39	28%	0.009		3%	0.86		3%	0.86
	Glacial	24	42%	0.54		0%	1		8%	0.34

Holm-Bonferroni significance levels: * p<0.05, **p<0.01, ***p<0.001

1 APPENDIX E: EFFECT OF FORESTRY ON LOW FLOWS

2 CONTENTS

3 Introduction 2

4 Data & Methods..... 2

5 Hypothesis Testing 2

6 Results 3

7 Power Analysis 7

8 Discussion..... 8

9 References 10

10

11 **Figures**

12 Figure E1: Spearman r correlations between filtered ECA coefficients and filtered $\log(Q7_{min})$ 5

13 Figure E2: The Type II (false negative) error rate for hypotheses H1 and H2..... 8

14

15 **Tables**

16 Table E 1 Results of hypothesis testing for H1, H2, and H3. H1 6

17

18

19 INTRODUCTION

20 Forest disturbance (wildfire, harvest, and/or insect-caused mortality) has been observed to both
21 increase and decrease warm-season low flows in the Pacific Northwest (Coble et al., 2020; Goeking &
22 Tarboton, 2020; Moore et al., 2020). Here we aim to apply longitudinal analysis techniques that have
23 been used on individual catchments by others (eg. Zhang & Wei, 2012). We aim to investigate the effect
24 that forest disturbance may have had on our 230 catchments.

25 Data & Methods

26 Hypothesis Testing

27 For each year from 1900-2022 we calculated forest age on a 30 m raster grid across British Columbia,
28 based on wildfire and forest harvest polygons (cutblocks). The cutblocks data includes forest harvest
29 records from crown land (95.5% of British Columbia), but not Private Managed Forests. For this analysis
30 we excluded 30 watersheds for which private lands constitute more than 10% of the watershed area.
31 We also excluded 97 watersheds for which less than 10% of the drainage area is recorded as having
32 been logged or burned since 1900.

33 Zhang and Wei (2012) calculated ECA coefficients based on tree age-height relationships that decrease
34 monotonically (but not linearly) from 100% at year 0 to between 0 and 15% at year 60. However, there
35 is evidence of a range of recovery times, as well as non-monotonic recovery curves (Coble et al., 2020;
36 Moore et al., 2020), so we chose to test four ECA coefficients which decrease from 100% to 0% over 5,
37 10, 20 and 60 years, respectively. We calculated the Equivalent Clearcut Area (ECA) for each watershed
38 and each year, based on these four ECA coefficients. This allows us to test a variety of hydrologic
39 recovery times.

40 We assess the Spearman rank correlation between ECA and $\log(Q7_{\min})$ after applying three data filtering
41 routines:

- 42 A) Jassby & Powell (1990) describe a method of drawing causal inferences from two autocorrelated,
43 possibly non-stationary time series. This method has applied in British Columbia and elsewhere
44 to study forestry effects on streamflow (Duan et al., 2017; Giles-Hansen et al., 2019; Li et al.,
45 2018; Zhang & Wei, 2012). First, both the independent variable time series (ECA) and the
46 dependent variable ($\log(Q7_{\min})$) are pre-whitened using an ARIMA model. We use the ARIMA
47 model with the best Akaike Information Criterion using the automated routine implemented in R
48 by Hyndman & Khandakar (2008).
- 49 B) We use the same pre-whitening strategy as 1) but for the dependent variable we use the
50 residuals from the optimized regression models (Section 3.4) instead of the time series of
51 $\log(Q7_{\min})$. This should remove the variability associated with climate from the dependent
52 variable.
- 53 C) We use the residuals from the optimized regression models (same as 2) but skip the pre-
54 whitening of both time series. This is done because pre-whitening can result in low-powered
55 statistical tests.

56 For each routine above, we then evaluate three hypotheses that, if true, would suggest a consistent
57 effect of forest disturbance on low flows:

- 58 H1: The number of significant ($p < 0.05$) correlations will be greater than expected by chance (5%).
59 This is evaluated using a one-sided binomial test with probability = 0.05.

60 H2: The fraction of positive/negative correlations will be greater than expected by chance. This is
61 evaluated using a two-sided binomial test with probability = 0.5.

62 H3: The strength of the effect will be largest in catchments that have been most disturbed. This is
63 evaluated by regressing the estimated correlation coefficients on the fraction of the catchment
64 that has been harvested or burned since 1900.

65

66 *Power Analysis*

67 The pre-whitening strategy used in routines 1 and 2 lacks statistical power if there is a causal
68 relationship between the two time series variables and a trend in the independent variable causes a
69 trend in the dependent variable (Jassby & Powell, 1990). This is because the pre-whitening has the
70 express purpose of removing trends and other non-stationarities in the time series. Many of ECA times
71 series in our sample do show strong trends (mostly increasing since the 1950s), so it is likely that these
72 analyses have low statistical power. We therefore tested the statistical power of hypotheses H1 and H2
73 using Monte Carlo analysis.

74 First, we found the Type I (false positive) error rate. For each catchment we:

- 75 1) Reordered the time series of $\log(Q7_{\min})$ 1000 times.
- 76 2) Fit ARIMA models to each reordered series.
- 77 3) For each of the 1000 simulations, we calculated Spearman's rank correlation coefficient
78 between the filtered ECA time series and the filtered $\log(Q7_{\min})$ series.
- 79 4) We noted the fraction of simulations resulting in significant (H1) and negative (H2) correlations.

80 We then evaluated H1 and H2 for each regime:

- 81 5) We simulated 10000 tests of H1 and H2 using the fractions derived in step 4. The number of
82 significant results for H1 and H2 is the Type I error rate.

83 We then explicitly included a causal relationship between ECA and $\log(Q7_{\min})$. After step 1 above, we
84 subtract a value proportional to the ECA from the reordered $\log(Q7_{\min})$ time series:

$$85 \log(Q7_{\min})'_t = \log(Q7_{\min})_t - \sigma \times ECA_t \times k \quad (A1)$$

86 Where ' denotes the perturbed value, t is the time step, σ is the standard deviation of $\log(Q7_{\min})$,
87 ECA_t is the value of ECA at time t , and k is a scaling factor which we term the 'Harvest Effect'.

88 After perturbation, we repeat steps 1-5. The result of step 5 is now the statistical power (1- Type II error
89 rate) for a particular Harvest Effect. We test Harvest Effects from 1 to 100.

90 **Results**

91 Hypothesis Testing

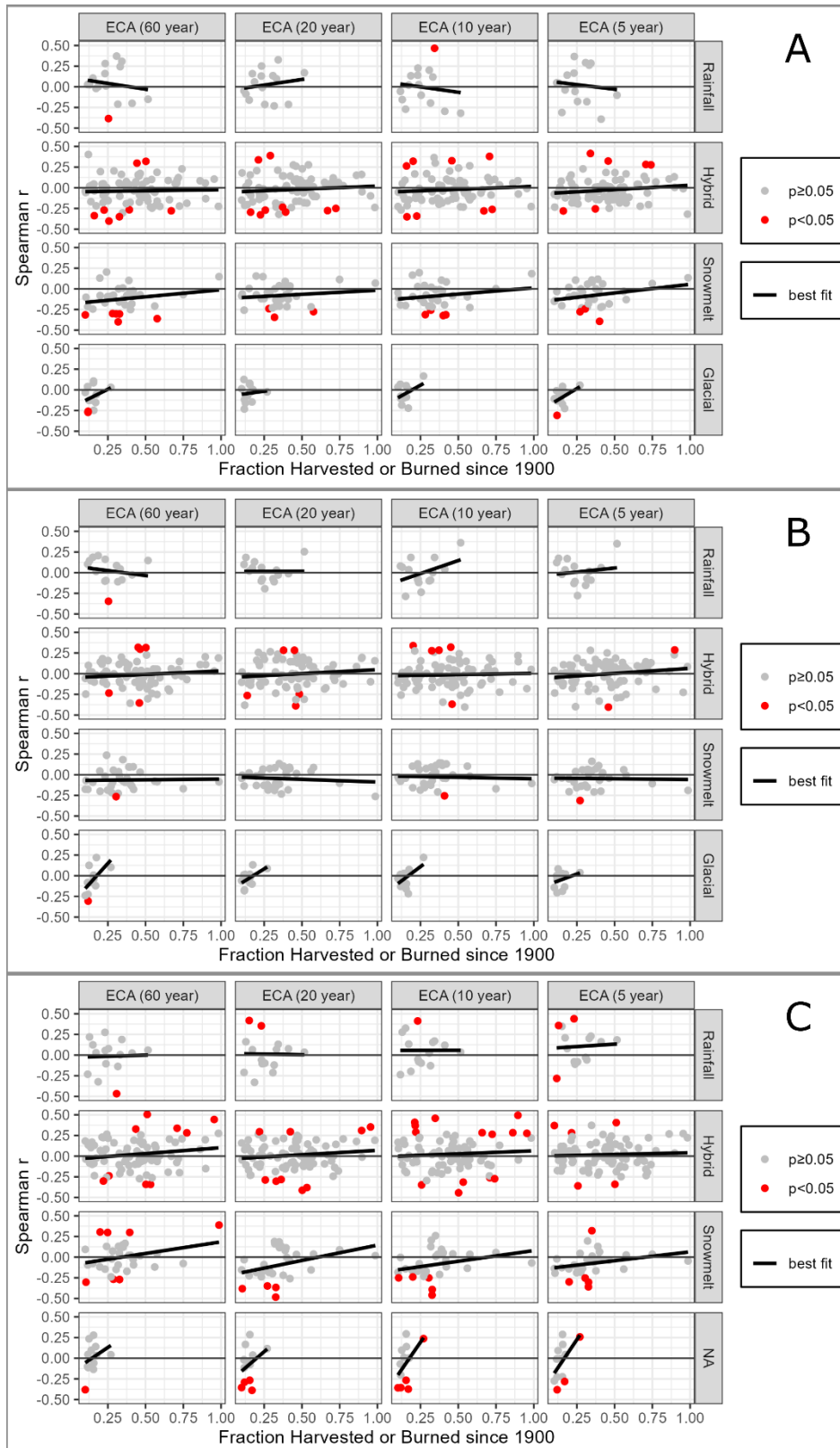
92 Figure A1 shows the Spearman correlations disaggregated by regime, and by ECA coefficient (60, 20, 10,
93 and 5 year recovery times), for routines A, B, and C. Table A1 shows the results of the hypothesis testing.
94 Each row of Table A1 corresponds to a panel in Figure A1.

95 For rainfall regimes, we cannot reject the null hypothesis for any of H1, H2, or H3, using any of the ECA
96 recovery times.

97 For hybrid regimes, we found very little evidence of any effect. Using routine A, we could reject H2 for
98 the 10-year recovery time (more negative correlations than expected by chance), suggesting a
99 downwards effect on low flows. On the other hand, using routine C we could also reject H1 for the 10-
100 year recovery time (more significant positive correlations than expected by chance), which implies the
101 opposite inference. We note that if we were to correct for the family-wise error rate using the Holm-
102 Bonferroni method, these results would not be considered statistically significant.

103 For snowmelt regimes, we found some evidence for both H1 and H2 using all three routines, suggesting
104 that forest disturbance tends to reduce low flows in these catchments. We found at least one significant
105 result for each recovery time. However, we note that the regressions against total disturbed area
106 suggest the smallest effects for the most disturbed catchments.

107 For glacial catchments we found limited evidence that forest disturbance reduces low flows. H1 has
108 significant for 10 and 20 year recovery times using routine C, and H2 was significant for a 5-year
109 recovery time using routine A.



110
111
112

Figure E1: Spearman r correlations between filtered ECA coefficients and filtered $\log(Q7_{\min})$. Panel A corresponds to filtering routine A, panel B to routine B, and panel C to routine C.

113
114
115

Table E 1 Results of hypothesis testing for H1, H2, and H3. H1: Binomial test for more significant ($p < 0.05$) correlations than expected by chance. H2: Binomial test for more positive/negative correlations than expected by chance. H3: linear regression between Spearman r and fraction harvested or burned since 1900.

Filtering Routine	Regime	ECA Recovery Time (years)	H1 (+ve)	H1 (-ve)	H2		H3		N
			p-value	p-value	% positive	p-value	slope	p-value	
A	Rainfall	60	1	0.54	67	0.30	-0.28	0.60	15
		20	1	1	53	1	0.27	0.55	15
		10	0.54	1	53	1	-0.26	0.65	15
		5	1	1	53	1	-0.22	0.70	15
	Hybrid	60	0.92	0.22	44	0.37	0.03	0.76	81
		20	0.92	0.11	46	0.51	0.07	0.39	81
		10	0.58	0.58	38	0.04	0.07	0.40	81
		5	0.58	0.92	41	0.12	0.11	0.16	81
	Snowmelt	60	1	0.01	18	0.0003	0.17	0.25	33
		20	1	0.23	30	0.04	0.10	0.45	33
		10	1	0.08	27	0.01	0.15	0.29	33
		5	1	0.23	30	0.04	0.21	0.11	33
	Glacial	60	1	0.12	33	0.39	0.91	0.34	12
		20	1	1	42	0.77	0.25	0.75	12
		10	1	1	33	0.39	1.02	0.19	12
		5	1	0.46	17	0.04	1.10	0.14	12
B	Rainfall	60	1	0.54	60	0.61	-0.24	0.53	15
		20	1	1	53	1	0.01	0.98	15
		10	1	1	53	1	0.63	0.13	15
		5	1	1	53	1	0.19	0.63	15
	Hybrid	60	0.78	0.92	43	0.27	0.08	0.27	81
		20	0.92	0.78	44	0.37	0.10	0.24	81
		10	0.58	0.98	47	0.66	0.03	0.72	81
		5	0.98	0.98	59	0.12	0.12	0.12	81
	Snowmelt	60	1	0.82	27	0.01	0.02	0.89	33
		20	1	1	42	0.49	-0.06	0.58	33
		10	1	0.82	36	0.16	-0.04	0.77	33
		5	1	0.82	39	0.30	-0.02	0.87	33
	Glacial	60	1	0.46	33	0.39	2.03	0.05	12
		20	1	1	42	0.77	1.14	0.07	12
		10	1	1	50	1	1.37	0.08	12
		5	1	1	50	1	0.67	0.33	12
C	Rainfall	60	1	0.54	67	0.30	0.06	0.91	15
		20	0.17	1	53	1	-0.03	0.96	15
		10	0.54	1	60	0.61	0.004	0.99	15
		5	0.17	0.54	60	0.61	0.12	0.82	15
	Hybrid	60	0.22	0.58	52	0.82	0.13	0.19	81
		20	0.22	0.38	56	0.37	0.10	0.29	81
		10	0.01	0.38	51	1	0.08	0.43	81
		5	0.58	0.92	52	0.82	0.10	0.25	81
	Snowmelt	60	0.08	0.08	48	1	0.25	0.22	33
		20	1	0.02	33	0.08	0.34	0.07	33
		10	1	0.01	33	0.08	0.23	0.19	33
		5	0.82	0.02	24	0.005	0.19	0.25	33
	Glacial	60	1	0.46	58	0.77	1.23	0.34	12
		20	1	0.002	33	0.39	1.58	0.30	12
		10	0.46	0.002	50	1	2.66	0.10	12
		5	0.46	0.12	42	0.77	2.71	0.08	12

116 Power Analysis

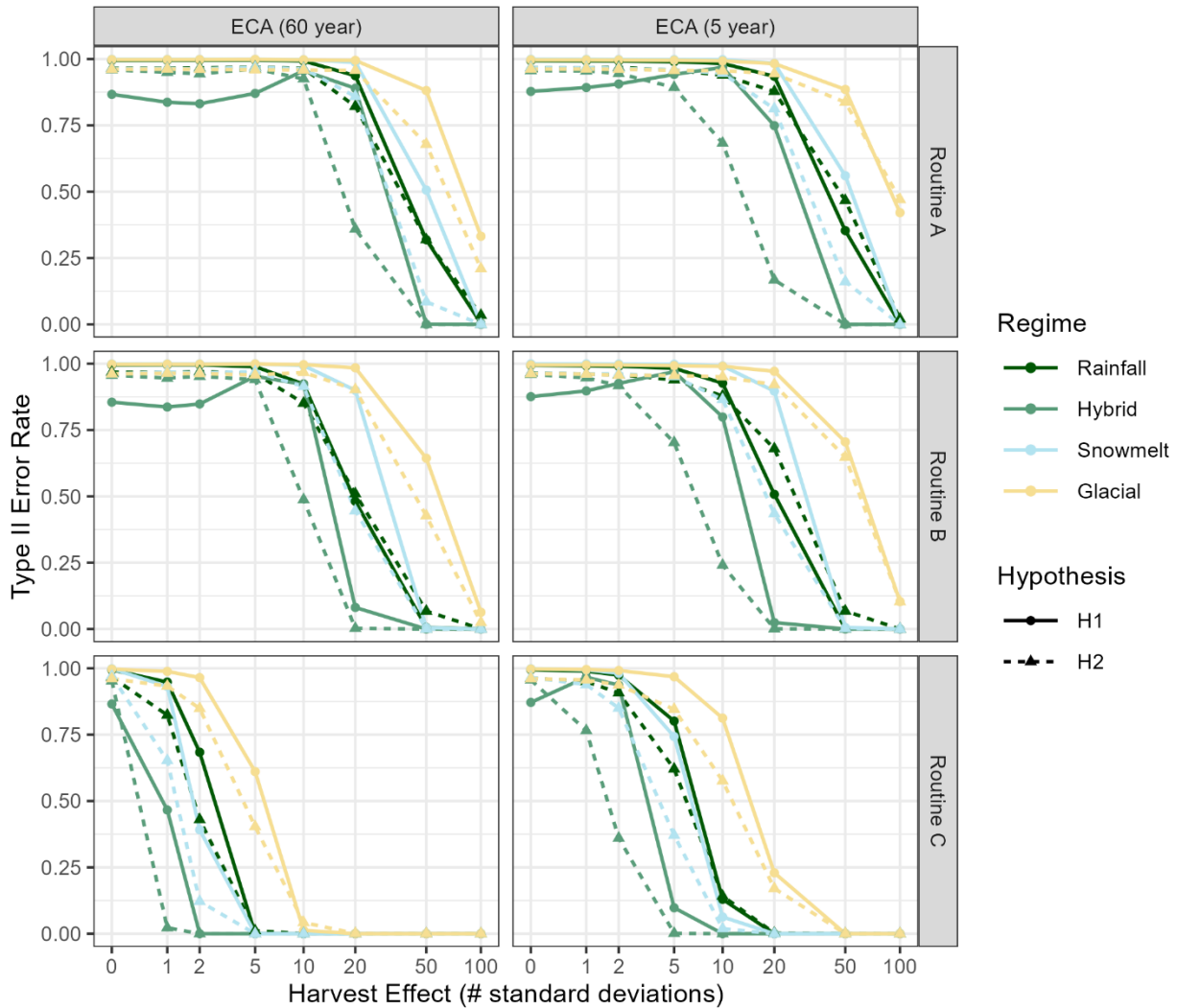
117 Figure A2 shows the results of the power analysis for 60-year and 5-year ECA coefficients. The x-axis of
118 each plot is the Harvest Effect (k) in Equation A1. This is the number of standard deviations by which an
119 ECA of 1 would be expected to perturb the low flow time series. For example, a harvest effect of 1
120 suggests that a clearcut of the entire catchment would reduce $\log(Q7_{\min})$ by 1 standard deviation. The y--
121 axis is the Type II error (false negative) error rate, or $1-(\text{statistical power})$. For a Harvest Effect of 0 there
122 is no genuine effect, so the x-intercept can be interpreted as $1-(\text{Type I error rate})$.

123 Routine A results in very low statistical power. This is the pre-whitening strategy suggested by Jassby &
124 Powell (1990) and used extensively by Zhang & Wei (2012), Li et al. (2018), and others. The test will
125 almost always fail to detect a true effect, except for Harvest Effects exceeding about 10. Hybrid regimes
126 are slightly more likely to produce a significant result, even when there is no genuine effect.

127 Routine B is only slightly more powerful than routine A. However, most of the statistical tests will still
128 fail to detect a true effect for all but the largest Harvest Effects.

129 Routine C (no pre-whitening) has better statistical power than routines A and B. For a Harvest Effect of
130 2, the Type II error rate drops to almost 0 for the hybrid regime, for a 60-year recovery time, for both H1
131 and H2. The x-intercept for routine C is similar to the x-intercept for routines A and B, which suggests
132 that the pre-whitening strategy does not reduce the Type I error rate (false positives).

133 In general, the statistical power is greatest for the Hybrid regime and weakest for the Rainfall and Glacial
134 regimes, because there are many Hybrid catchments (81) and few Rainfall (15) and Glacial (12)
135 catchments. The power also tends to be greater for a 60-year recovery time than a 5-year recovery time
136 because ECA (60 year) is always larger than ECA (5 year), so the perturbation applied in Equation A1 is
137 larger than for ECA (60 year). However, ECA (60 year) also tends to show stronger autocorrelation, so
138 the pre-whitening strategy in routines A and B removes more of the variance, reducing the statistical
139 power.



141
142 **Figure E2: The Type II (false negative) error rate for hypotheses H1 and H2.**

143 **Discussion**

144 Overall, the evidence of increases or decreases in low flows following forest disturbance is
145 weak. We tried many statistical tests here and few produced significant results. This could be
146 due to a genuine absence of substantial effects, or because the tests applied are statistically
147 weak.

148 The weak statistical power found in the power analysis arises for several reasons. First, the pre-
149 whitening strategy is recognized to reduce power where a trend in the independent variable
150 manifests as a trend in the dependent variable (Jassby & Powell, 1990). Second, most of the
151 catchments analysed here have only been moderately disturbed, so the signal to noise ratio in
152 these data is smaller than in studies of small catchments that have been entirely harvested.
153 Third, for many of the catchments studied here, harvesting has progressed at a relatively

154 consistent pace, so there are few ‘shocks’ that would produce dramatic changes in low flows
155 from year to year.

156 Despite these shortcomings, we found relatively consistent evidence of low-flow reductions in
157 snowmelt-dominated catchments. We found weaker evidence of reductions in glacial
158 catchments. Despite high statistical power in hybrid catchments, we did not find consistent
159 evidence of low-flow increases or decreases in these catchments.

160 These results contrast somewhat with the literature. First, we did not observe short-term
161 increases in low flows that have been reported, particularly for warmer catchments (Coble et
162 al., 2020; Moore et al., 2020). Second, we found the most consistent evidence of decreases to
163 low flows in colder, snowmelt-dominated catchments, which contrasts with the findings of
164 Moore et al. (2020) that results in colder catchments are the most mixed.

165 In the main text we found that snowmelt-dominated catchments are most sensitive to summer
166 precipitation, so we hypothesize that quicker runoff is the primary mechanism that causes a
167 reduction in low flows following forest disturbance in these catchments. Given that low flows in
168 these catchments are not very sensitive to temperature or winter snow accumulation, we argue
169 that disturbance-induced changes to spring snowmelt and to summer evapotranspiration
170 probably have minor impacts.

171

172 **References**

- 173 Coble, A. A., Barnard, H., Du, E., Johnson, S., Jones, J., Keppeler, E., Kwon, H., Link, T. E., Penaluna, B. E.,
174 Reiter, M., River, M., Puettmann, K., & Wagenbrenner, J. (2020). Long-term hydrological
175 response to forest harvest during seasonal low flow: Potential implications for current forest
176 practices. *Science of The Total Environment*, 730, 138926.
177 <https://doi.org/10.1016/j.scitotenv.2020.138926>
- 178 Duan, L., Man, X., Kurylyk, B. L., Cai, T., & Li, Q. (2017). Distinguishing streamflow trends caused by
179 changes in climate, forest cover, and permafrost in a large watershed in northeastern China.
180 *Hydrological Processes*, 31(10), 1938–1951. <https://doi.org/10.1002/hyp.11160>
- 181 Giles-Hansen, K., Li, Q., & Wei, X. (2019). The Cumulative Effects of Forest Disturbance and Climate
182 Variability on Streamflow in the Deadman River Watershed. *Forests*, 10(2), Article 2.
183 <https://doi.org/10.3390/f10020196>
- 184 Goeking, S. A., & Tarboton, D. G. (2020). Forests and Water Yield: A Synthesis of Disturbance Effects on
185 Streamflow and Snowpack in Western Coniferous Forests. *Journal of Forestry*, 118(2), 172–192.
186 <https://doi.org/10.1093/jofore/fvz069>
- 187 Hyndman, R. J., & Khandakar, Y. (2008). Automatic Time Series Forecasting: The forecast Package for R.
188 *Journal of Statistical Software*, 27, 1–22. <https://doi.org/10.18637/jss.v027.i03>
- 189 Jassby, A. D., & Powell, T. M. (1990). Detecting Changes in Ecological Time Series. *Ecology*, 71(6), 2044–
190 2052. <https://doi.org/10.2307/1938618>
- 191 Li, Q., Wei, X., Zhang, M., Liu, W., Giles-Hansen, K., & Wang, Y. (2018). The cumulative effects of forest
192 disturbance and climate variability on streamflow components in a large forest-dominated
193 watershed. *Journal of Hydrology*, 557, 448–459. <https://doi.org/10.1016/j.jhydrol.2017.12.056>
- 194 Moore, R. D. (Dan), Gronsdahl, S., & McCleary, R. (2020). Effects of Forest Harvesting on Warm-Season
195 Low Flows in the Pacific Northwest: A Review: *Confluence: Journal of Watershed Science and*
196 *Management*, 4(1), Article 1. <https://doi.org/10.22230/jwsm.2020v4n1a35>
- 197 Zhang, M., & Wei, X. (2012). The effects of cumulative forest disturbance on streamflow in a large
198 watershed in the central interior of British Columbia, Canada. *Hydrology and Earth System*
199 *Sciences*, 16(7), 2021–2034. <https://doi.org/10.5194/hess-16-2021-2012>

200

1 **Appendix F: Model Performance for Long Time Series**

2

3 These figures show the results of historical simulations for individual stations along with measured data for select stations.
4 For hybrid, snowmelt-dominated, and glacial regimes we show stations with mostly continuous data beginning before
5 1950. No rainfall-dominated stations have continuous data beginning before 1950, so we show four stations with time
6 series beginning in the 1950's.

7 The figures show the 10-year running mean of $Q7_{min}$ for both predicted and measured time series. We allow up to 5 years
8 of missing data in the 10-year mean, and show the degree of missingness by the transparency of the lines.

9 **Table of Figures**

10 Figure F1: Gauge ID 08DB001, Nass River Above Shumal Creek 2

11 Figure F2: Gauge ID 08EE004, Bulkley River at Quick 2

12 Figure F3: Gauge ID 08EF001, Skeena River at Usk..... 3

13 Figure F4: Gauge ID 08HA001, Chemainus River near Westholme 3

14 Figure F5: Gauge ID 08HA003, Koksilah River at Cowichan Station 4

15 Figure F6: Gauge ID 08HB014, Sarita River near Bamfield 4

16 Figure F7: Gauge ID 08HB024, Tsable River near Fanny Bay 5

17 Figure F8: Gauge ID 08JE001, Stuart River near Fort St. James 5

18 Figure F9: Gauge ID 08KH001, Quesnel River at Likely 6

19 Figure F10: Gauge ID 08KH006, Quesnel River near Quesnel 6

20 Figure F11: Gauge ID 08LA001, Clearwater River near Clearwater Station..... 7

21 Figure F12: Gauge ID 08LB020, Barriere River at the Mouth..... 7

22 Figure F13: Gauge ID 08LD001, Adams River near Squilax 8

23 Figure F14: Gauge ID 08LE031, South Thompson River at Chase 8

24 Figure F15: Gauge ID 08MA001, Chilko River near Redstone..... 9

25 Figure F16: Gauge ID 08MA002, Chilko River at Outlet of Chilko Lake 9

26 Figure F17: Gauge ID 08MG005, Lillooet River near Pemberton..... 10

27 Figure F19: Gauge ID 08MG016, Chilliwack River at Outlet of Chilliwack Lake 10

28 Figure F18: Gauge ID 08MH001, Chilliwack River at Vedder Crossing 11

29 Figure F20: Gauge ID 08NA002, Columbia River at Nicholson..... 11

30 Figure F21: Gauge ID 08NH006, Moyie River at Eastport 12

31 Figure F22: Gauge ID 08NH032, Boundary Creek near Porthill 12

32 Figure F23: Gauge ID 08NJ013, Slocan River near Crescent Valley 13

33 Figure F24: Gauge ID 08NN012, Kettle River Near Laurier 13

34 Figure F25: Gauge ID 08NN013, Kettle River Near Ferry 14

35 Figure F26: Gauge ID 08NP001, Flathead River at Flathead 14

36

37

38

39

40

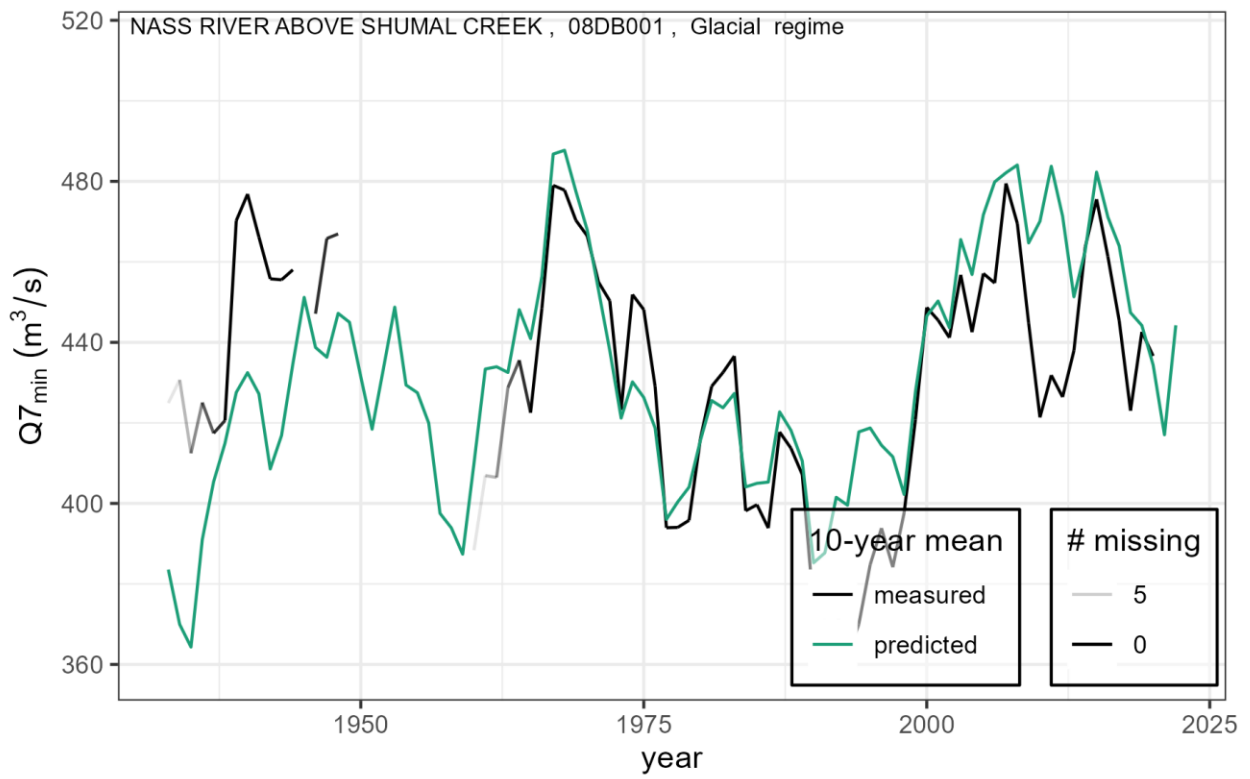


Figure F1: Gauge ID 08DB001, Nass River Above Shumal Creek

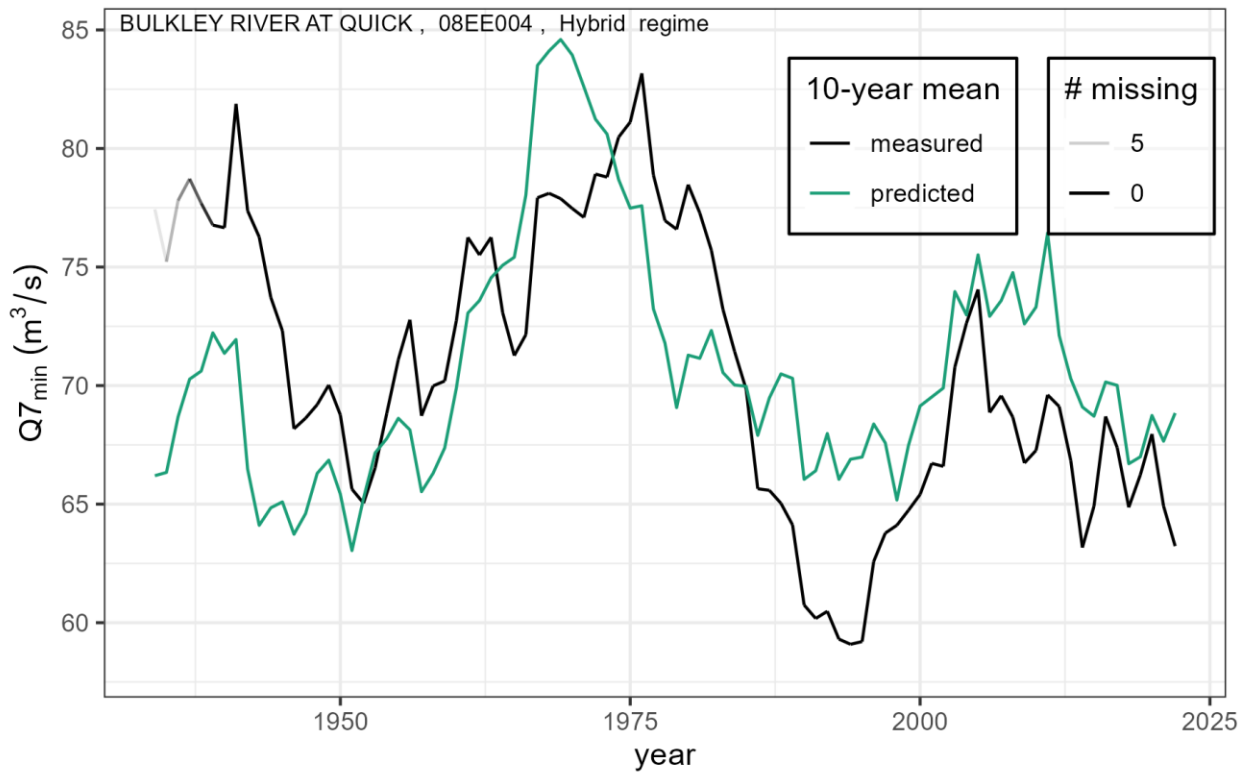


Figure F2: Gauge ID 08EE004, Bulkley River at Quick

41
42

43
44

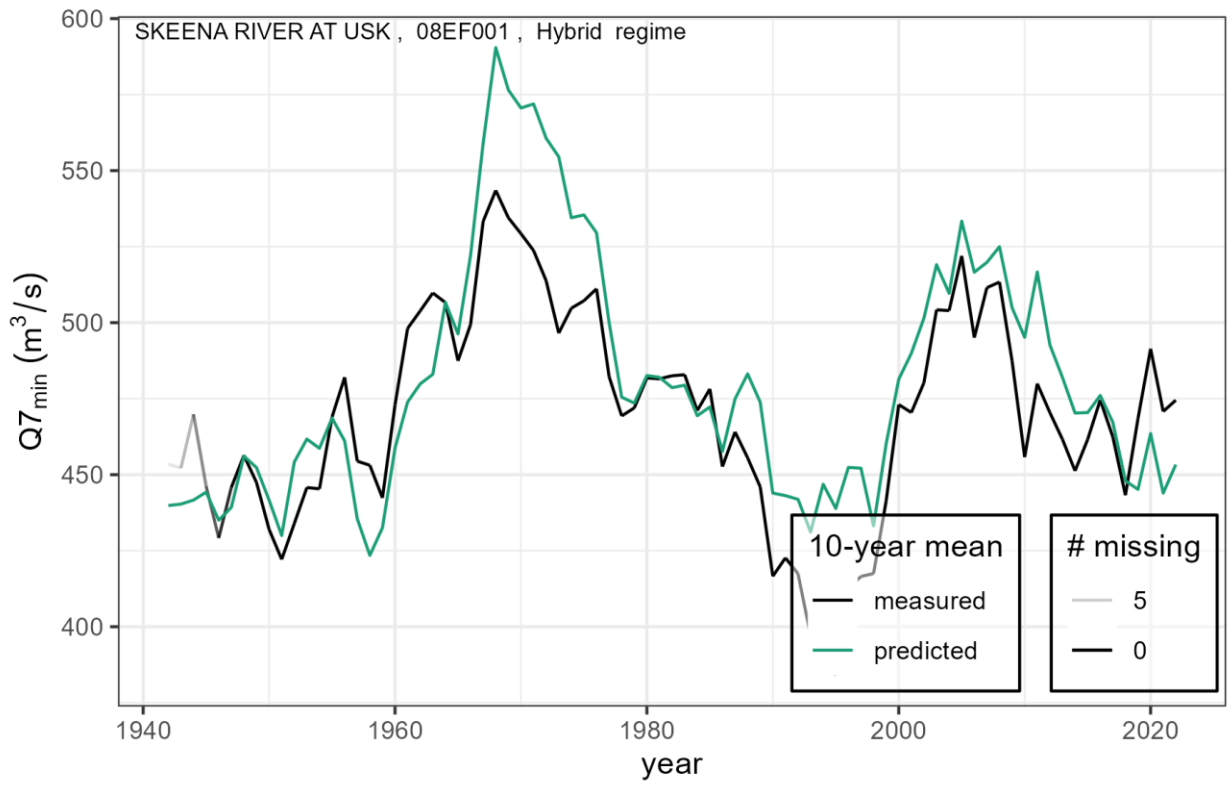


Figure F3: Gauge ID 08EF001, Skeena River at Usk

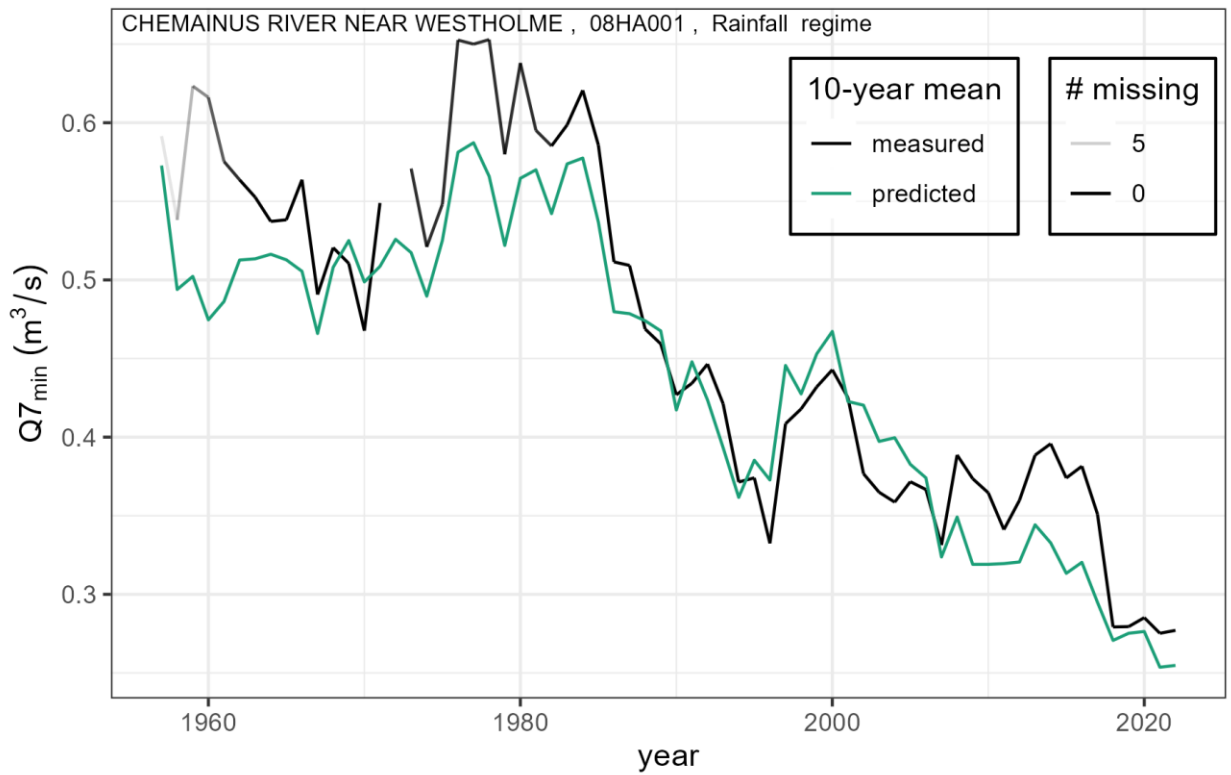


Figure F4: Gauge ID 08HA001, Chemainus River near Westholme

45
46

47
48

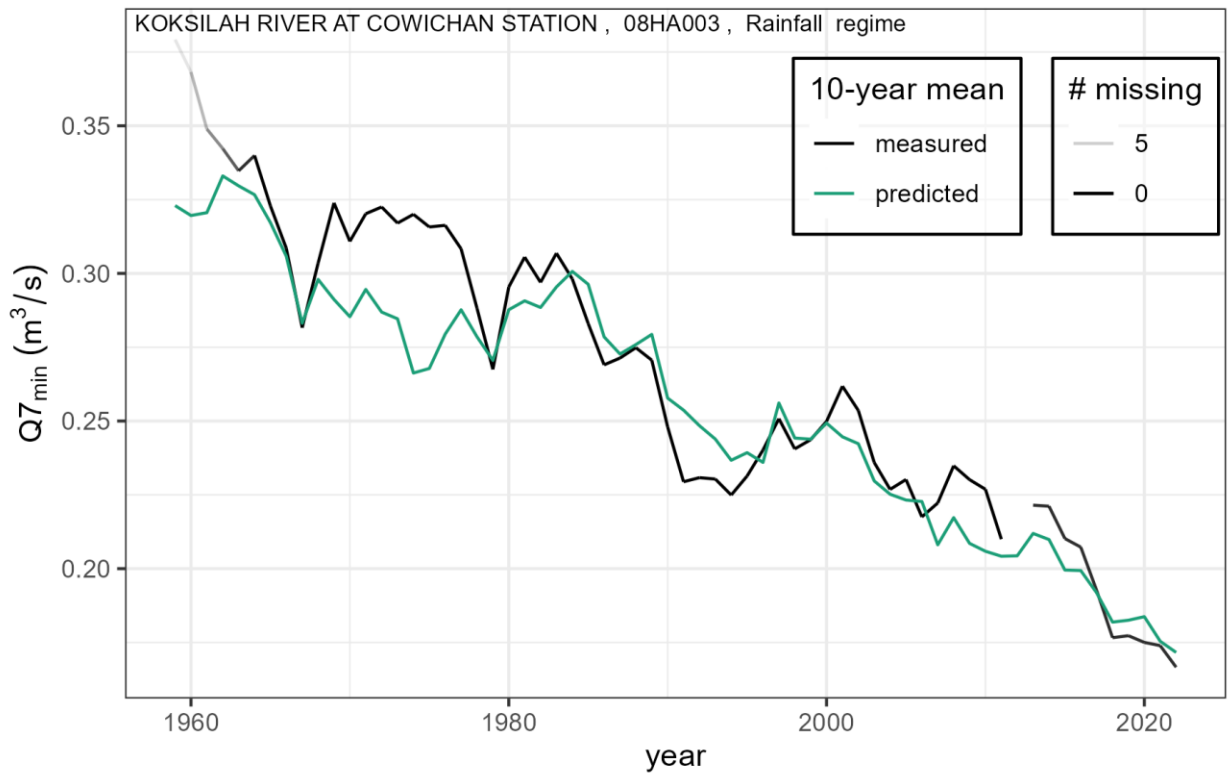


Figure F5: Gauge ID 08HA003, Koksilah River at Cowichan Station

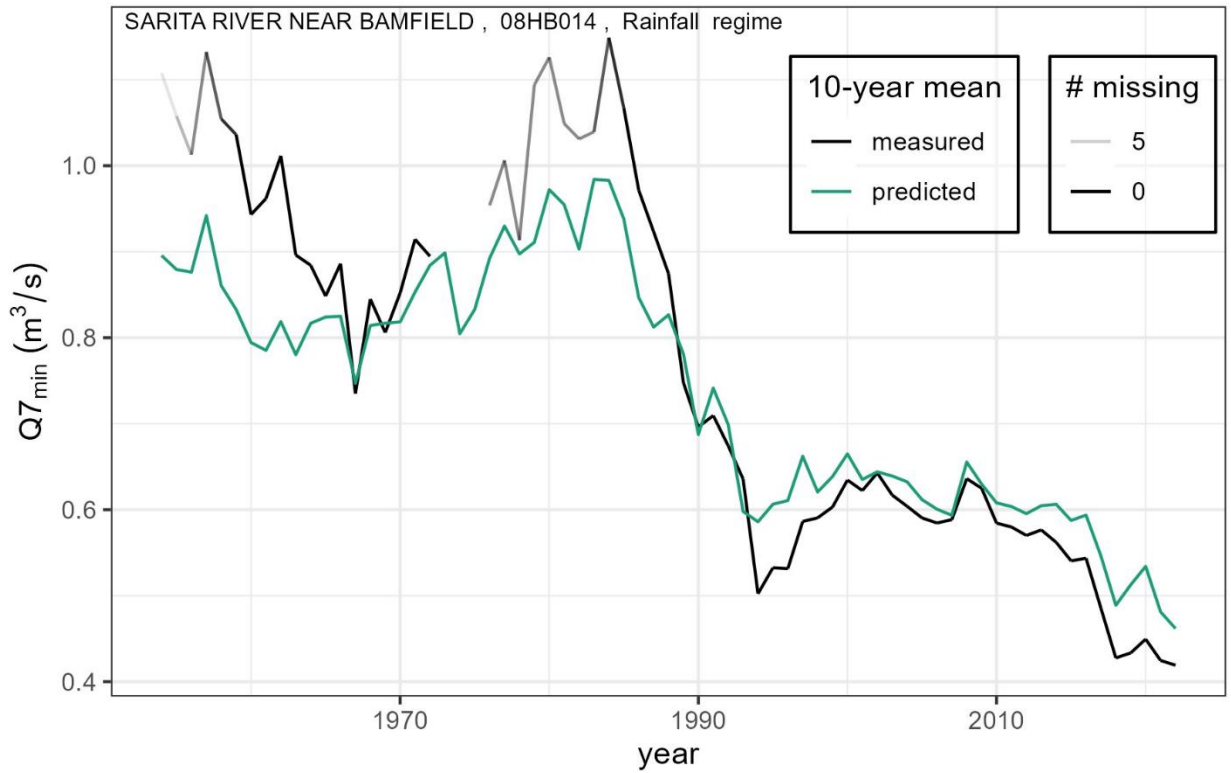


Figure F6: Gauge ID 08HB014, Sarita River near Bamfield

49
50

51
52
53

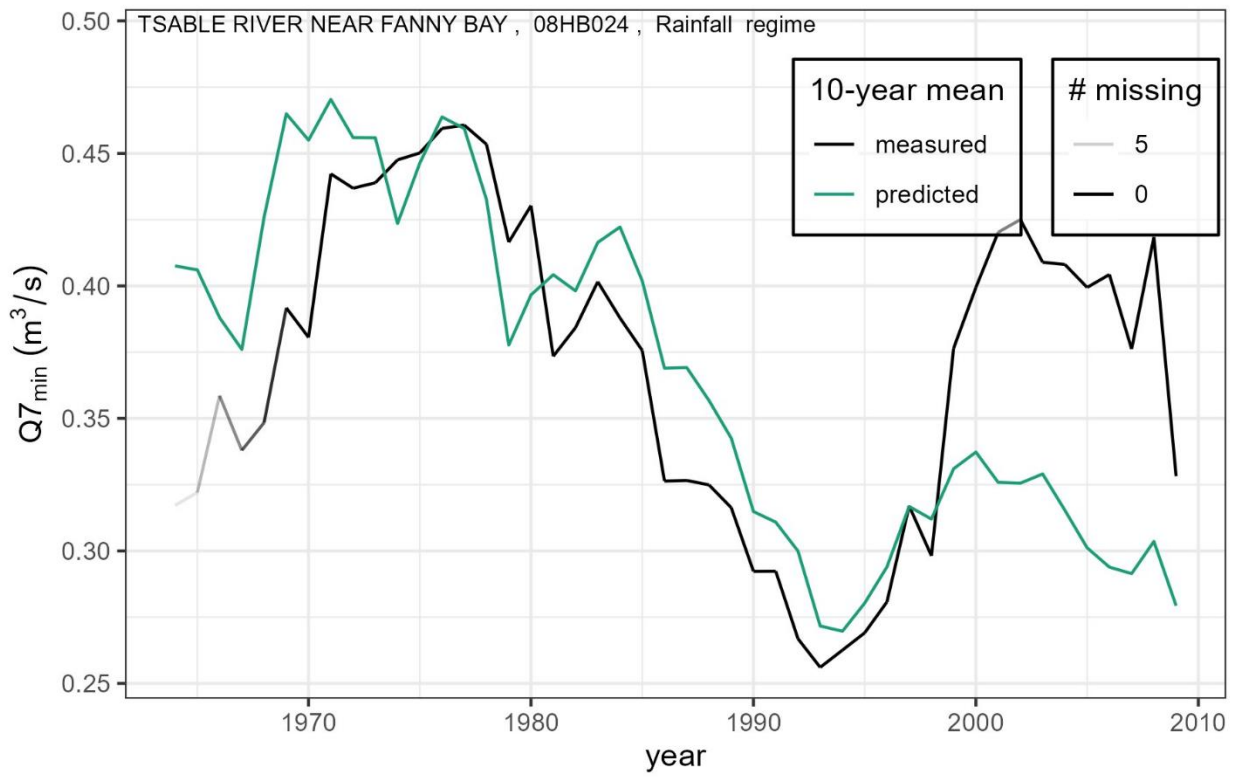


Figure F7: Gauge ID 08HB024, Tsable River near Fanny Bay

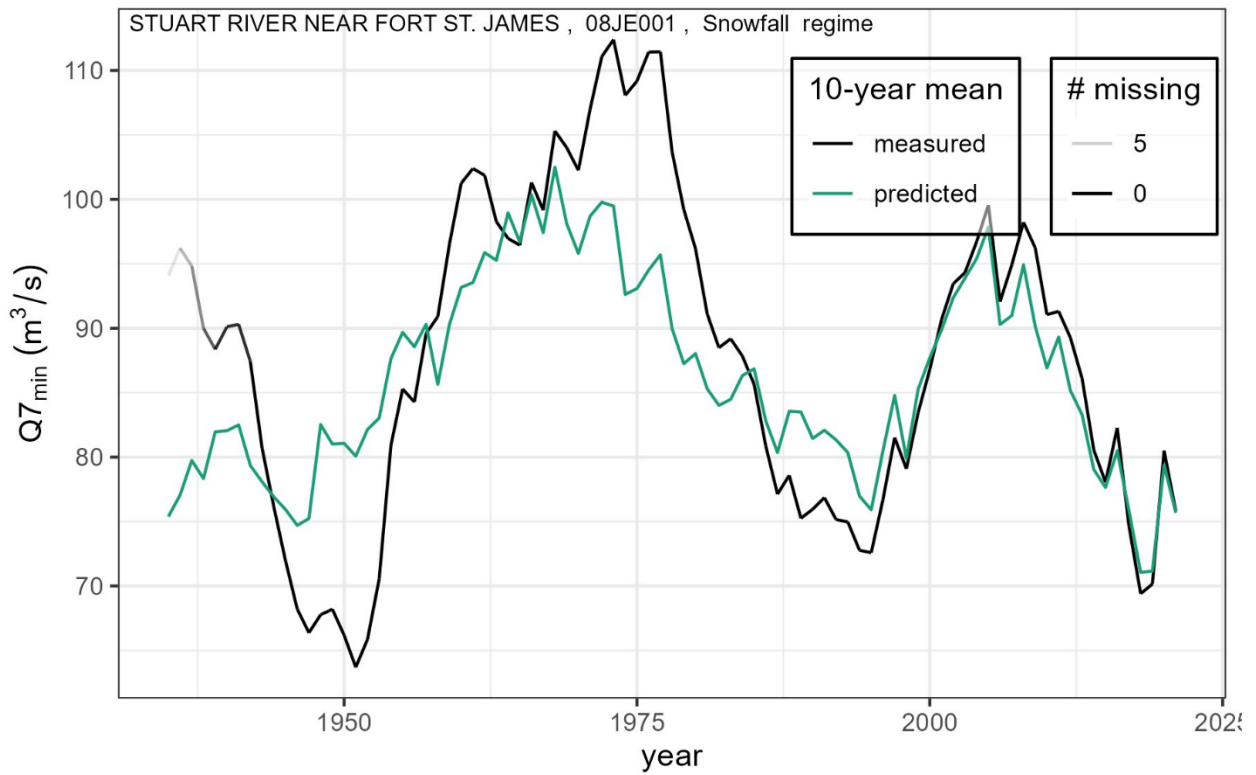


Figure F8: Gauge ID 08JE001, Stuart River near Fort St. James

54
55

56
57

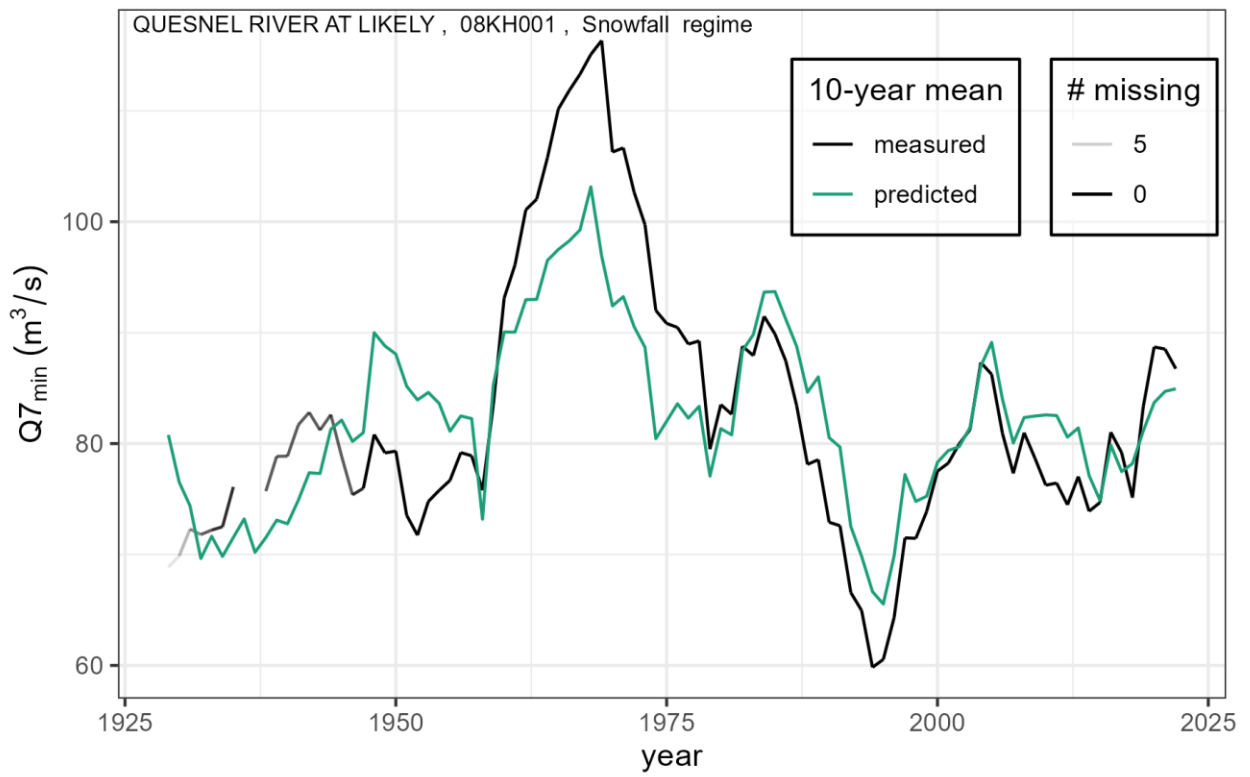


Figure F9: Gauge ID 08KH001, Quesnel River at Likely

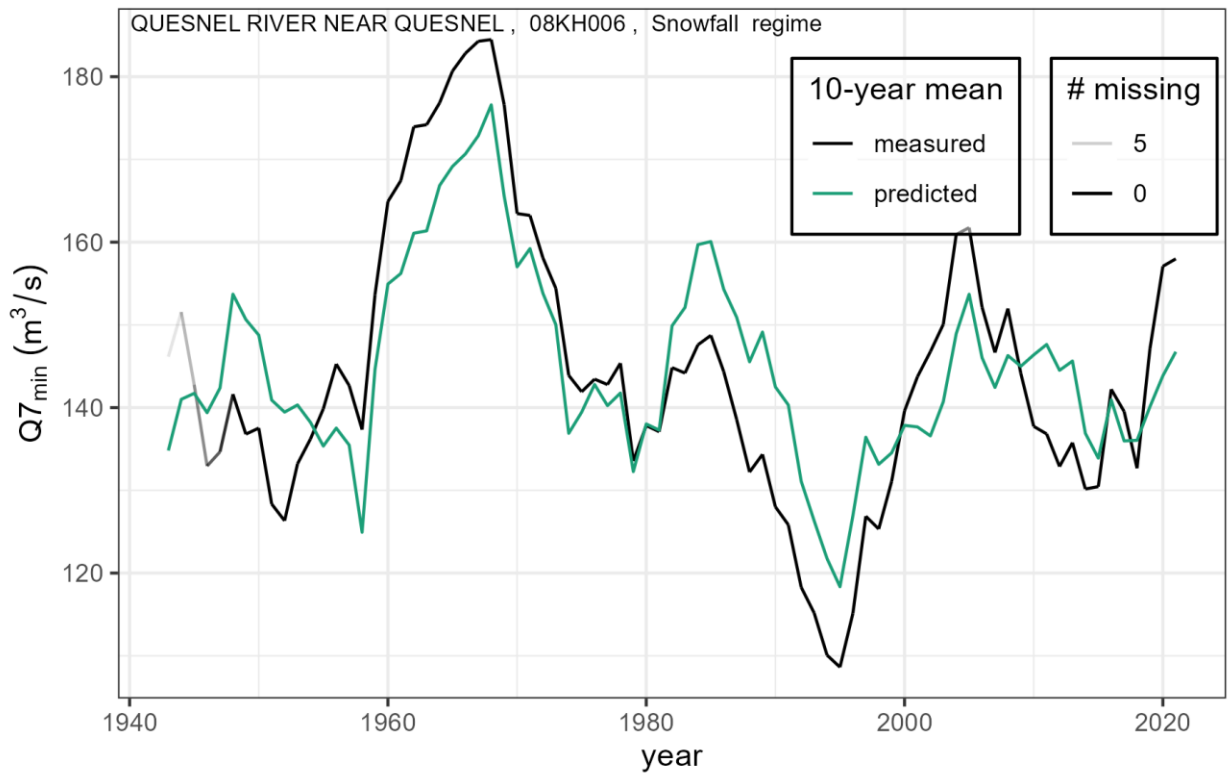


Figure F10: Gauge ID 08KH006, Quesnel River near Quesnel

58
59

60
61
62

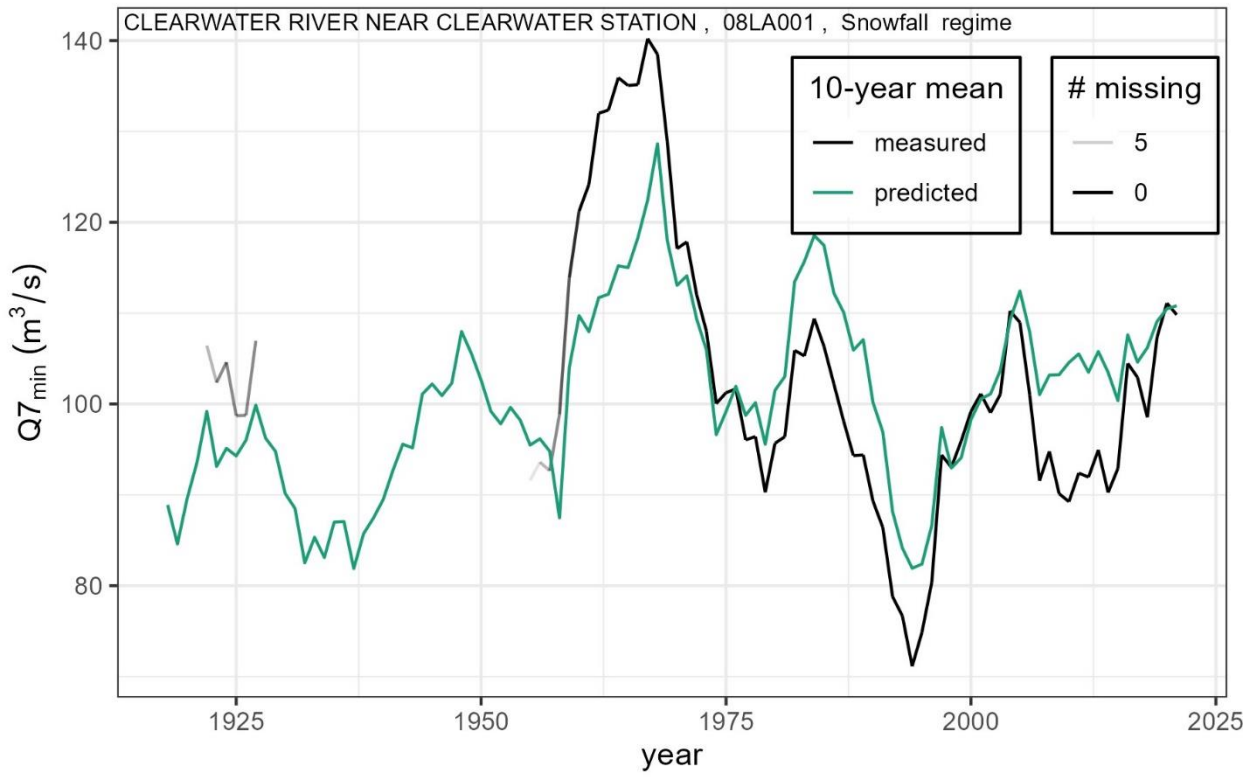


Figure F11: Gauge ID 08LA001, Clearwater River near Clearwater Station

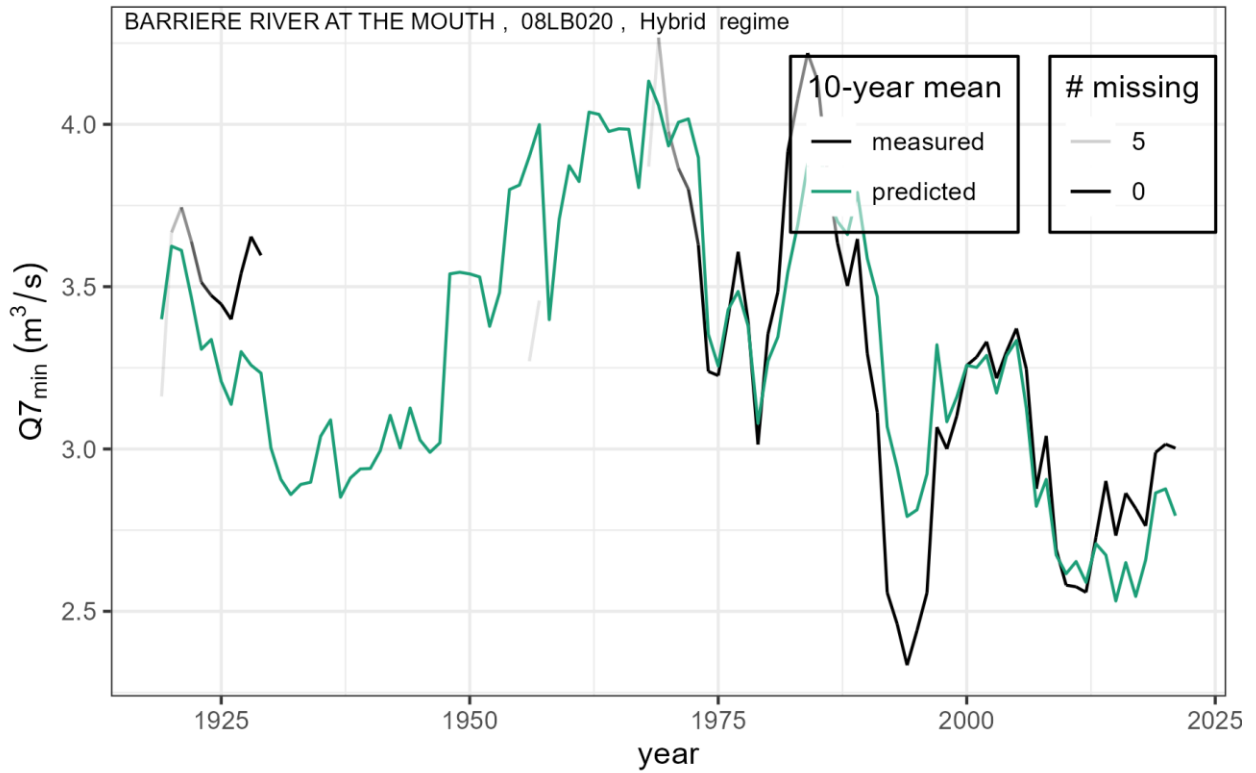


Figure F12: Gauge ID 08LB020, Barriere River at the Mouth

63
64

65
66

67

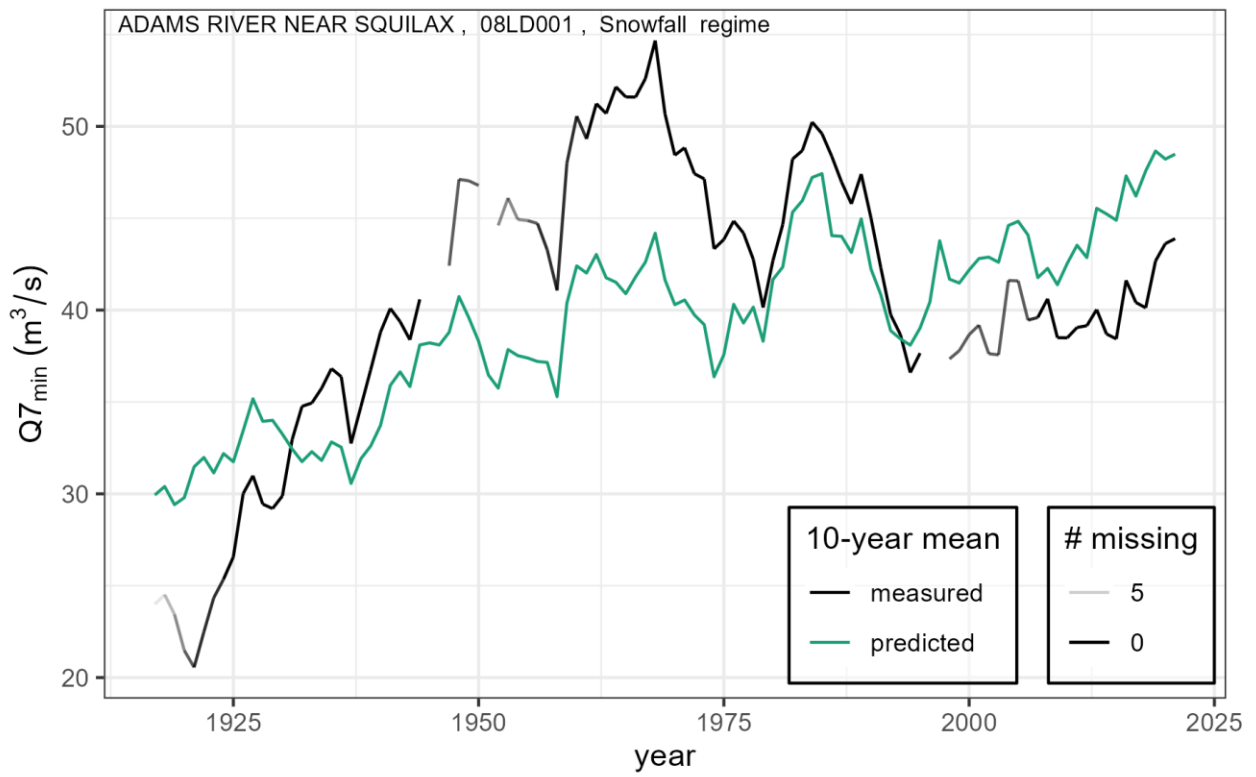


Figure F13: Gauge ID 08LD001, Adams River near Squilax

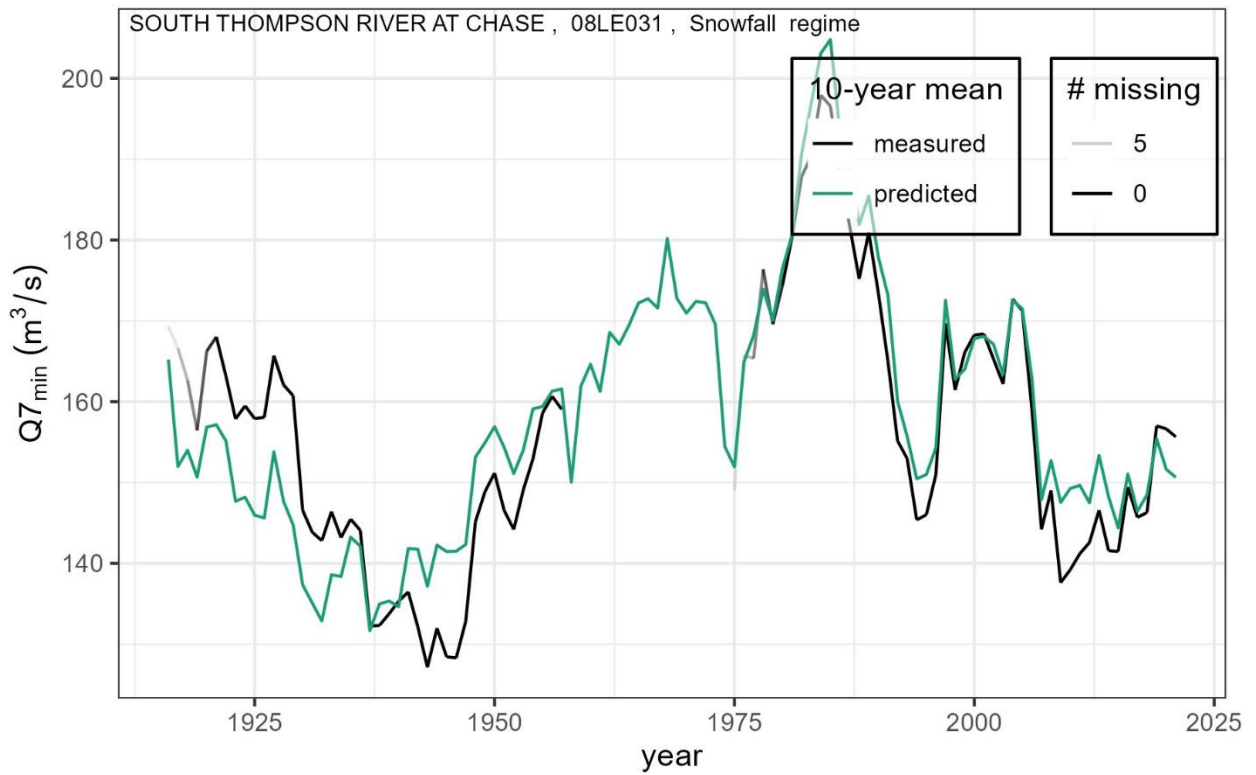


Figure F14: Gauge ID 08LE031, South Thompson River at Chase

68
69

70
71

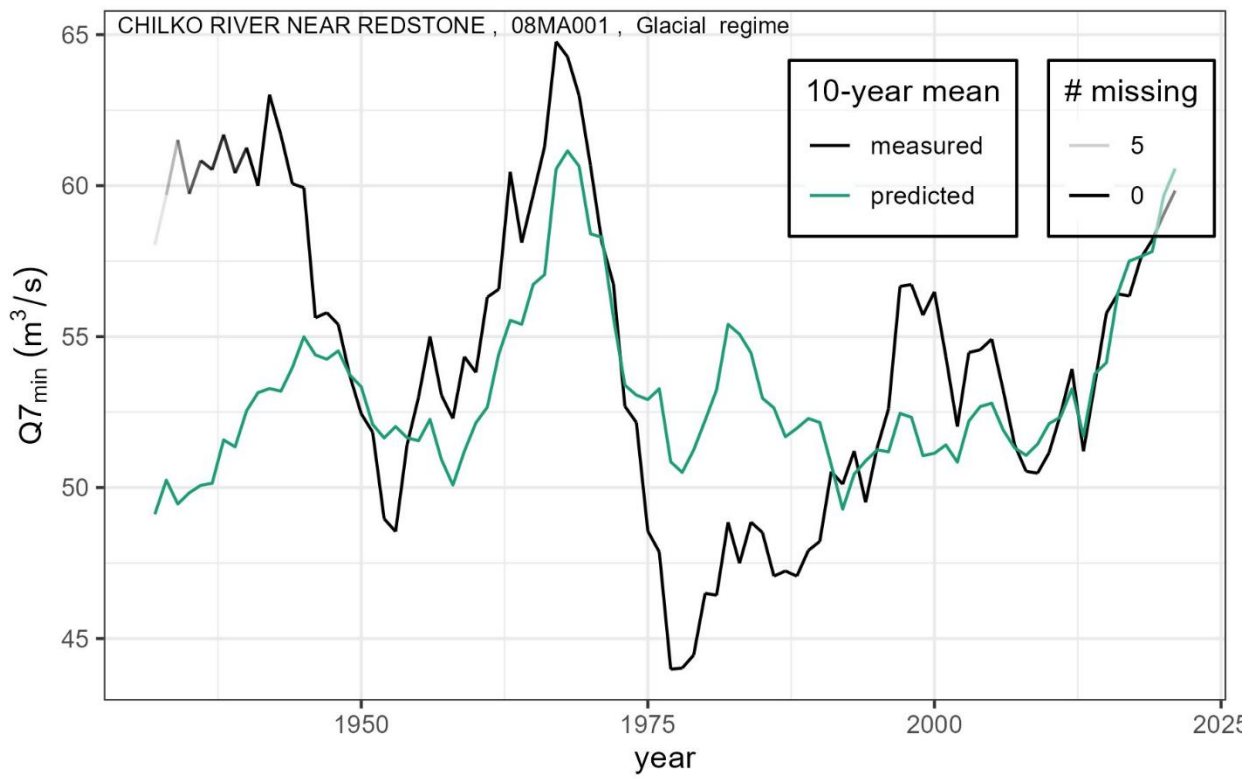


Figure F15: Gauge ID 08MA001, Chilkco River near Redstone

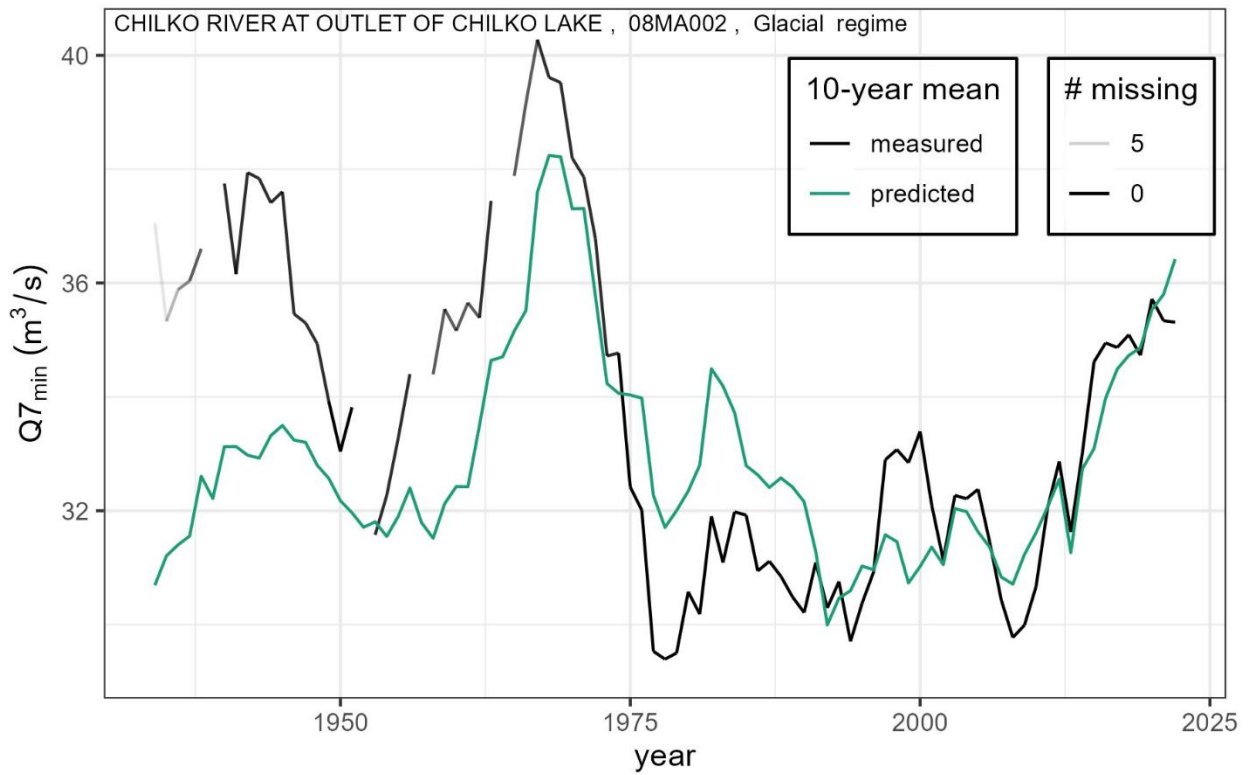


Figure F16: Gauge ID 08MA002, Chilkco River at Outlet of Chilkco Lake

72
73

74
75

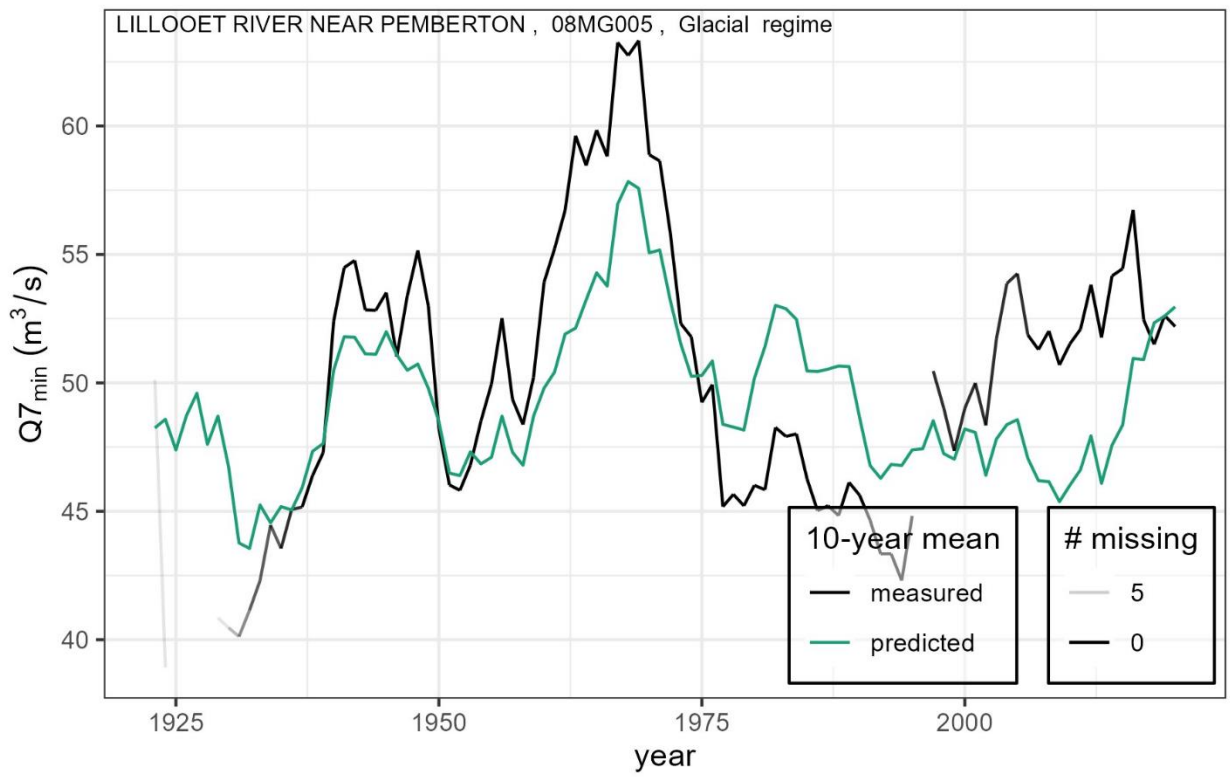


Figure F17: Gauge ID 08MG005, Lillooet River near Pemberton

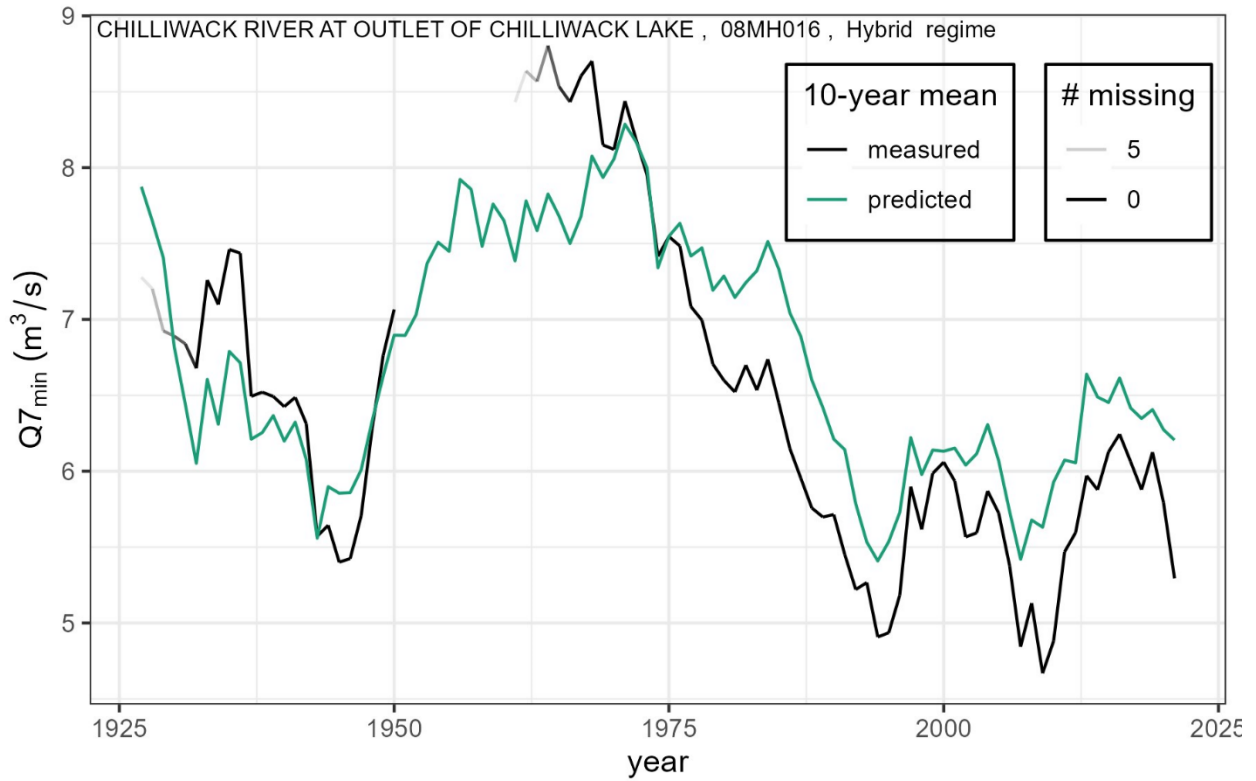


Figure F18: Gauge ID 08MG016, Chilliwack River at Outlet of Chilliwack Lake

76
77

78
79
80

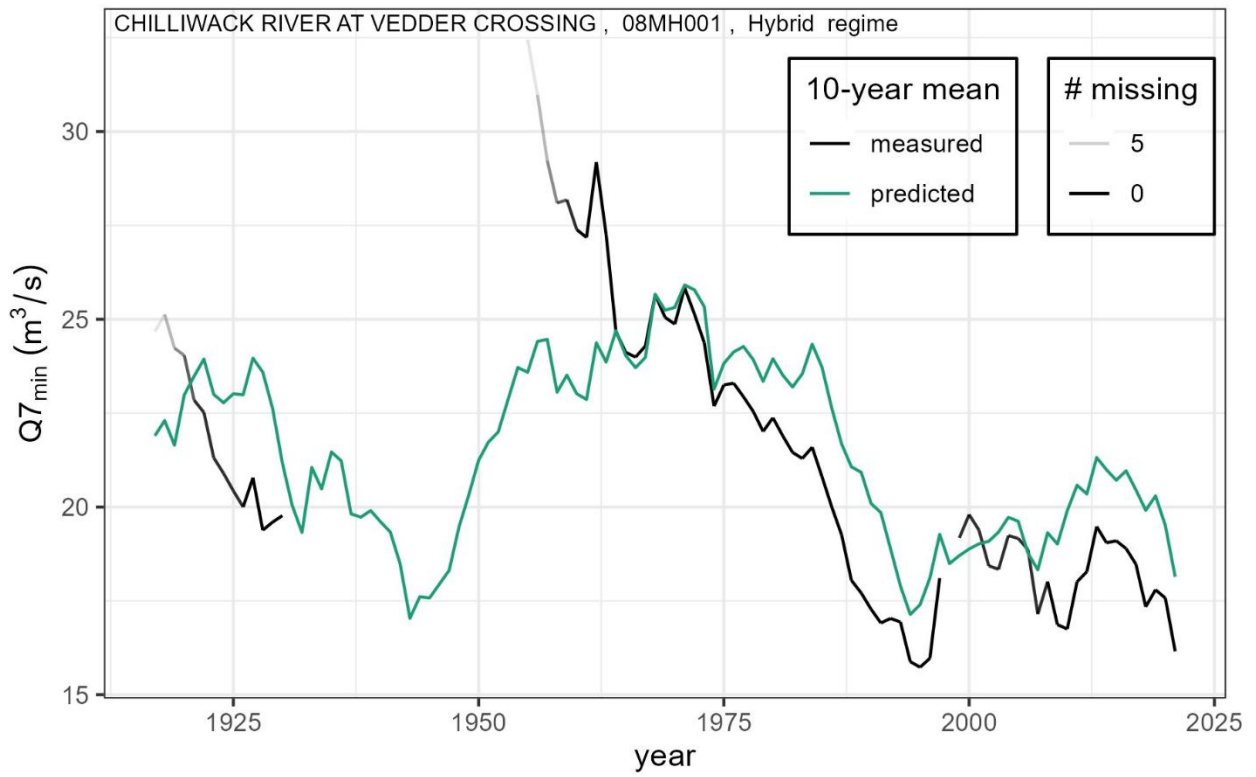


Figure F19: Gauge ID 08MH001, Chilliwack River at Vedder Crossing

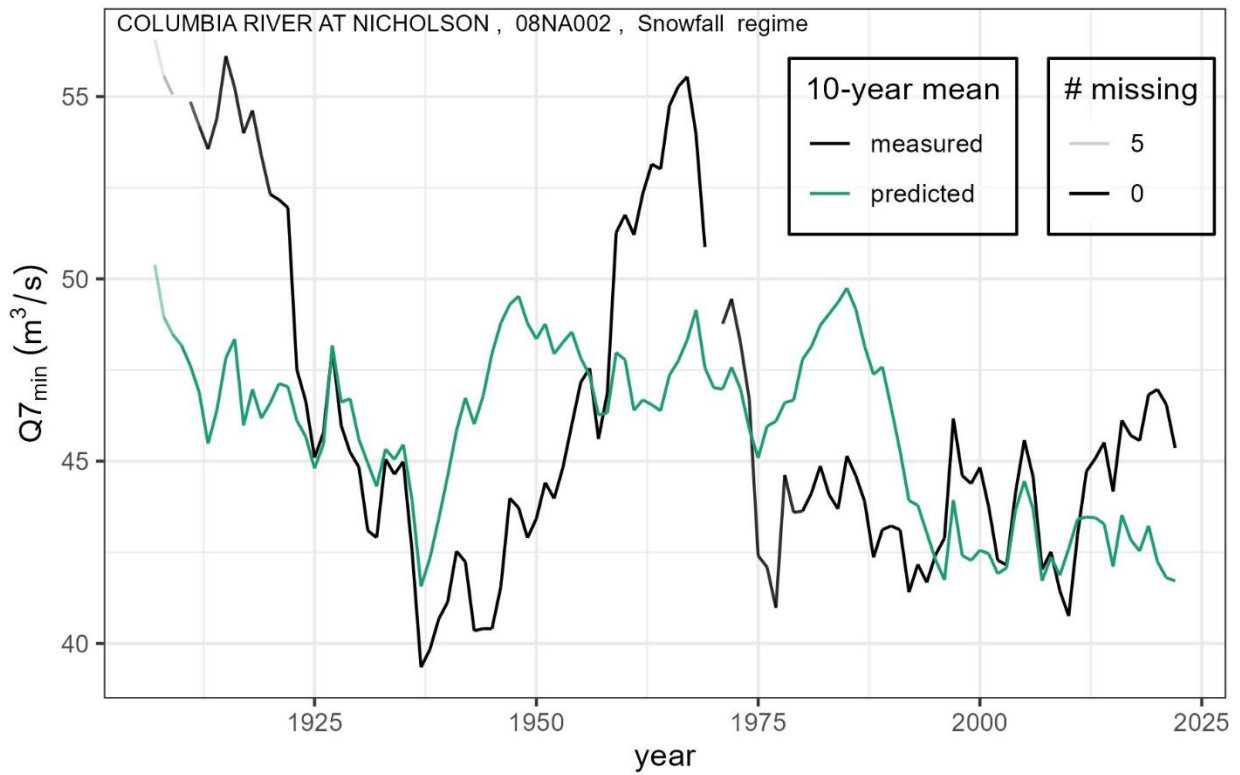


Figure F20: Gauge ID 08NA002, Columbia River at Nicholson

81
82

83
84

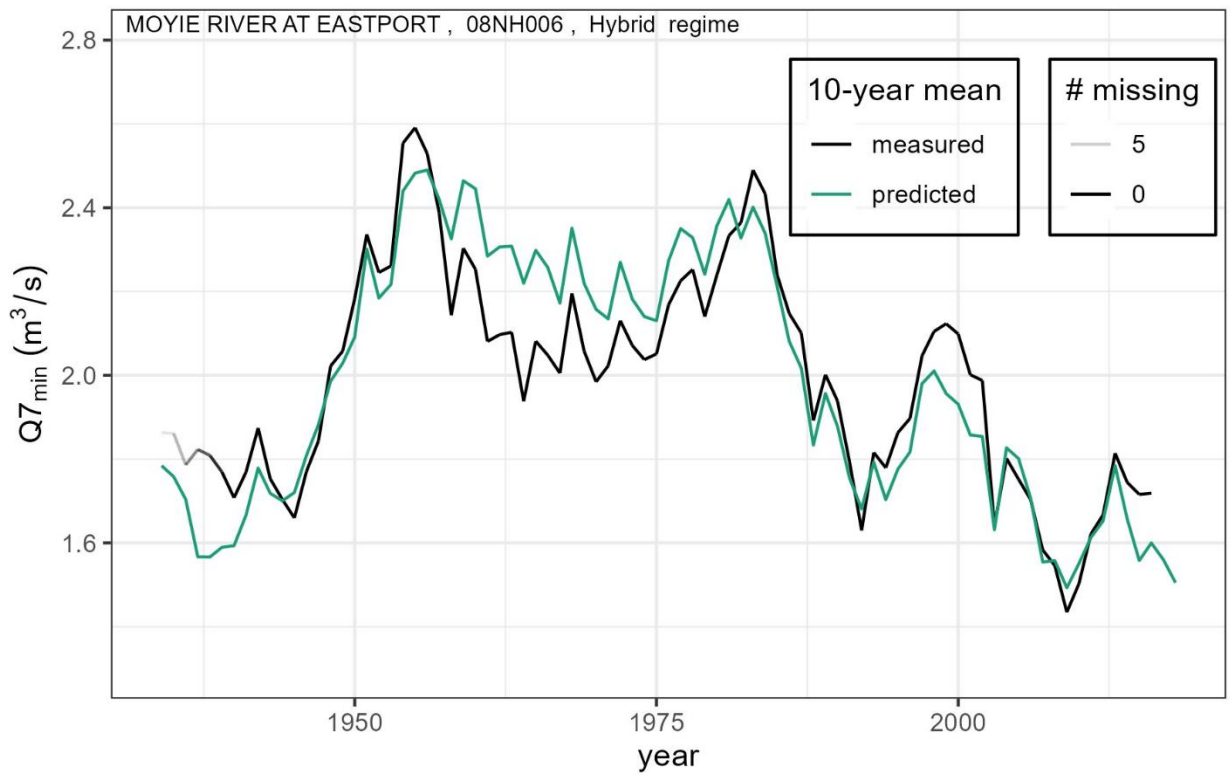


Figure F21: Gauge ID 08NH006, Moyie River at Eastport

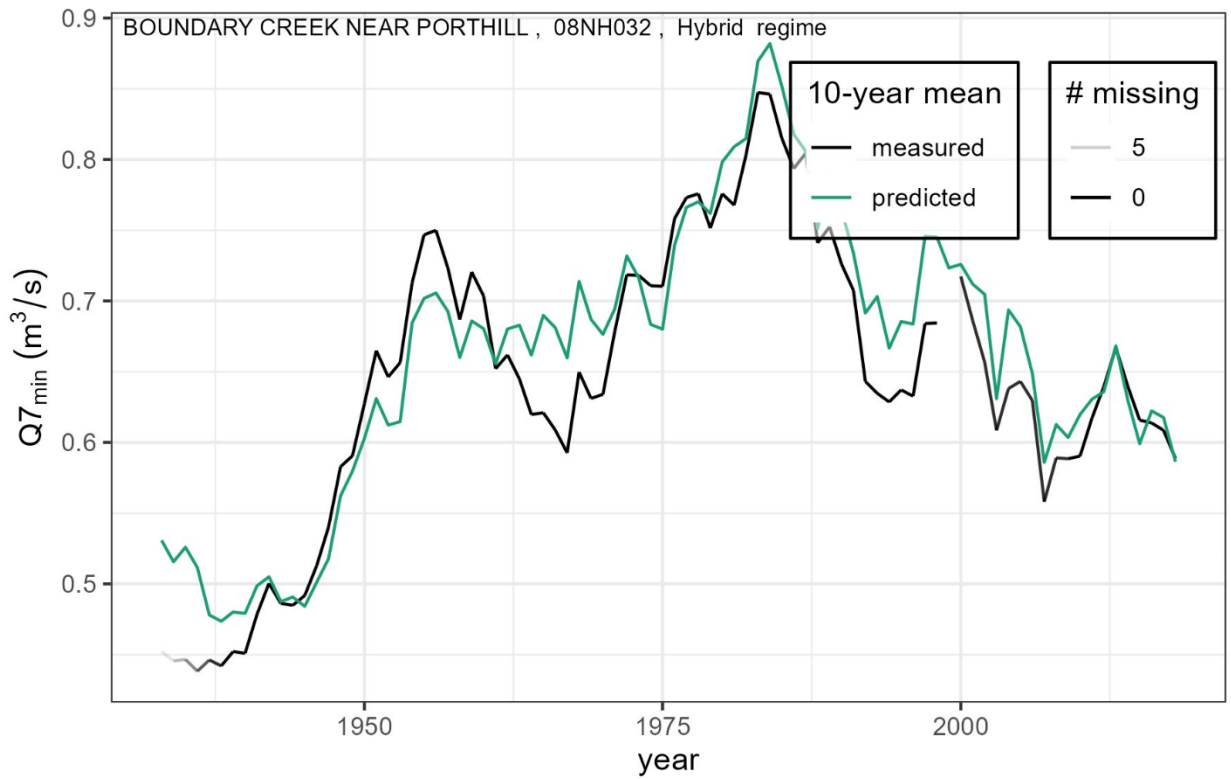


Figure F22: Gauge ID 08NH032, Boundary Creek near Porthill

85
86

87
88

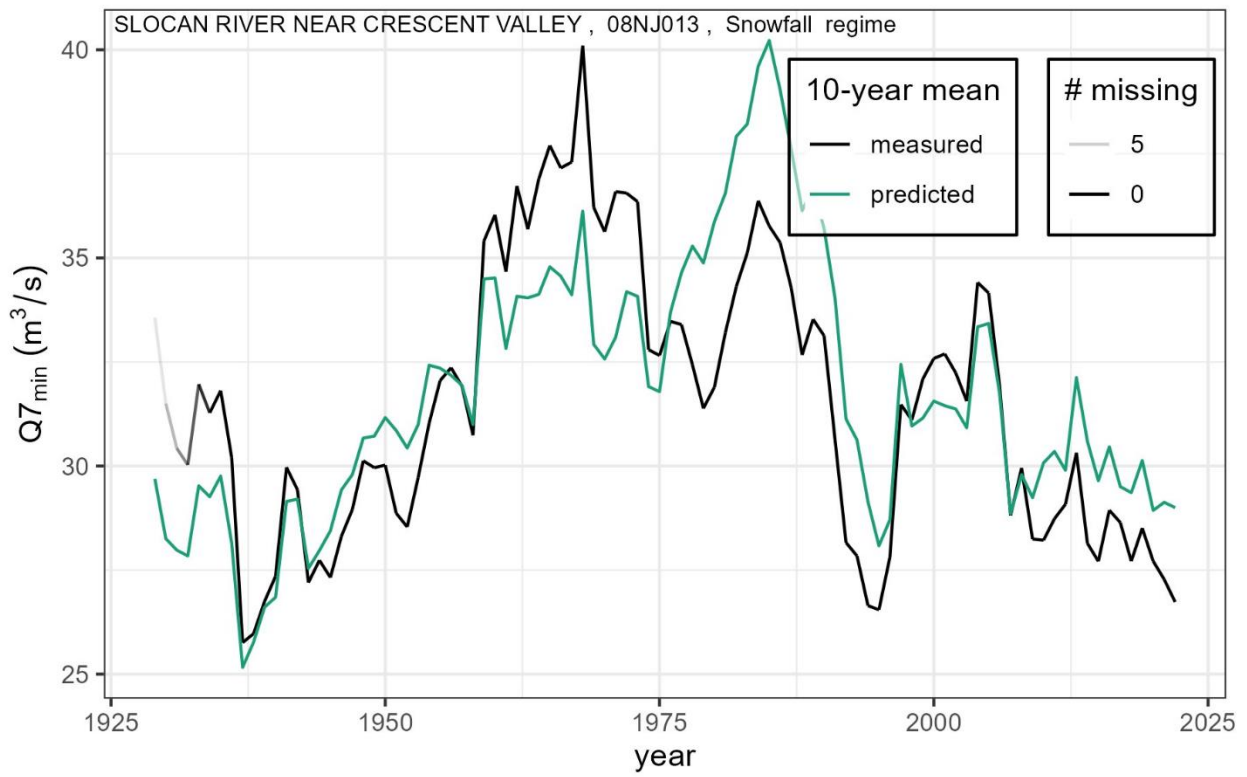


Figure F23: Gauge ID 08NJ013, Slocan River near Crescent Valley

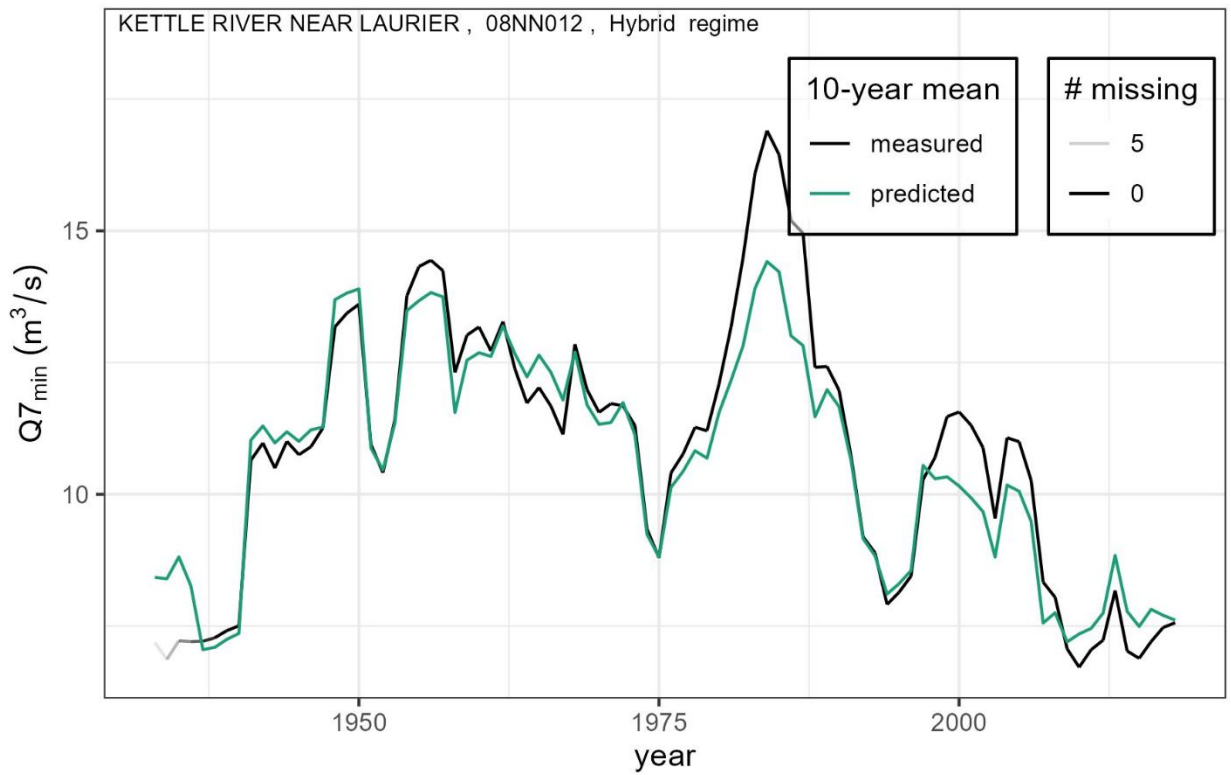


Figure F24: Gauge ID 08NN012, Kettle River Near Laurier

89
90

91
92

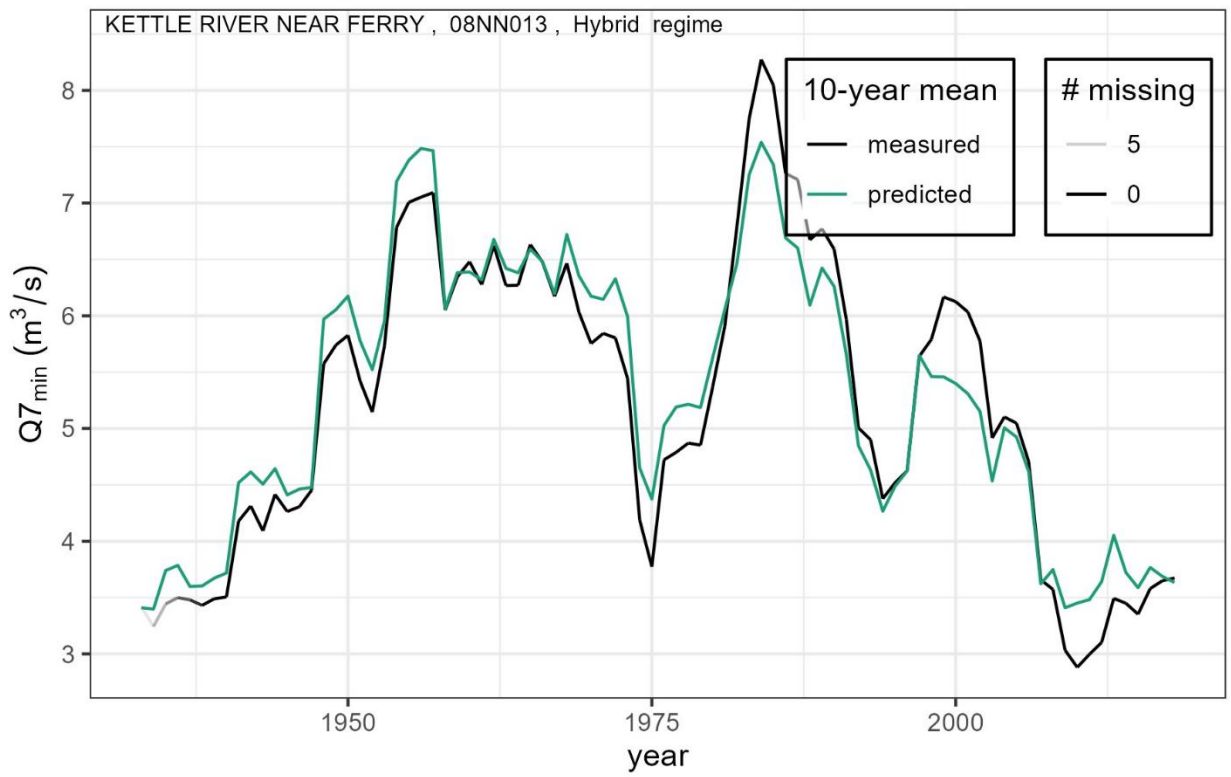


Figure F25: Gauge ID 08NN013, Kettle River Near Ferry

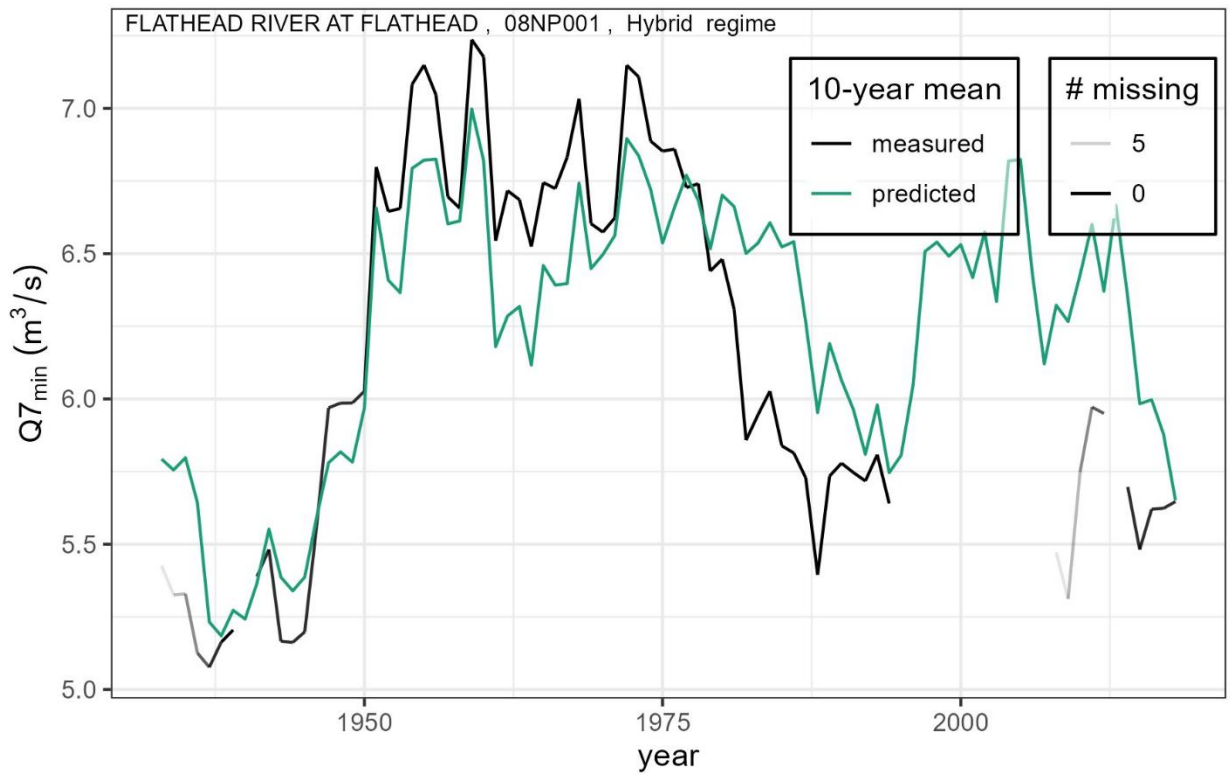


Figure F26: Gauge ID 08NP001, Flathead River at Flathead

93
94

95
96